# DEFINING THE NEUROMUSCULAR MECHANISMS OF VOCAL MOTOR CONTROL

A Thesis

Presented to

The Academic Faculty

by

Kyle Harish Srivastava

In Partial Fulfillment

of the Requirements for the Degree

Doctor of Philosophy in the

School of Biomedical Engineering

Georgia Institute of Technology

May 2016

# DEFINING THE NEUROMUSCULAR MECHANISMS OF VOCAL

# MOTOR CONTROL

Approved by:


Dr. Samuel Sober, Advisor
Department of Biology
*Emory University*


Dr. T. Richard Nichols
School of Applied Physiology
*Georgia Institute of Technology*


Dr. Garrett Stanley
Department of Biomedical Engineering
*Georgia Institute of Technology*

Dr. Lena Ting
Department of Biomedical Engineering
*Emory University*


Dr. Arthur English
Department of Cell Biology
*Emory University*


Date Approved:  March 7, 2016

*To my loving parents, who have always supported me no matter what I have decided to do with my life*

# ACKNOWLEDGEMENTS

classroom, departmental administration, and on my committee. His first semester course helped to shape my research interests, his positions within the department helped me understand the graduate process, and his presence on my committee helped elucidate my research findings. Dr. Ting's tough demeanor helped harden me as a scientist while also encouraging me to give my best effort. All of my committee members were always friendly and collaborative, both with me and each other, which made the entire process both productive and enjoyable. I also want to thank Dr. Elemans, Dr. Nemenman, and Caroline Holmes, who were all great collaborators for conducting meaningful research.

I want to thank my family for all their support over the past 28 years. My parents may not understand what I have been doing for the past six years, but they tell everyone they know about every small accomplishment of mine. My father has always taught me to appreciate knowledge and to learn as much as I can about everything. My mother has inspired me with her work ethic, as she is one of the hardest working people I know. Both of them are role models that have driven me to accomplish my goals.

My wife has been my biggest cheerleader since I started graduate school. She always tells me I am better than I think I am and constantly encourages me to strive for the best. Our relationship has grown so much over the past six years, and I would not be where I am today without her love and support.

Finally, I want to thank everyone over the past six years who asked me when I was going to graduate and, finally, get a job. I never knew the answer then, but it made me want to find out.

# TABLE OF CONTENTS

# LIST OF FIGURES

# LIST OF SYMBOLS AND ABBREVIATIONS

ACh          acetylcholine

AFP          anterior forebrain pathway

ANOVA       analysis of variance

BOS          bird's own song

CBT          corticobulbar tract

CON          conspecific song

CPG          central pattern generator

CT           cricothyroid muscle

DLM          dorsolateral nucleus of the anterior thalamus

DS           *m. syringealis dorsalis*

DTB          *m. tracheobronchialis dorsalis*

EMG         electromyography

EXP          expiratory muscle group

GABA        $\gamma$-aminobutyric acid

HVC          used as a proper noun, the nucleus upstream from RA

LCA          lateral cricoarytenoid

LDS          *m. syringealis dorsalis lateralis*

LMAN       lateral magnocellular nucleus of the anterior nidopallium

M1           primary motor cortex

MEAD       myo-elastic aerodynamic theory

NA           nucleus ambiguous

NMF          nonnegative matrix factorization

| | |
|---|---|
| nXIIts | tracheosyringeal portion of the $12^{th}$ (hypoglossal) nucleus of the medulla |
| PAm | nucleus para-ambiguus |
| PCA | posterior cricoarytenoid |
| RA | robust nucleus of arcopallium |
| RAm | nucleus retro-ambiguus |
| REV | reversed bird's own song |
| stEMG | spike-triggered electromyography |
| suEMG | single-unit electromyography |
| TA | transverse arytenoid muscle |
| TL | *m. tracheolateralis* |
| VS | *m. syringealis ventralis* |
| VTB | *m. tracheobronchialis ventralis* |
| wfANOVA | wavelet-based functional ANOVA |

# SUMMARY

The manner in which the brain sends commands to muscles to enact behavior is instrumental to our ability to interact with our environment. Moreover, the control of complex vocalizations is crucial for communicating with those around us. Therefore, in order to fully understand the neuromuscular mechanisms underlying vocal motor control, we must determine how the brain controls muscles and how those muscles' activity translates into vocal behavior. The objective of this thesis is to quantify how patterns of vocal muscle activity are transformed into acoustic output, controlled by individual premotor neurons in the avian nucleus RA (robust nucleus of arcopallium), and modulated by spike timing of motor neurons, which directly activate muscle fibers.

We first demonstrated that vocal muscles can both control multiple acoustic parameters, and do so in a context-dependent manner. We accomplished this goal by performing electromyographic recordings and targeted electrical stimulation of muscles during vocalization in addition to stimulating muscle in an *ex vivo* assay, in which the vocal organ is extracted and kept alive during the experiment. Next, we explored whether single premotor neurons control single or multiple muscles, with the implication that each scenario presents a different challenge to how the brain controls and modulates behavior. This experiment involved acutely recording from the brain and vocal muscles simultaneously and then using those recordings to determine functional connectivity. Finally, we showed how the brain uses spike timing in addition to spike rate to form a code that drives motor behavior. This was accomplished by recording single motor unit activity and stimulating respiratory muscles during quiet breathing. The work of this thesis elucidates how the brain controls vocal muscles and, subsequently, behavior, while

laying a foundation for future studies to further define the functional relationship between

the brain and muscles.

# CHAPTER 1

# INTRODUCTION

Humans are capable of generating a multitude of complex behaviors as they interact with their environment. To accomplish these feats, the nervous system must coordinate incoming sensory information with outgoing motor commands to properly drive muscles to enact the desired behaviors. The transformation of neural signals to muscle activity to behavioral output defines how the brain controls the body, and a full account of brain function demands that we understand this transformation. Moreover, vocal motor control is critical to our ability to communicate, and yet we still do not understand how single premotor neurons control vocal muscle activity and, subsequently, behavior. This gap in knowledge hinders our ability to understand the general principles of vocal behavior and develop effective treatments for the various speech disorders affecting millions of Americans [1]. This work will advance our understanding of vocal motor control by revealing how single neuron activity is transformed into vocal muscle activity and how muscle activity produces vocal behavior in songbirds.

## 1.1    Songbirds as a model system

Vocal learning is a rare behavior in the animal kingdom, but birdsong provides one of the very few examples in nonhumans. Like speech, birdsong must be learned from other members of its species, unlike innate calls that are more common in other animals [2]. In addition, songbirds, like humans, rely heavily on auditory feedback during both the juvenile development and adult error-correction of their songs [3]. The well-defined neural anatomy [4, 5] and physiological accessibility of songbirds make them an excellent system for investigating the neuromuscular mechanisms of vocal behavior.

1

More broadly, this system is a good model for general motor control as songbirds learn complex and sequenced behaviors. For more detail on the songbird system, refer to 3.1.

## 1.2 Clinical significance

Millions of Americans suffer from a variety of diseases in motor control, including those that affect people's ability to communicate [1, 6-8]. Communication is critical to our interactions with others in the environment, yet we do not fully understand the mechanisms behind the generation of vocalizations. Pathologies in motor control can have devastating effects on the patient. Any disruption of the neural circuits underlying speech control due to neural insult can harm a person's ability to communicate. Understanding the neuromuscular circuitry and vocal plasticity involved in speech will considerably help our ability to treat speech disorders. Specific disorders such as spasmodic dysphonia and dysarthrias resulting from stroke or Parkinson's disease have been shown to cause abnormal muscle activation, thus disrupting the acoustic structure of speech [9, 10]. Our ability to treat disorders is inhibited by our lack of understanding of the neuromuscular circuitry. For example, a common treatment for stuttering involves altering auditory feedback, yet even this treatment is only successful in less than half the cases [11]. Furthermore, the mechanisms for how this treatment works are poorly understood, and thus these treatments and modifications represent "shots-in-the-dark" [11]. Understanding the mechanisms for this vocal plasticity would not only help clinicians refine and better target current therapies but also develop better ones by targeting the correct portions of the pathways.

Before we can develop optimal tools for treating motor diseases, we must first understand how the brain controls muscles in a healthy state in order to interact with the human body's environment. Within the field of motor control, the songbird model presents an ideal platform for studying the neuromuscular control of vocalizations, a critical behavior in both songbirds and humans. While many studies have looked at the

2

neural mechanisms of vocal behavior in songbirds [12-17], none have bridged neural activity through muscular activity to vocal behavior. It is imperative to illuminate the full pathway from brain to behavior in order to begin to understand the mechanisms of both healthy and diseased motor control.

# CHAPTER 2

# SPECIFIC AIMS AND HYPOTHESES
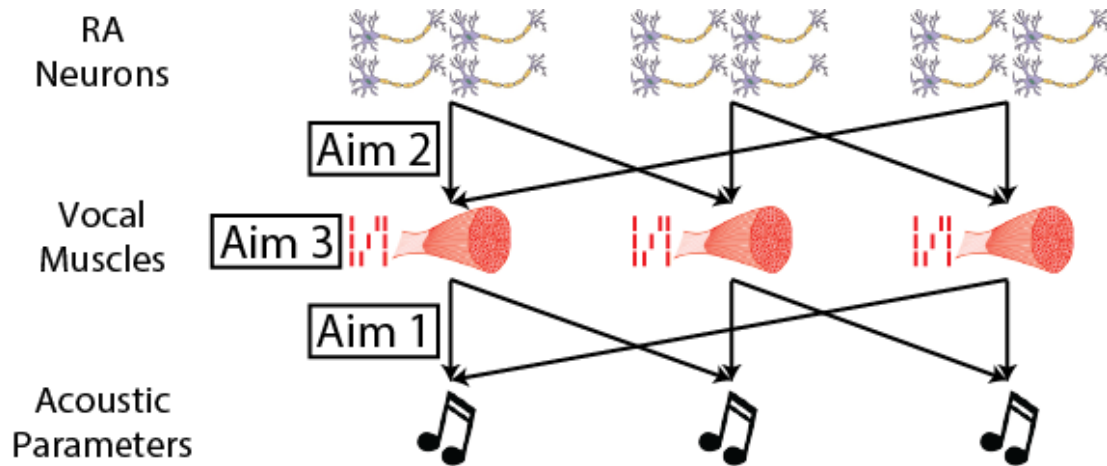


Figure 1: Central hypothesis depicts the three aims of this thesis. In this thesis, it is hypothesized that vocal muscles control multiple acoustic parameters (Aim 1), while each upstream RA neuron controls multiple muscles (Aim 2), by altering the timing of their spike patterns (Aim 3).

The long term goal of this project is to define the neuromuscular mechanisms behind vocal motor control in birdsong. The objective of this thesis was to quantify how patterns of vocal muscle activity are transformed into acoustic output, controlled by individual premotor neurons in nucleus RA (robust nucleus of arcopallium), and modulated by spike timing of motor neurons. This was accomplished using electromyography (EMG) to record vocal muscle activity (Aims 1, 2 and 3), vocal muscle stimulation to drive changes in behavior (Aims 1 and 3), and electrophysiology to record premotor neuron activity (Aim 2) to define how this system controls and modifies motor patterns during song. Furthermore, spike-triggered EMG (stEMG) [18, 19] was used to establish the functional connectivity between premotor neurons and vocal muscles (Aim 2). The central hypothesis (depicted in Figure 1) was that individual RA neurons, by altering the timing

of their spike patterns, control multiple muscles, each of which, in turn, controls multiple acoustic parameters. I tested this hypothesis using the following three Specific Aims:

**Aim 1: Reveal the mechanics of the transformation from vocal muscle activity to acoustic parameters.** To establish the mechanics of the vocal muscles' effects on song, I studied how single muscles control the acoustic parameters of song. Here, I implanted electrodes in vocal muscles to both record EMG activity and drove acoustic changes using muscle stimulation, a first in vocal motor control research. *I hypothesized that single vocal muscles control multiple acoustic parameters during song.* With respect to the central hypothesis, this Aim elucidated the transformation from muscle activity to acoustic parameters during song.

**Aim 2: Characterize functional projections of nucleus RA to the vocal muscles.** Despite the importance of premotor neurons to vocal control, the functional connections between individual premotor neurons and particular vocal muscles are unclear. While anatomical tracer studies in songbirds suggest a one-to-one mapping [20, 21], studies in other systems using a neurophysiological approach (spike-triggered EMG, or stEMG) indicate single premotor neurons can control multiple muscles [22, 23]. It is unknown whether these results reflect a difference in techniques or a fundamental difference in motor control organization. Here, I combined neural recording and EMG to perform stEMG, which might identify the functional connectivity between RA and vocal muscles. *I hypothesized that the functional circuitry is defined by one-to-many mapping (Figure 1) rather than each neuron activating a single vocal muscle as currently believed [20, 21].* If each RA neuron controls a single muscle that controls multiple acoustic parameters, then each RA neuron would be forced to control multiple acoustic parameters. However, a one-to-many mapping between each RA neuron and vocal muscles would allow single neurons to tune individual acoustic parameters given appropriate synaptic weights. The results of this Aim might allow us to differentiate models of motor control.

**Aim 3: Determine the role of motor neuron spike timing in driving vocal muscle behavior.** While motor neurons are typically modelled to drive muscle behavior using a rate code [24, 25], it is unclear whether the force production of vocal muscles is sensitive to small timing changes on the order of milliseconds. While some studies have investigated precise motor timing in motor neurons and its effect on muscle force [26-28], no study has been able to connect this precision from motor neuron activity to muscle force and, finally, to behavior. *I hypothesized that variations in vertebrate behavior can be driven by varying the timing, in addition to the rate, of vocal muscle activation.* With respect to the central hypothesis, this Aim shed light on how the brain controls behavior at the interface between the nervous and muscular system.

# CHAPTER 3

# LITERATURE REVIEW

## 3.1 Songbirds, as a model system

Despite the wealth of human behavioral studies investigating motor control and sensorimotor learning [29, 30], our understanding of the underlying mechanisms controlling these phenomena is limited by our ability to replicate these behaviors in animals from which we can directly record neurons and muscles.

### 3.1.1 The song system

Songbirds have been studied for several decades because they represent an excellent model system for vocal motor control and learning [31]. The well-defined neural anatomy (Figure 2) of the Bengalese finch makes it appropriate and feasible to study the mechanisms of vocalizations [4, 5]. In fact, because these song nuclei are specialized for producing vocalizations (rather than other behaviors that involve the muscles of the face and throat), experimental outcomes can be predominantly attributed to vocalizing behaviors instead of others, like eating [4, 31, 32]. In the vocal motor pathway, nucleus HVC (used as a proper name) [33] projects to the premotor nucleus RA, which projects onto the motor nuclei which control the vocal muscles (Figure 2) [34]. HVC also projects onto Area X as part of the anterior forebrain pathway (AFP) [35]. This branch of the song system injects variability for motor exploration into song via RA [36]. It is also believed to implement vocal learning by strengthening and weakening synaptic connections within RA based on feedback delivered through dopamine neurons [37, 38]. The experiments in this thesis focus on RA and downstream motor nuclei and muscles, though it is important to consider where they stand in the context of the song system. In addition to a mapped

anatomy, this species allows for experimental accessibility and has plastic song, which is susceptible to learning. Their song is stereotyped enough to yield high statistical power, but maintains some variability, which is crucial for inducing vocal learning. The songbird model is therefore an ideal one for studying the neuromuscular mechanisms of vocalizations.
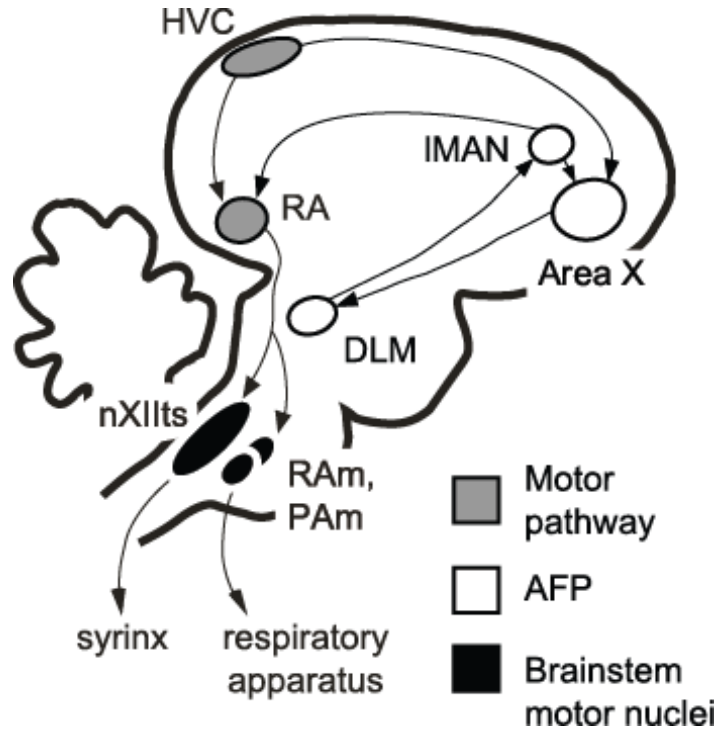


Figure 2: Schematic of the songbird motor pathway. Nucleus HVC projects to both the motor pathway, including premotor nucleus RA, subsequent motor nuclei, and vocal muscles, as well as the Anterior Forebrain Pathway (AFP), which injects variability and implements vocal learning in the song system. Figure reproduced with permission from [15].

In order to produce vocalizations in humans, the brain must precisely coordinate the contractions of several vocal muscles. Birdsong provides an excellent platform for studying the neuromuscular control because, like humans, they must learn the correct neural patterns of activity to generate the acoustics of song via the vocal muscles. Although previous work has helped to explain articulatory control in humans [39, 40], the

dynamics of the neural circuits behind speech remain largely unknown. In birdsong, the neural circuitry has been studied extensively, but the manner in which that activity is converted to song is unclear. Therefore, understanding how birds transform neural activity into song (as in Aim 2) will help overcome a critical barrier to understanding the general principles of vocal control. Figure 3 clarifies the neuromuscular anatomies of the vocalization system between humans and songbirds. Though the muscles differ morphologically, their analogous functions and structures are sufficient to allow study of the birdsong model to significantly advance our understanding of vocal motor control. For example, both the avian ventral syringeal (VS) muscle and the human cricothyroid (CT) muscle regulate the tension of the vibrating membrane for pitch control during vocalization [41, 42].
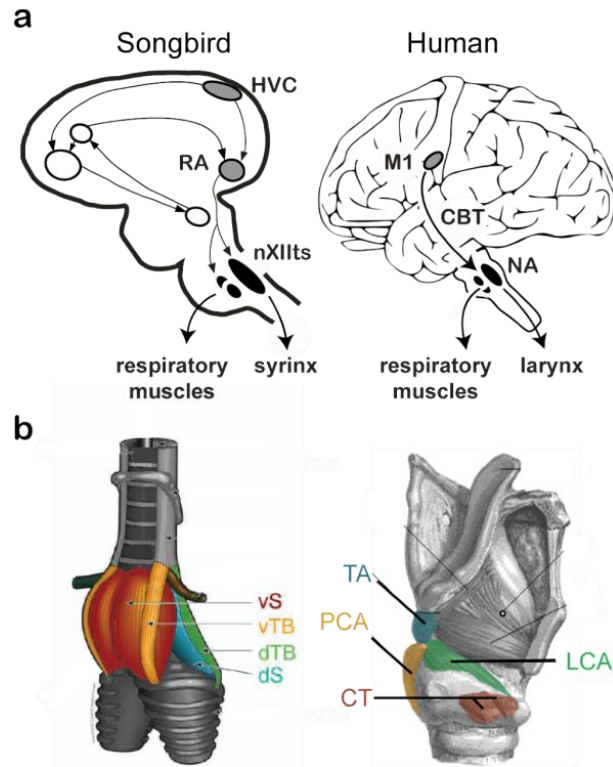
Figure 3: Comparative look at the neural and muscular anatomies of vocalization in humans and songbirds. (a) In songbirds, premotor nucleus RA (robust nucleus of the arcopallium) connects to the 12th motor nucleus (nXIIts) which innervates the vocal muscles [20, 21, 43]. In humans, the primary motor cortex (M1) projects along the corticobulbar tract (CBT) to the nucleus ambiguous (NA), which innervates the vocal muscles. (b) In songbirds, the dorsal syringeal (DS) and dorsal tracheobronchial (DTB) muscles adduct the vocal membrane, while the ventral tracheoobronchial (VTB) muscle abducts it. The ventral syringeal (VS) muscle controls membrane tension [44]. In humans, transverse arytenoid (TA) and lateral cricoarytenoid (LCA) adducts the vocal membrane, while the posterior cricoarytenoid (PCA) abducts it. The cricothyroid (CT) muscles control membrane tension. Figure designed by Sam Sober and adapted from [44].

Birdsong and human speech both exhibit vocal learning and can be modified in adulthood by altering auditory feedback. Both song and speech exhibit degradation after deafening [45, 46] and compensate for imposed auditory errors [47, 48]. Therefore, songbirds offer a unique model for investigating the role of neural plasticity in vocal production as well as insight into how sensory feedback regulates motor control.

Identifying how songbirds implement vocal learning will enhance our understanding of vocal motor plasticity and sensorimotor learning in humans.

The muscles' neural control and role in vocal learning have not yet been studied. In the songbird field, much research has been dedicated to the motor pathways used for producing song [13, 15-17], as well as the auditory pathways responsible for incorporating auditory feedback into song production [49-51]. Additionally, some studies have demonstrated behavioral phenomena common to birds and humans, such as adaptively correcting for perturbed auditory feedback [48, 52]. While some songbird research has studied the importance of the vocal musculature [41, 44, 53], the size of the literature pales in comparison to neural and behavioral studies. In order to grasp how the songbird model produces and modifies vocalizations, we must understand the role of the musculature in transforming neural input into acoustic output.

### 3.1.2 Production of acoustic signals by the vocal organ

Once neural signals leave the songbird brain, they must be converted to a vocal behavior by the vocal organ called the syrinx (Figure 3b). In order to produce vocalizations, the brain takes over the respiratory circuits to control expiratory pulses through the syrinx while abducting and adducting a vibrating membrane into the passing air. The syrinx is made up of tens of muscles that surround the bifurcation between the trachea and the two bronchi [54]. Because the syrinx is located at this branching point in Bengalese and zebra finches, among other songbirds, the bird can produce two "voices" at the same time. In fact, even without an anatomical difference between the two sides, specialization is observed in the types of sounds the two sides make. In most songbirds, like domestic canaries, zebra finches, brown-headed cowbirds, grey catbirds, northern cardinals, and brown thrashers, the left side of the syrinx produces low-frequency, noisy sounds, while the right side of the syrinx produces high-frequency tonal sounds [41, 55-62]. However,

11

in the Bengalese finch, this specialization is reversed, with the left side of the syrinx producing high-frequency, tonal sounds and the right side producing low-frequency, noisy sounds [63]. While syringeal activity is lateralized, the respiratory activity is symmetric as EMG activity in the left and right abdominal muscles are equal during song [64]. Though the abdominal expiratory muscles on each side compress ipsilateral air sacs, connections between them via the unpaired intraclavicular air sac lead to relatively uniform pressure throughout the system [65-68]. Thus, the vocal organ must use symmetric respiratory drive to produce asymmetric vocalizations across the bilateral syrinx, which can be accomplished using ipsilateral neural control that switches sides during vocalizations [69, 70]. Though the site of sound production can switch sides, neural control may still be occurring on the side without vocalization.

Pressure patterns are key to generating sounds as they combine with muscle contractions to force vibrations in the tissue (labia) that gate airflow to produce sound. In songbirds, the vocal organ is housed in an empty space called the air sac. Songbirds have many connected air sacs that help to create pressure to drive vocalizations when the expiratory muscles are active. The pressure within the system is thought to be well-controlled via feedback loops mediated by stretch receptors in the air sac [71]. According to myo-elastic aerodynamic (MEAD) theory [72], the vibrating tissue in the vocal organ maintains its oscillations through air-tissue interactions and restoring myo-elastic forces from the muscle [73-76], eliminating the need for muscles to contract at rates comparable to the output acoustic frequency [77]. Airflow through the oscillating tissue then becomes pulsatile [75], resulting in acoustic output, which is modulated by the resonance properties of the tissue and the driving airflow [78-81]. In fact, the biophysical mechanisms used to generate sound are not only common across birds but also mammals, including humans [72]. Small changes in pressure can also have effects on the amplitude

and frequency of produced sound [82, 83]. While the pressure patterns primarily help to shape the envelope of sound production into discrete units called syllables, the muscles of the syrinx form the fine acoustics of each syllable.

Understanding the transformation from neural signals to muscle activity to vocal behavior is critical to describing the full system. Early work demonstrated that VS (Figure 3) is a key vocal muscle for controlling pitch, or syllable frequency, as it regulates the tension in the vibrating labia [41]. Dorsal muscles like DS and DTB reduce airflow through adduction while VTB increases airflow through abduction [59]. These vocal muscles are in fact capable of modulating airflow at frequencies above 150 Hz, making them faster than most muscle tissue in the animal kingdom [53]. EMG studies have shown that many of the muscles are co-activated during vocalization, making it difficult to discern which muscles are driving acoustic changes [41, 59]. It is believed that all of the muscles activate to stabilize the vocal organ during vocalization, allowing one side of the syrinx to vocalize at a time in some cases. Once sound is produced at the vocal organ, it travels up the trachea where it can still be modulated by the upper vocal tract to emphasize certain frequencies before leaving the mouth [84]. Though many in the songbird field view the system as a very complex, nonlinear, and redundant process [72, 85], some have attempted to simplify the transformation as an invertible one governed by labial tension and air sac pressure [86-88]. More work is necessary to fully understand the transformation from neural signals through muscle activity to acoustic behavior.

### 3.2    Muscles as a transformer from neural activity to behavior

Muscles are the interface between the nervous system and the environment. The brain relies on the muscles to perform tasks and react to that environment with accuracy. At the

transition point between the nervous system and the muscular system, a motor neuron innervates a motor unit, made up of several muscle fibers, ranging from a few in very small muscles to thousands in larger ones [89, 90]. When a motor neuron spikes, it releases acetylcholine (ACh) at the neuromuscular junction to activate all of the muscle fibers in the motor unit, causing them to contract and produce force. Traditionally, this output muscle force has been modeled with the muscle acting as a low-pass filter on the firing rate of the motor neuron [91]. A critical exception to this thought is the phenomenon of motor units firing doublets, which are two action potentials separated by a short interval of time between 2.5 ms and 20 ms [92, 93]. These doublets are often found during the onset of muscle activation and are hypothesized to ramp up muscle force quickly relying on nonlinear dynamics in contrast to that of a low-pass filter [94, 95]. Some in the motor control field believe that doublets represent the physiological manifestation of the "catch effect," where moving a single stimulation pulse in a fixed-rate stimulation pattern results in a significant change in force output [26, 27]. Others have contested whether or not doublets are physiologically meaningful, or just an artifact of the experimental preparation [96, 97]. The controversial interpretation of these results demands that the topic be addressed further to determine the relevant timescale of muscle excitation.

Understanding the effects of timing based on electrical stimulation of muscles requires us to look at the signals going to the muscle and the behavior resulting from the muscles. To this point, the only study to play back physiological relevant motor unit firing patterns including doublets to induce variations in muscle force was in the invertebrate *Aplysia* [28]. A study in hawkmoths demonstrated that the nervous system could use control of opposing flight muscles on a millisecond scale to modulate flight torque [98]. It is important to note that among the differences between invertebrate and vertebrate motor control, invertebrate muscle can be innervated by multiple motor neurons, both excitatory and inhibitory, while vertebrate muscles are innervated by a

single excitatory motor neuron, which can itself be inhibited [99]. Therefore, it is not clear what the conclusions from invertebrate studies can reveal about whether the vertebrate brain also uses a spike-timing code. While muscles may not act as simple low-pass filters for incoming neural signals, it is still unclear how relative timing within motor neuron firing affects muscle activity and, subsequently, behavior. A next step for the motor control field is to push these muscles to their temporal limits to see how they handle quickly changing dynamics in neural firing. Determining whether the central nervous system generates precisely timed spike sequences in motor commands would unlock an immense amount of information from the neural code.

# CHAPTER 4

# MULTIFUNCTIONAL AND CONTEXT-DEPENDENT CONTROL OF VOCAL ACOUSTICS BY INDIVIDUAL MUSCLES [1]

A similar version of this chapter was originally published in [100].

## 4.1 Abstract

The relationship between muscle activity and behavioral output determines how the brain controls and modifies complex skills. In vocal control, ensembles of muscles are used to precisely tune single acoustic parameters independently such as fundamental frequency and sound amplitude. If individual vocal muscles were dedicated to the control of single parameters, then the brain could control each parameter independently by modulating the appropriate muscle or muscles. Alternatively, if each muscle influenced multiple parameters, a more complex control strategy would be required to selectively modulate a single parameter. Additionally, it is unknown whether the function of single muscles is fixed or varies across different vocal gestures. A fixed relationship would allow the brain to use the same changes in muscle activation to, for example, increase the fundamental frequency of different vocal gestures, whereas a context-dependent scheme would require the brain to calculate different motor modifications in each case. We tested the hypothesis that single muscles control multiple acoustic parameters and that the function of single

muscles varies across gestures using three complementary approaches. First, we recorded electromyographic data from vocal muscles in singing Bengalese finches. Second, we electrically perturbed the activity of single muscles during song. Third, we developed an *ex vivo* technique to analyze the biomechanical and acoustic consequences of single-muscle perturbations. We found that single muscles drive changes in multiple parameters and that the function of single muscles differs across vocal gestures, suggesting that the brain uses a complex, gesture-dependent control scheme to regulate vocal output.

### 4.2    Introduction

The transformation from neural signals to muscle performance to behavioral output defines how the brain controls behavior. During both speech and birdsong, the coordinated activity of vocal muscles regulates the tension of vibrating tissue and gates airflow in order to generate vocalizations [44, 101]. Behavioral studies have demonstrated that both humans and songbirds can selectively modulate single acoustic parameters such as fundamental frequency [48, 102, 103], raising the question of how the vocal system might selectively alter a single parameter. Although single muscles have been shown to control multiple behavioral parameters in other systems [104, 105], the functional role of individual vocal muscles remains poorly understood. The difficulty in accessing human vocal muscles hinders our understanding of how individual muscles shape speech [106]. Furthermore, although studies in both humans and songbirds have demonstrated correlations between electromyographic (EMG) activity and various acoustic parameters [41, 53, 107, 108], it is difficult to isolate the independent contributions of individual vocal muscles because the activities of different muscles can

be strongly correlated [41, 59, 109]. Here, we test the hypothesis that single vocal muscles control multiple acoustic parameters in songbirds by combining traditional EMG measurements with online stimulation techniques that perturb the activity of single muscles.

A distinct but equally important issue is whether the transformation from muscle activation to behavior is fixed or context-dependent across different vocal gestures. If fixed, single muscles would have the same effect on acoustics regardless of the performed gesture. Alternatively, the transformation could be context-dependent, where the effect of a change in a muscle's activity depends on muscle performance and the biomechanical context of the vocal organ (including the activity of other muscles). A fixed transformation would allow the brain to increase activation of a particular muscle to enact a specific change in fundamental frequency, for instance, regardless of the vocal gesture being produced. However, a context-dependent transformation would force the brain to account for the current state of the vocal organ when implementing acoustic changes. Though the transformation from muscle activation to behavior is strongly context-dependent in some systems [110, 111], this question has not been examined in vocal control. We hypothesize that individual muscles have context-dependent effects on acoustic parameters during song.

We used three approaches to test our hypotheses. First, we examined correlations between EMG activity recorded from single muscles with the acoustic parameters of individual vocal gestures. Second, we developed a novel stimulation assay in which individual muscles are electrically stimulated during behavior to measure the marginal effect of their increased activity on acoustic output. Third, we devised an *ex vivo* assay in

which the vocal organ produced sound in isolation from the nervous system, allowing us to visualize the dynamics of the vocal organ and the effects of stimulation.

## 4.3 Methods

### 4.3.1 Surgical procedures

We used EMG and *in vivo* electrical stimulation to determine the function of vocal muscles during birdsong. All procedures were approved by the Emory University Institutional Animal Care and Use Committee. Prior to surgery, adult (>90 days old) male Bengalese finches (*Lonchura striata domestica*) were anesthetized using 40 mg/kg of ketamine and 3 mg/kg of midazolam injected intramuscularly. Proper levels of anesthesia were maintained using 0-3% isoflurane in oxygen gas. Across all experiments, *m. syringealis ventralis* (VS), *m. tracheobronchialis dorsalis* (DTB), and the expiratory muscle group (EXP) were implanted, though not necessarily all at once. Note that EXP is comprised of three sheet-like overlapping muscles (*m. obliquus externus abdominis*, *m. obliquus internus*, and *m. transversus abdominis*). As in prior studies [43, 64, 112, 113], we did not attempt to distinguish signals arising from these three muscles. We focused our experiments on VS, DTB, and EXP because their surfaces are comparatively large (1 mm x 3 mm) and easy to access; we were unable to reliably target other smaller muscles of the syrinx. The implanted muscles reflected a range of biomechanical functions. VS activity is highly correlated with fundamental frequency in brown thrashers (*Toxostoma rufum*) [59] and based on morphological position is suggested to modulate medial labial tension in zebra finches (*Taenopygia guttata*) [54]. Direct observations during micro-stimulation in anesthetized northern cardinals (*Cardinalis cardinalis*) showed that DTB adducts the lateral labia [44] and micro-stimulation of DTB in anesthetized starlings

19

(*Sturnus vulgaris*) modulated and decreased air flow and sound amplitude [53]. EXP drives expiration during breathing and song, with the majority of sound production taking place during the expiratory phase of the respiratory rhythm [112]. EXP drives expiration by regulating pressure in the system of air sacs that both supply and surround the vocal organ. The relationship between EXP activity and air sac pressure (a key parameter for vocal production) is complex and poorly understood, and appears to depend on syringeal gating of airflow and the volume of air in the air sac, which varies during expiration [114].

The syrinx was accessed for electrode implantation via a midline incision between the furcula into the intraclavicular air sac. VS is located on the ventral portion of the syrinx near the midline (Figure 4b). DTB is located just dorsally to a prominent blood vessel on the lateral and rostral portion of the syrinx. One pair of insulated single-stranded stainless steel (25 μm diameter, California Fine Wire Co., Grover Beach, CA, USA) or multi-stranded nickel-copper alloy (50 μm diameter Phoenix Wire Inc., South Hero, VT, USA) wires (0.5 mm of insulation was stripped from the end) were inserted into VS and/or DTB muscles (Figure 4). Wires were secured using either a small amount of tissue adhesive or 10-0 suture (Ethicon, Inc., Somerville, NJ, USA) and run from the syrinx to the scalp subcutaneously where the wires were soldered to a plug. The air sac was sealed using additional tissue adhesive. The skin was closed with 5-0 sutures (Ethicon, Inc.). For surgeries to record from EXP, an incision was made dorsal to the femoral joint, rostral to the pubic bone. One pair of the same wires was inserted into EXP and secured using tissue adhesive or a suture and routed subcutaneously to a plug on the head as described above. Birds typically began singing within a week after the surgery. Voltage signals were amplified using a 10X headstage and a differential AC amplifier (A-M Systems Model 1700, Sequim, WA, USA). EMG data were bandpass filtered between 300 Hz and 5 kHz, then digitized, rectified and smoothed (5 ms box filter).

Acoustic data were also recorded using a microphone (Countryman Associates Inc., Isomax 2 omnidirectional, Menlo Park, CA, USA) and digitally bandpass filtered between 200 Hz and 10 kHz prior to analysis. The microphone was fixed 3 cm above the cage (28 cm x 28 cm x 28 cm), which sat in the middle of a semi-anechoic chamber (66 cm x 71 cm x 71 cm). Both acoustic and EMG signals were sampled at 32 kHz and digitized using an NI board (National Instruments, BNC-2090A, Austin, TX, USA).
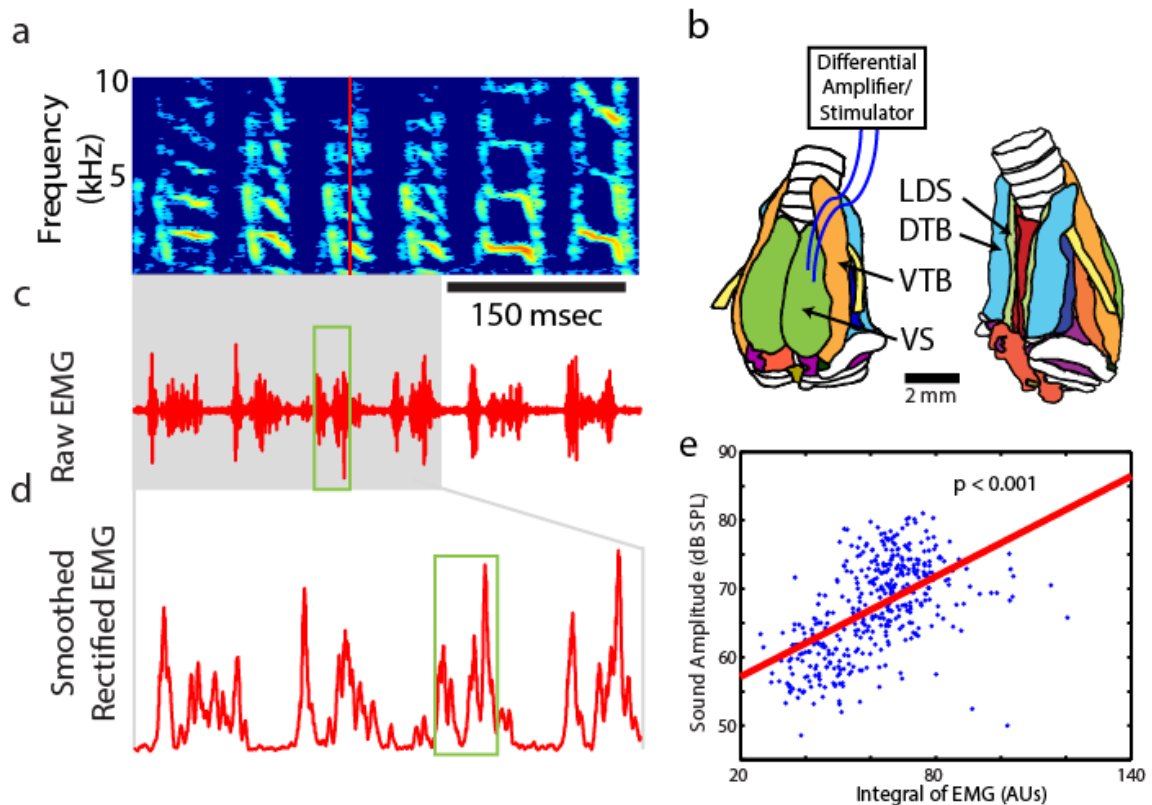


Figure 4: Vocal muscle activity correlates with vocal acoustics in Bengalese finch song. Birdsong is made up of vocal gestures called syllables, labeled "A" through "F" above the spectrogram, which shows the power at different acoustic frequencies as a function of time. The vertical red line represents the time at which acoustic parameters were measured during syllable "C" (see Methods). (b) To measure EMG activity and electrically stimulate single muscles, pairs of electrodes were inserted in individual vocal muscles (DTB: *m. tracheobronchialis dorsalis*, and VS: *m. syringealis ventralis*). VTB (*m. tracheobronchialis ventralis*) and LDS (*m. syringealis dorsalis lateralis*), which were used as reference muscles in the *ex vivo* experiments, are also shown. Anatomy illustration modified and used with permission from [54]. Muscles are shown as colored structures while the trachea (top) and bronchi (bottom) are shown in white. (c) The raw EMG signal and (d) smoothed, rectified EMG signal from the expiratory muscle group (EXP). Red box shows the time window over which EMG activity was quantified just

prior to acoustic measurement time. (e) A linear regression was then calculated between the smoothed, rectified EMG and each acoustic parameter (sound amplitude is shown).

### 4.3.2   Regression analysis

To relate muscle activity to acoustic variation, we measured the acoustic properties of each syllable rendition as well as the EMG activity associated with each syllable. For these experiments, 11 VS muscles (8 from the left side of the syrinx and 3 from the right side), 8 DTB muscles (all from the left side), and 9 EXP muscles (7 from the left side and 2 from the right side) across 20 adult male Bengalese finches were used. EMG activity was measured as the mean smoothed, rectified EMG in the 16 ms preceding the time of fundamental frequency measurement (Figure 4c-d). The preceding time delay was determined by calculating the cross-correlation between EMG and sound, which typically reached a peak value between a 6 and 16 ms lag. To ensure that our regression results did not depend on our choice of a 16 ms-wide time window, we performed additional analyses in which we performed regressions using the EMG signal from 8, 12, and 20 ms prior to the time of acoustic measurement. As described in Results, these alternate latencies yielded nearly identical results to those obtained using a 16 ms latency. Previous analysis using principal components analysis has identified fundamental frequency, amplitude, and spectral entropy as important axes of acoustic variation in Bengalese finch song [15]. These acoustic parameters were therefore selected to reveal the behavioral effect of trial-by-trial variations in EMG activity. For each syllable, we defined a measurement time relative to syllable onset (vertical red line in Figure 4a) that corresponded to a well-defined spectral feature. Syllable onsets were defined based on amplitude threshold crossings. Fundamental frequency was quantified at the selected

measurement time by quantifying peaks in spectral power as described previously [15]. Amplitude was defined as the root-mean-square (RMS) amplitude in the 16 ms window surrounding the time of fundamental frequency measurement. This amplitude measurement was then converted to sound pressure level (dB SPL) by using a sound level calibrator (CAL73, BK Precision, Yorba Linda, CA, USA), which generated a 1 kHz sound wave at 94 dB SPL re 20 µPa, at the microphone. The following equation was used to calculated sound pressure level (dB SPL)

$$SPL = 20 * log_{10}\left(\frac{V_{measured}}{V_{calibrated,94dB}}\right) + 94,$$

where *SPL* is the sound pressure level (dB SPL), $V_{measured}$ is the measured RMS voltage, and $V_{calibrated, 94dB}$ is the measured RMS voltage during calibration with a 94 dB SPL re 20 µPa, 1 kHz sound wave. We calculated sound pressure at the microphone (i.e. measured level) and not at the bird's beak (i.e. source level). When time-varying sound amplitude waveforms were calculated, a sliding 16 ms window was used to calculate RMS throughout the waveform, before being calculated in dB SPL. Spectral entropy was defined as the entropy of spectral power at the time of fundamental frequency measurement within a one octave window centered on the peak power according to the equation

$$E = -\sum_{f_{min}}^{f_{max}} (P(f) * log_{10} P(f)),$$

where *E* is the spectral entropy, *P(f)* is the probability distribution of spectral power, and $f_{min}$ and $f_{max}$ are the frequency bounds surrounding the first harmonic (one half octave below and above the first harmonic, respectively).

Linear regressions were computed between EMG activity and each of the three acoustic parameters for each muscle-syllable pair (example shown in Figure 4e). Here, a muscle-syllable pair refers to the EMG activity from one muscle associated with one vocal gesture. Therefore, if a bird sang 5 different syllables, while having 2 muscles implanted, it would contribute 10 muscle-syllable pairs to the data set. Because no significant difference in proportion of significant regressions (regression slope significantly different from zero, $p < 0.05$) was found between muscles on the left and right side, they were combined for our analysis.

Because of the large number of linear regressions performed (336), we needed to confirm that the number of significant regressions we discovered were more than that found at chance. To do so, we permuted each of the four measured parameters (fundamental frequency, amplitude, spectral entropy, and EMG) for each muscle-syllable pair in order to break any correlations that may exist in the dataset. We then calculated a linear regression for every muscle-syllable pair in the permuted datasets and measured the proportion of significant regressions. This process was repeated one thousand times to establish the $95^{th}$ percentile for the proportion of significant regressions. This value was then compared to what we found in the original dataset to determine if the number of significant regressions found in the study were more than those that would be found by chance. This process was also used to determine whether the number of muscle-syllable pairs with significant regressions with two, three, and multiple (i.e. two or three) acoustic parameters in our dataset were more than expected by chance. All analysis was conducted in MATLAB (Mathworks, Natick, MA).

### 4.3.3  Muscle stimulation

Muscle stimulation experiments were conducted using the same type of electrodes implanted for recording experiments, as described above. For stimulation experiments, 9

vocal muscles (4 left VS, 3 left DTB, and 2 EXP) were implanted in 9 adult male Bengalese finches, in which 5 syllables were stimulated across all VS experiments, 6 syllables across all DTB experiments, and 2 syllables across all EXP experiments. Using custom LabView code [115], a specific syllable was detected using a spectral template. The template was created by taking the average spectrum of the target syllable across hundreds of unperturbed trials. A template match triggered the onset of stimulation (train burst width: 18.5 ms, pulse duration: 0.5 ms, interpulse period: 3 ms, 7 pulses) at a latency calibrated so that stimulation would perturb the subsequent syllable. Note that because our analysis focuses on the effects of stimulation at a minimal latency rather than maximal effects (see below), the duration of the stimulation train is unlikely to significantly affect our results. A stimulator (A-M Systems, Model 2100) was used to pass current through the electrodes to perturb the implanted muscle in 50% of the trials (to allow comparison with control, or "catch" trials). We determined the appropriate current level by first titrating the current amplitude to the lowest level at which we could observe acoustic effects in any parameter. Our stimulation experiments encompassed currents ranging from 75 μA to 500 μA. Our *ex vivo* data (see Results) show 500 μA was a suitable maximum for avoiding activation of neighboring muscles. Though there are differences between the *in vivo* and *ex vivo* paradigms that could cause the recruited volume of muscle tissue to differ at the same stimulating current (see Discussion), we believe that the *ex vivo* preparation suggests a reasonable range for stimulating currents. Acoustic data from stimulation experimented were measured in the same manner that is described in the correlation approach above.
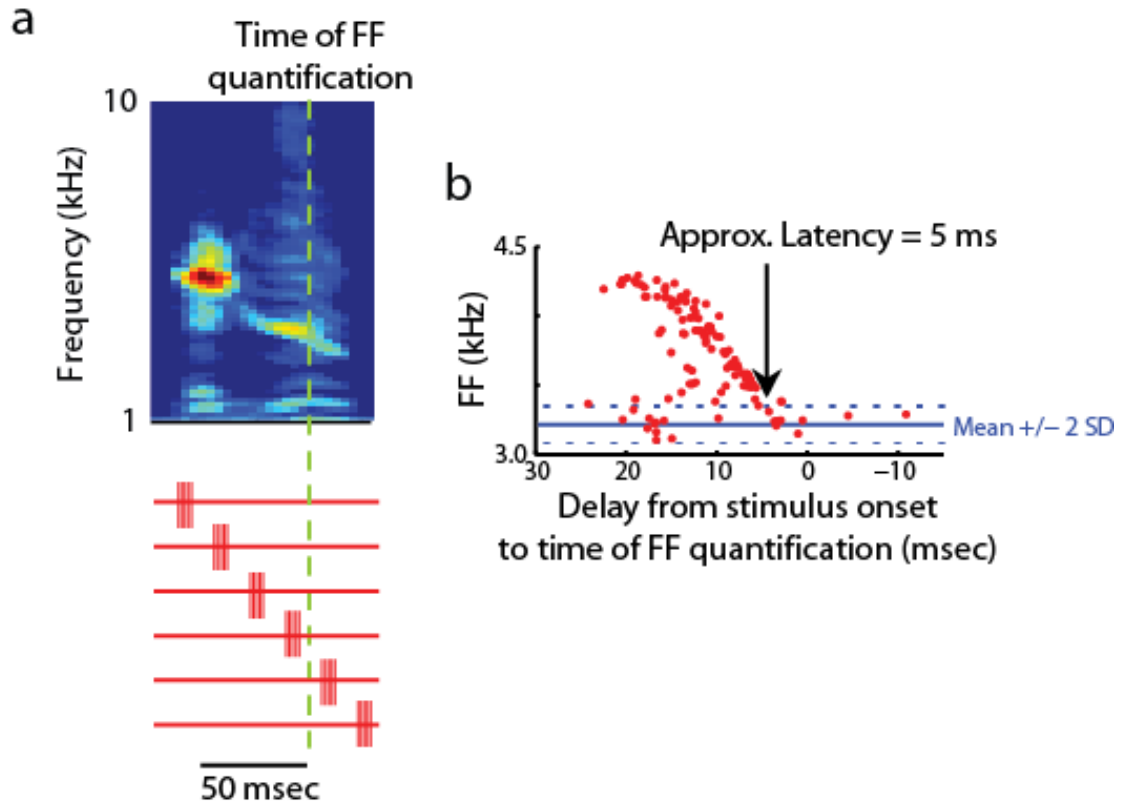
Figure 5: Measuring the latency of muscle stimulation effects. (a) The timing of stimulation was varied relative to the time of fundamental frequency (FF) quantification (green dashed line). The red traces schematize six different stimulation times relative to the syllable. (b) Across all experiments, the minimum latency for detected acoustic effects was 5 ms. Acoustic effects measured later than this latency were similar in direction but could be larger in magnitude. In all stimulation analysis, acoustic effects were measured between 5 ms and up to 30 ms after stimulation onset, depending on the number of datapoints available (see Methods).

To avoid the possibility of neural reflex loops affecting our results, we determined the minimum delay after stimulation onset at which the acoustic effects of stimulation could be observed. Because of timing variability in template recognition and natural variability in the song, the timing of stimulation fluctuated relative to the time of acoustic measurement (Figure 5). As a result, we were able to analyze the effect of stimulation timing on acoustics. We were able to observe acoustic effects as early as 5 ms after stimulation Figure 5b), which corresponds well to maximum force generation at 4-5 ms

26

in isolated zebra finch vocal muscle fibers [53]. At longer latencies, the absolute magnitude of acoustic effects could increase, but remained the same sign in all cases. Acoustic effects for stimulation experiments were grouped by the delay between the time of stimulation and the time of acoustic measurements. To minimize the risk of capturing reflex effects, we used data in the range of a 5-20 ms delay. In one of the eleven stimulation experiments, there were not enough data points in this range, so we expanded the range up to 5-30 ms. This range is still smaller than the latency of a reflex loop estimated to be between 35 ms and 70 ms in a songbird study of somatosensory reflexes in the abdominal expiratory muscle group [71]. Furthermore, our analysis window falls below the delay for auditory feedback to influence vocal motor output, which based on prior studies we estimate to be at least 40 ms [12, 116]. Therefore, analyses like the one shown in Figure 5b were used to make sure that acoustic effects at longer latencies were not different in sign from those at a shorter latency. All stimulation trials that took place within the appropriate delay interval were compared to the catch trials using a t-test on all three acoustic parameters. Finally, to determine whether stimulation effects were fixed for a given acoustic parameter, the fraction of stimulation experiments for a given muscle that elicited a significant increase in a given acoustic parameter as opposed to a decrease were tested against a binomial distribution with a probability of 0.5. Finding significance in this test indicated whether the effect distribution was significantly different from a 50/50 chance of getting an increase or decrease in that acoustic parameter.

In contrast to muscles in the syrinx, stimulation of EXP did not evoke measureable effects on vocal output. We believe that this was the case because the magnitude of stimulation necessary to measurably perturb vocal output would have

27

caused significant discomfort to our subjects. Current amplitudes as high as 1 mA applied to EXP did not produce detectable changes in song output. However, at this current level, birds often truncated their song bouts even after repeated exposure to stimulation, a potential indication of discomfort. We consequently did not increase stimulation currents higher than 1mA. Therefore, we were unable to assess whether EXP might drive modulations in multiple acoustic parameters using *in vivo* stimulation.

### 4.3.4  *Ex vivo* syrinx
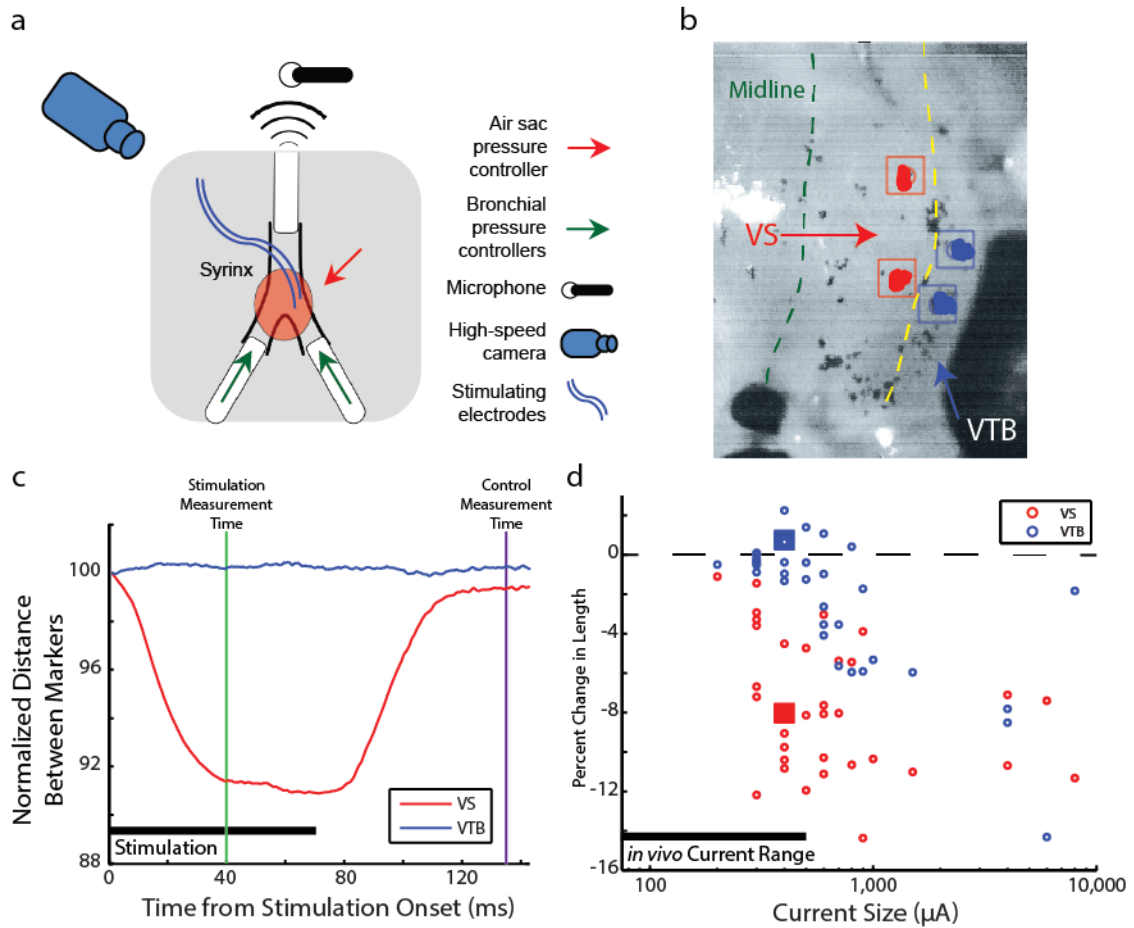


Figure 6: Image analysis of ex vivo muscle perturbation suggests stimulation currents used in the in vivo experiments specifically shortened targeted muscle. (a) Schematic of experimental setup (see Methods). (b) Markers were selected on the first image of an *ex vivo* stimulation run. (c) The distances between selected markers were tracked over the course of the video. Strain (change on y-axis label) is shown for a stimulation current of 400 μA for syringeal muscles VS (red) and VTB (blue). (d) Percent change in length

during stimulation is plotted against the magnitude of the stimulating current. Data points from example in (c) are shown as squares. While VS (red) showed significant contraction at low currents (t(16) = 7.8, p < 0.01, two-tailed, paired t-test), VTB (blue) did not begin to significantly contract until the current size reaches 600 µA (t(16) = 0.51, p = 0.62, two-tailed, paired t-test).

We developed an *ex vivo* assay (Figure 6a) to quantify 1) the muscle recruitment specificity as a function of currents used in the *in vivo* stimulation paradigm and 2) the resulting acoustic effects of targeted stimulation. We will briefly describe the setup here, while a more detailed description can be found in [72].

### 4.3.4.1 Experimental setup

Animals were euthanized with isoflurane, and then the syrinx and associated blood vessels were removed from the animal. The syrinx was then moved to a covered petri dish (Sylgard, Dow Corning, Midland, MI, USA), which sat on ice and contained oxygenated Ringer solution. The bronchi and trachea were connected to tubing (Instech Solomon, PA, USA) in the chamber with 10-0 nylon suture (S&T, Neuhausen, Switzerland). The syrinx was then perfused through its vasculature using oxygenated Ringer solution. The syrinx was mounted in the chamber (Figure 6a) with the ventral side up for VS experiments and the dorsal side up for DTB experiments. This chamber was covered by an airtight glass lid that allowed pressurization and visualization of the syrinx. Bronchial and chamber pressures were controlled separately via dual valve differential pressure PID controllers (model PCD, 0-10 kPa, Alicat Scientific, AZ, USA), referenced to atmospheric pressure. Imaging of the syrinx was performed with a high-speed camera (MotionPro-X4, 12 bit CMOS sensor, IDT, Coralville, IA) mounted on a stereomicroscope (M165-FC, Leica Microsystems, Buffalo Grove, IL, USA). During experiments, a 1/4 inch microphone (model 4939 with preamplifier 2669, Bruel & Kjær, Denmark) was placed 4 cm from the trachea to record sound, which was then bandpass filtered (20 Hz − 22.4 kHz) and amplified (Nexus 2690-OS2, Bruel & Kjær, Denmark).

The acoustic, camera trigger, and muscle stimulator trigger signals were digitized at 50 kHz (USB 6259, 16 bit, National Instruments). All control and analysis software was written in Labview (National Instruments) or MATLAB.

### 4.3.4.2 Muscle recruitment specificity

We perturbed VS and DTB *ex vivo* using electrical stimulation to ensure that the currents used during *in vivo* stimulation specifically recruited the targeted muscle. We used the same electrode design and placement as those used *in vivo*. We used length change of muscle fibers to assess specificity of muscle recruitment. Fiber length was quantified *ex vivo* by placing spherical carbon beads of 40-200 μm diameter onto muscle fibers. Carbon beads are light, adhere well, provide stark visual contrast, and precisely follow length changes of muscle fibers [117]. The position of the carbon beads was determined using an automated autocorrelation function adapted from Elemans et al. (2011), which then tracked the position of the bead frame-by-frame throughout the video (Figure 6b). On both the stimulated muscle and the neighboring muscle, we selected and tracked the distance between two spots to measure muscle contraction during the stimulation. The neighboring muscles for VS and DTB were *m. tracheobronchialis ventralis* (VTB) and *m. syringealis dorsalis lateralis* (LDS) [54]), respectively. Muscle length was low-pass filtered with a cutoff of 50 Hz to remove the effects of labial oscillation. We calculated muscle shortening during stimulation as Lagrangian strain, i.e. the percent difference between muscle length at 40 ms after stimulation onset and at 135 ms after stimulation onset:

$$\varepsilon = \frac{L_{40\,ms}}{L_{135\,ms}} * 100\%$$

where $\varepsilon$ is the percent strain, $L_{40\ ms}$ is the length at 40 ms and $L_{135\ ms}$ is the length at 135 ms. The value 40 ms was chosen because it reflected the full amount of contraction whereas 135 ms was selected because contraction had already returned to baseline for tens of milliseconds (Figure 6c). We selected a time after stimulation as opposed to before stimulation because the high-speed camera was triggered at stimulation onset. The strain was then plotted over several trials at currents ranging from 200 µA to 8 mA (note that all current amplitudes used *in vivo* were less than 1 mA). To test muscle recruitment specificity, we compared muscle length changes for the neighboring muscles (VTB and LDS) relative to the targeted muscles (VS and DTB, respectively). We used a t-test to determine if any length changes of the stimulated and/or neighboring muscles were significant.

### 4.3.4.3 *Ex vivo* acoustic effects

The acoustic effects of muscle activation *ex vivo* were quantified in a manner similar to that used *in vivo*. Acoustic parameters were quantified (see above) 30 ms after stimulation onset. This delay was slightly larger than the one used *in vivo* because the temperature of the syrinx was lower in the *ex vivo* assay (~ 26 °C) compared to *in vivo* (41 °C) and thus muscle fiber shortening took slightly longer [118]. The parameters measured here were compared to the parameters measured 20 ms before stimulation onset. Changes in amplitude and spectral entropy were measured as the difference between stimulation and control values. To allow us to combine data from different *ex vivo* preparations (where baseline fundamental frequency varied somewhat across specimens), each iteration's fundamental frequency (in Hz) was converted to the fractional change from the control fundamental frequency (in cents) as defined below:

$$\Delta FF = 1200 \log_2 \frac{h_s}{h_c},$$

where $\Delta FF$ is the change in fundamental frequency in cents, $h_s$ is the fundamental frequency 30 ms after stimulation onset in Hz, and $h_c$ is the control (unstimulated) fundamental frequency in Hz. A shift of 100 cents corresponds to one semitone (approximately a 6% change in fundamental frequency). Shifts in all three parameters were then regressed against current size for current levels up to 1,000 µA using linear regression.

## 4.4     Results

### 4.4.1   Vocal muscles control multiple acoustic parameters

To examine the relationship between the effects of vocal muscle activity and vocal behavior, we implanted EMG electrodes into 28 vocal muscles (11 VS, 8 DTB, and 9 EXP) in 20 adult male Bengalese finches. Following electrode implantation, we assessed any postsurgical changes in the acoustic structure of song by visually assessing spectrographic representations of vocal output. If surgery resulted in gross changes in acoustic structure such that pre-surgery song syllables could not be discerned following implantation, the resulting data were excluded from subsequent analysis. Data from two DTB cases and one VS case were excluded for this reason, resulting in 25 total muscles across 17 birds being used for our analysis. In these remaining cases, implantation had minimal effect on vocal acoustics. By calculating linear regressions between EMG and each of three acoustic parameters (fundamental frequency, amplitude, and spectral entropy), we determined how small variations in vocal muscle activity related to changes in acoustics. In these experiments, 78% (87 of 112 muscle-syllable pairs) of all pairs had a significant linear regression between EMG activity and at least one acoustic parameter ($p < 0.05$, linear regression slope significantly different from zero, Figure 7). Here, a

muscle-syllable pair referred to the EMG activity from one muscle associated with one vocal gesture. Therefore, if a bird sang 5 different syllables, while having 2 muscles implanted, it would contribute 10 muscle-syllable pairs to the data set. These results demonstrate that our EMG and acoustic analyses were sufficiently sensitive to detect significant relationships between trial-by-trial variations in muscle activity and vocal behavior.
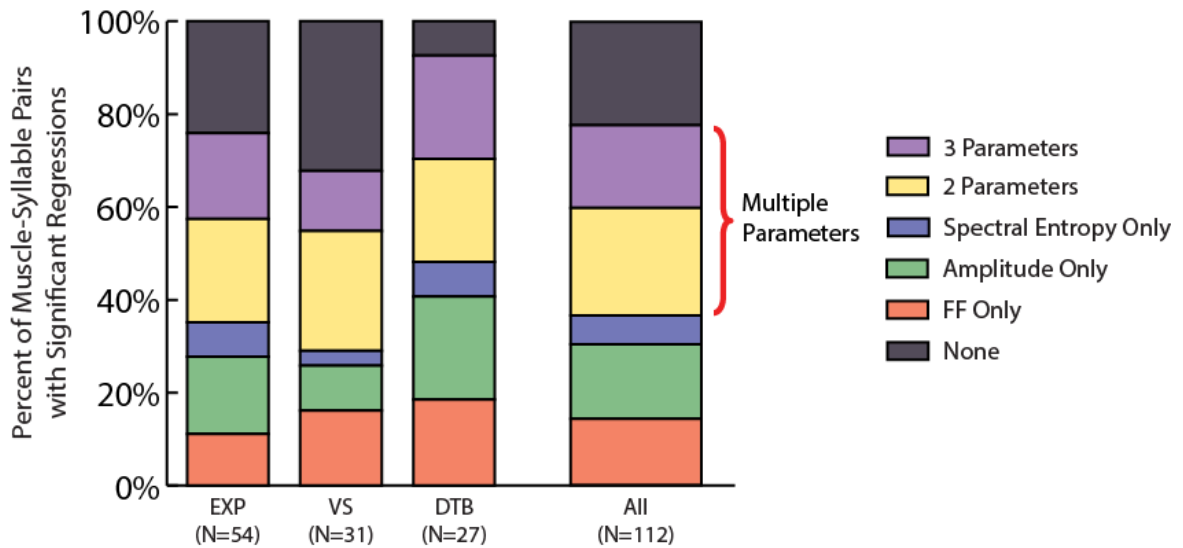


Figure 7: EMG activity had significant regressions with multiple acoustic parameters across vocal muscles. Significant linear regressions were found between EMG activity and multiple acoustic parameters in all muscles recorded. Across all muscle-syllable pairs (N = 112), 78% featured significant regression slopes with at least one acoustic parameter. 53% of those (41% overall) exhibited significant regressions with multiple acoustic parameters.

To investigate whether individual vocal muscles control multiple acoustic parameters, we counted the number of cases in which a muscle had significant regressions with at least two of the measured acoustic parameters. Importantly, 41% of all pairs (53% of pairs with at least one correlation) had significant regressions between EMG activity and at least two of the measured acoustic parameters (Figure 7, purple and yellow regions). There were instances of pairs with multiple significant regressions

across all recorded muscles indicating that this observation was not specific to one of the three selected vocal muscles. Randomly permuting the dataset and recalculating the number of significant regressions revealed that the proportion of significant linear regressions found in our data was significantly greater than chance ($p < 0.001$, permutation test, see Methods). Using the same permutation test, we found that the proportions of significant regression slopes between EMG activity and two, three, and multiple (i.e. two or three) acoustic parameters were also significant ($p < 0.001$ in all cases). Furthermore, although our primary analysis quantified the relationship between vocal acoustics and EMG activity in a 16 ms-wide premotor window (see Methods), calculating EMG activity in a premotor window of 8, 12, or 20 ms width yielded results that were qualitatively identical to those of our primary analysis. These data suggest that individual vocal muscles are capable of modifying multiple acoustic parameters during song.

Because correlations typically exist between different vocal muscles' activity during singing [41, 59], a significant regression between a muscle and an acoustic parameter might have resulted from that muscle's activity having been correlated with the activity of another muscle that drove that parameter. To solve this problem, we developed a targeted stimulation technique (see Methods). This technique allowed us to perturb the activity of a single vocal muscle without altering other muscles' activity (see "*ex vivo syrinx tests stimulation specificity*" below), ensuring any acoustic effect was due to the marginal increase in the targeted muscle's activity. In these experiments, the syllable prior to the syllable of interest was detected using a spectral template (see Methods). Upon matching the template, half of the trials ("catch" trials) resulted in no stimulation (Figure 8a shows a typical example). In the other half of trials, a short train of biphasic current between 75 μA and 500 μA was passed between the EMG electrodes within the

34

implanted muscle (Figure 8b). Figure 8c shows the difference between the catch and stimulated trials' spectrograms, with a distinct upward shift in frequency toward the end of the syllable. Significant acoustic changes, measured in the 5-20 ms following stimulation (see Methods), appeared in all three acoustic parameters (Figure 9a-c) for the syllable shown in Figure 8 when the implanted muscle was stimulated with a current of 75 µA (note that Figure 8 depicts the effects of stimulation at 500 µA to illustrate a larger effect). Across all stimulation experiments, we stimulated using the minimum current capable of evoking detectable acoustic effects (75-500 µA) and found that significant changes ($p < 0.05$, two-tailed, two-sample t-test) were driven in at least two acoustic parameters in 80% of the experiments where VS was stimulated and 100% of the experiments where DTB was stimulated (Figure 9d). Although we cannot be certain that the spread of stimulating current *in vivo* was equal to that *ex vivo* (see Discussion), we believe that the stimulation likely activated nerve fibers within the implanted muscle, which in turn activated associated motor units, but did not activate muscle fibers directly. This notion is supported by a previous *in vitro* study [53], which directly activated isolated syringeal muscle fibers and required current sizes much greater than those used in the present study. The stimulation results suggest that single vocal muscles in the syrinx can drive changes in multiple acoustic parameters, in agreement with the regression-based analysis described above.
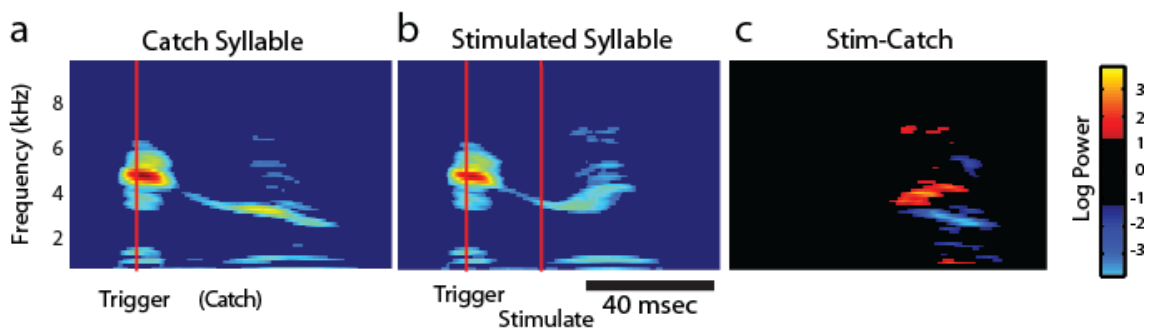


Figure 8: Targeted vocal muscle activation drives short-latency acoustic effects. (a) In a catch trial, online acoustic analysis (see Methods) detected the initial part of the syllable (red line), but no stimulation occurred. (b) In a stimulated trial (using a 500 µA current), the muscle is perturbed 20 ms after detection (first red line indicates detection time while

the second red line indicates the onset of stimulation). (c) The difference in spectrograms shows an increase in fundamental frequency. All plots show the mean spectrogram over all trials.
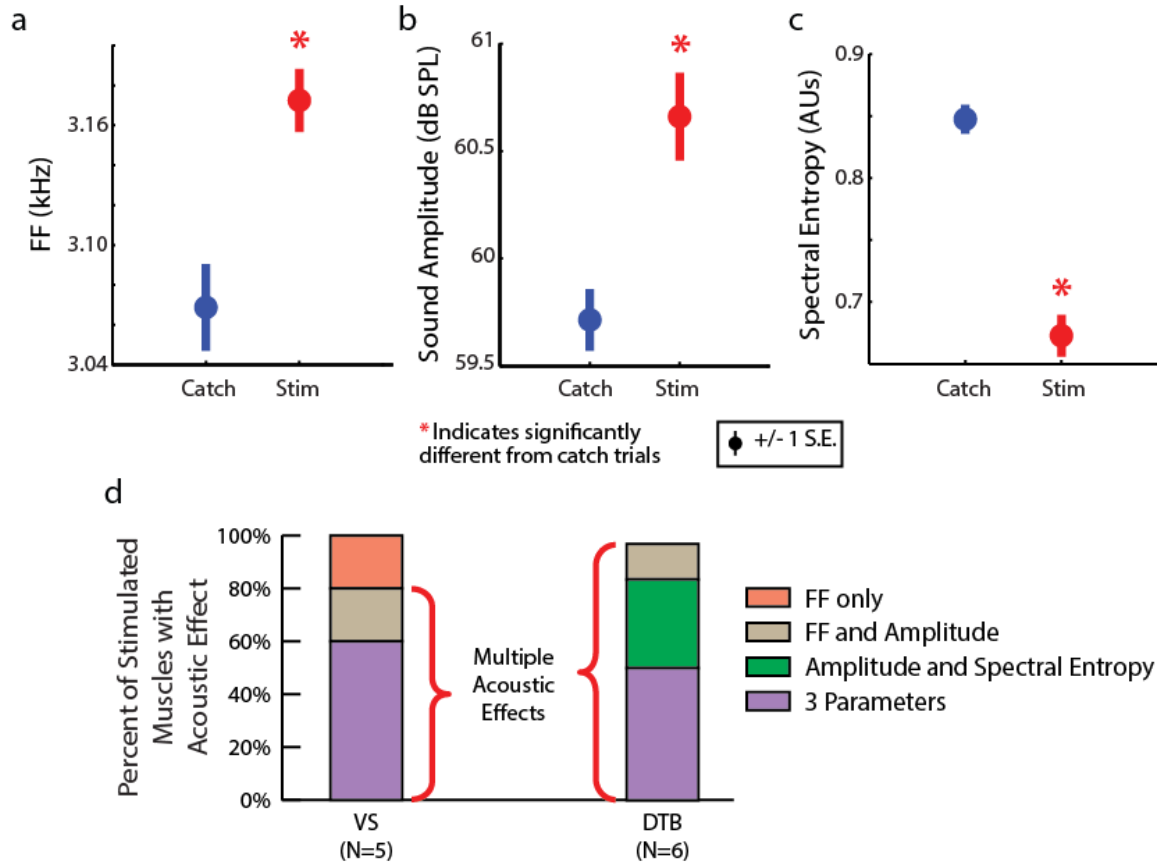


Figure 9: Targeted muscle stimulation drives significant changes in multiple acoustic parameters in singing birds. In the syllable and muscle shown in Figure 8b, a stimulating current of 75 µA caused (a) fundamental frequency (FF) to significantly increase (t(230) = 3.5, p < 0.01, two-tailed, two-sample t-test), (b) sound amplitude to significantly increase (t(230) = 3.9, p < 0.01, two-tailed, two-sample t-test), and (c) spectral entropy to significantly decrease (t(230) = 8.8, p < 0.01, two-tailed, two-sample t-test). (d) Perturbation of VS altered multiple acoustic parameters in 80% of cases (N = 5), while perturbation of DTB did so in 100% of cases (N = 6).

### 4.4.2 *Ex vivo* syrinx tests stimulation specificity

Because we wanted to test the effects of stimulation on individual muscles in our *in vivo* experiments, we needed to ensure that the stimulating current only caused contraction in the targeted muscle. The *ex vivo* syrinx assay (see Methods) allowed us to directly

visualize the effects of electrical stimulation and assess whether the stimulation parameters used in our *in vivo* studies produced muscle contractions that were restricted to the implanted muscles. Figure 6b-c show a trial where VS was stimulated with a current of 400 µA. While the length of VS changed appreciably ($t(16) = 7.8$, $p < 0.01$, two-tailed, paired t-test), the neighboring muscle VTB showed no significant changes in length (Figure 6c). Across all trials (Figure 6d), the change in length of VTB was not significantly different from zero for currents of 500 µA or smaller ($t(16) = 0.51$, $p = 0.62$, two-tailed, paired t-test). This finding suggests that 500 µA was an appropriate maximum current for *in vivo* perturbations of VS. This approach was also used to compare changes in muscle length for DTB with the neighboring lateral dorsal syringeal (LDS) muscle [54]. Similarly, changes in length of LDS were not found to be significant for currents of 600 µA or smaller ($t(10) = 1.5$, $p = 0.92$, two-tailed, paired t-test), while stimulation drove significant changes in the length of DTB ($t(10) = 5.5$, $p < 0.01$, two-tailed, paired t-test). This suggests that 600 µA is an appropriate maximum current for *in vivo* perturbations of DTB. Therefore, although the *in vivo* and *ex vivo* conditions differed in some respects (including electrode implant duration, temperature, etc.; see Discussion), these analyses suggest that the stimulation current amplitudes used in our *in vivo* experiments were sufficiently small so as not to evoke contraction in non-implanted muscles.

### 4.4.3 Stimulation of single muscles *ex vivo* drives changes in multiple acoustic parameters

Additionally, we compared the acoustic effects of VS perturbation *ex vivo* to those found *in vivo*. This was an important experiment because the *ex vivo* paradigm allowed us to eliminate the descending neural control and feedback loops which could affect the observed acoustic effects *in vivo*. While the *ex vivo* syrinx produced sound, VS was perturbed using the same stimulation parameters from the *in vivo* experiments (Figure

10a). *Ex vivo* activation of VS showed a positive relationship between current size and fundamental frequency (p < 0.001, linear regression) and a negative relationship between current size and amplitude (p < 0.001, linear regression) (Figure 10b). These results were similar to those of our *in vivo* stimulation experiments, in which activation of vocal muscles drove changes in multiple acoustic parameters. There was no significant relationship between current size and spectral entropy.
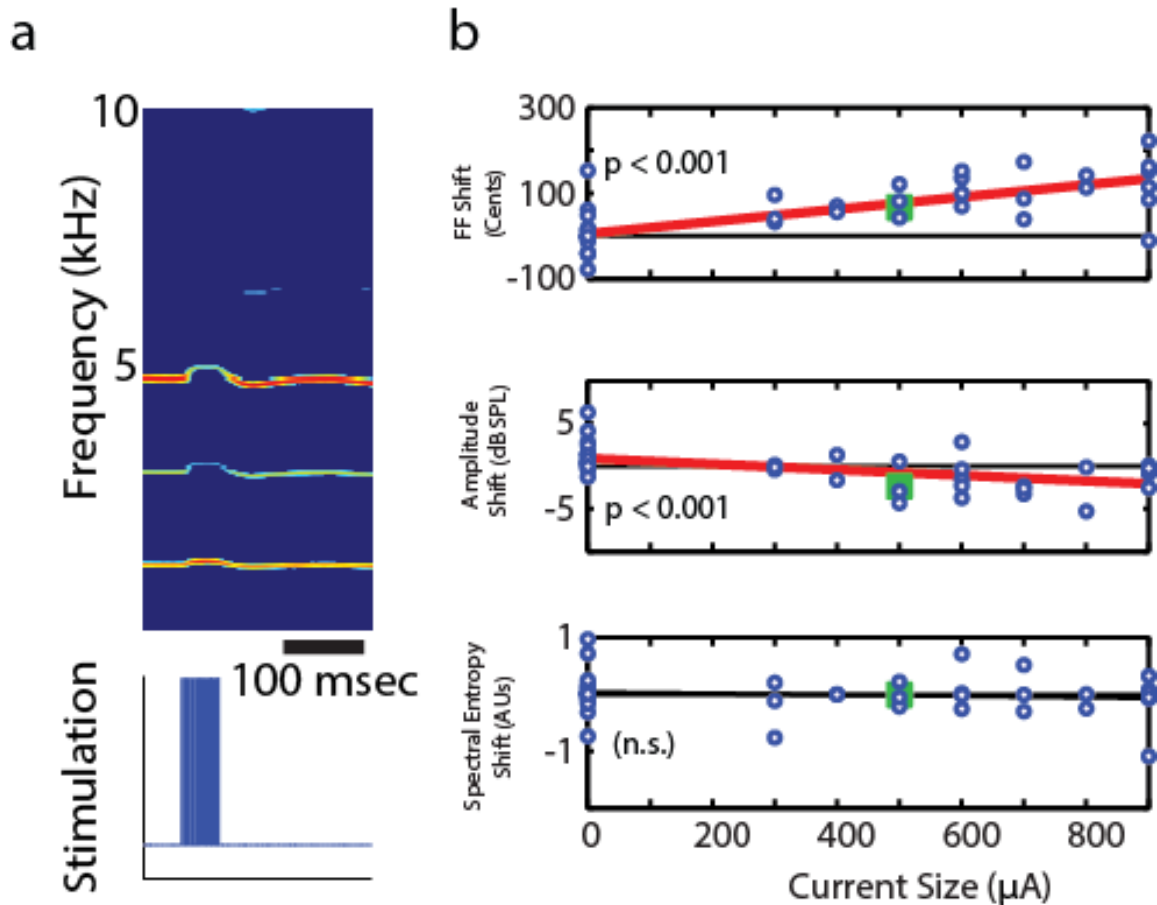


Figure 10: Ex vivo activation of VS demonstrates changes in multiple acoustic parameters. (a) Sound generated by an *ex vivo* syrinx displayed an upward shift in fundamental frequency (FF) when stimulation is delivered within VS. (b) Across all *ex vivo* trials activating VS, there was a significant increase in fundamental frequency and a significant decrease in amplitude, both of which varied with current size (p < 0.001, linear regression). The trial depicted in (a) was marked by an enlarged, green square for each parameter.

#### 4.4.4  Vocal muscles can have context-dependent effects on acoustic parameters
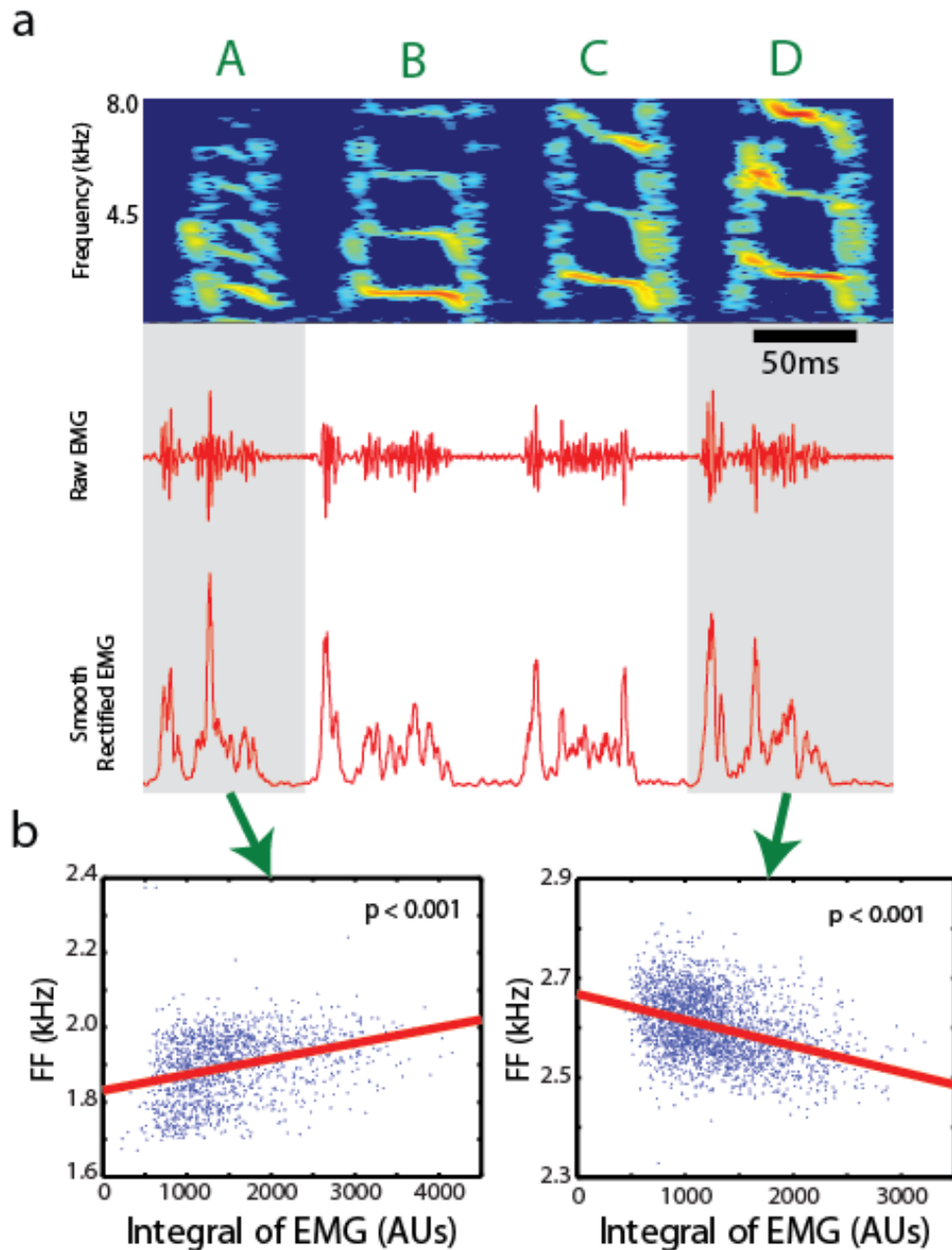


Figure 11: The sign of the correlation between single vocal muscles and acoustic parameters can vary depending on the syllable. (a) EMG activity in EXP was recorded during song (plotting conventions as in Figure 4a-c). (b) In syllable A, the linear regression between EMG activity and fundamental frequency (FF) had a positive slope, while in syllable D, the regression had a negative slope ($p < 0.001$, linear regression).

In addition to testing whether vocal muscles could control multiple acoustic parameters, we asked whether the transformation from vocal muscle activity to vocal behavior was

constant across different vocal gestures or changed depending on the gesture being produced. First, we investigated whether the sign of the regression slope between the activity of a single muscle and a given acoustic parameter changed across syllables within the same bird. While detecting cases with positive and negative regression slopes is a very simple analysis and might fail to capture more subtle context-dependent differences in muscle function, finding that a given muscle increased fundamental frequency during one syllable but decreased it during another syllable, for example, would provide unambiguous evidence of context-dependency. Figure 11a shows a recording of EXP in one individual during song. During syllable A, EMG activity had a positive relationship with fundamental frequency ($p < 0.001$, linear regression), while EMG activity had a negative relationship with fundamental frequency ($p < 0.001$, linear regression) during syllable D (Figure 11b). Across all muscles recorded from birds that produced more than one syllable with quantifiable acoustic structure, 50% (10 out of 20) of those muscles exhibited context-dependency for at least one acoustic parameter (i.e. had at least one syllable with a significant, positive linear regression slope and at least one with a significant, negative linear regression slope). Second, we tested this hypothesis by examining the variation in stimulation effects within the same muscle. In the syllable of one individual, VS stimulation caused amplitude to significantly decrease ($t(1537) = 16.2$, $p < 0.01$, two-tailed, two-sample t-test), while in another individual's syllable, perturbation of VS caused amplitude to significantly increase ($t(511) = 2.8$, $p < 0.01$, two-tailed, two-sample t-test, Figure 12a-d). Similarly, DTB perturbation caused a significant decrease in fundamental frequency ($t(108) = 3.5$, $p < 0.01$, two-tailed, two-sample t-test), while the same DTB stimulation during a syllable in another bird caused a significant increase in fundamental frequency ($t(109) = 4.3$, $p < 0.01$, two-tailed, two-sample t-test, Figure 12e-h). In one case, we were able to stimulate DTB during three different syllables in the same bird. While stimulation significantly increased entropy in two cases, it significantly decreased that parameter in the third case. Together, the results

40

from EMG recording and stimulation data suggest that single vocal muscles can have context-dependent effects on acoustic parameters.
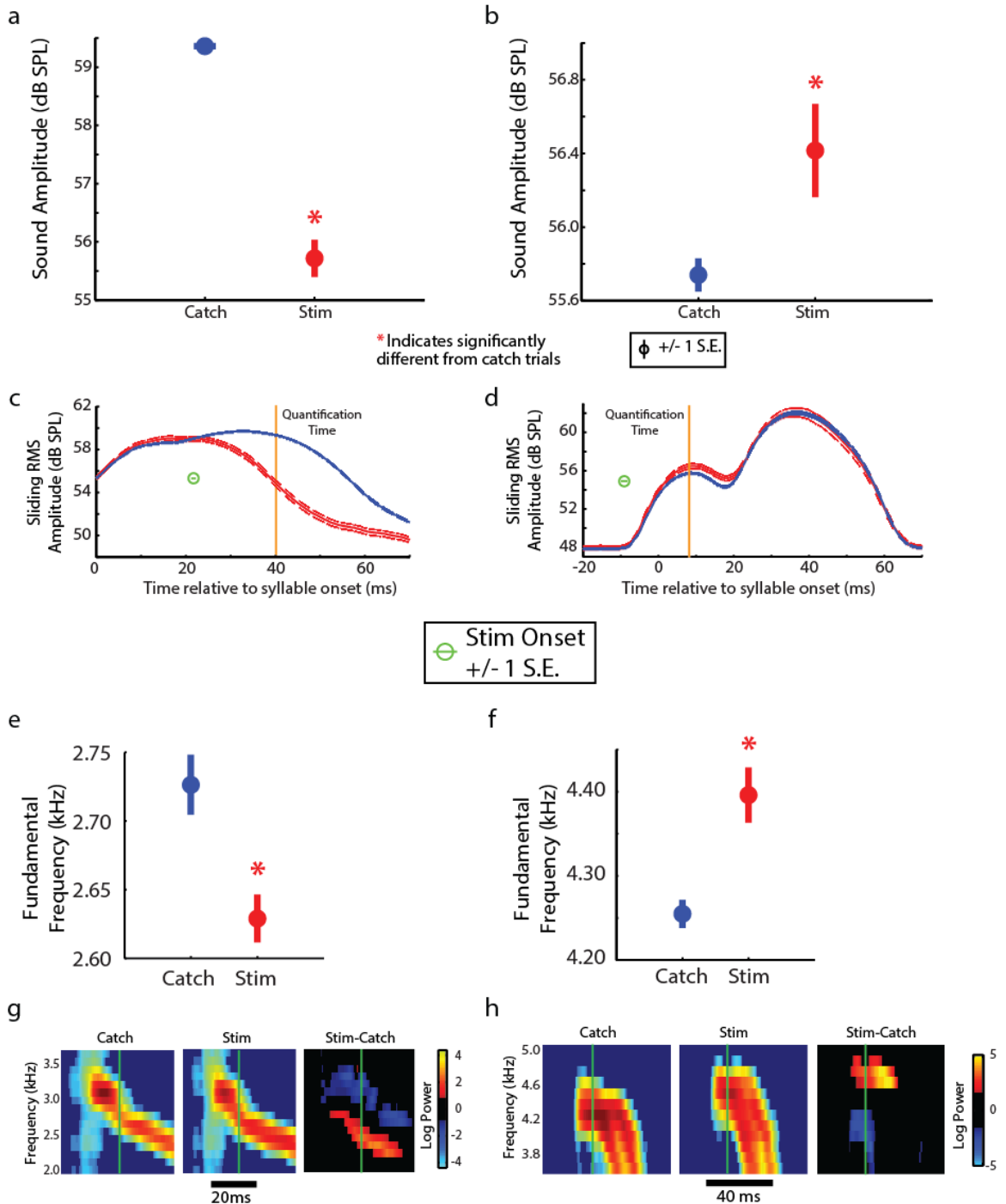


Figure 12: Vocal muscle activation drives opposite acoustic effects during different syllables. (a) In one syllable, VS stimulation (500 µA) caused a significant decrease in amplitude (t(1537) = 16.2, p < 0.01, two-tailed, two-sample t-test), while (b) perturbation (500 µA) during another syllable caused a significant increase in amplitude (t(511) = 2.8,

41

p < 0.01, two-tailed, two-sample t-test). Their respective sliding RMS amplitudes showed a visible decrease (c) and increase (d) in amplitude. Dashed lines indicate mean amplitude trace plus/minus one standard error. Orange lines indicate where sound amplitudes were quantified for (c) and (d). (e) In a third syllable, DTB perturbation (500 µA) caused a significant decrease in fundamental frequency (FF) ($t(108) = 3.5$, $p < 0.01$, two-tailed, two-sample t-test), while (f) perturbation (500 µA) during another syllable caused a significant increase in fundamental frequency ($t(109) = 4.3$, $p < 0.01$, two-tailed, two-sample t-test). Their respective spectrograms showed the difference after stimulation (red bands in Stim-Catch spectrograms) with the first syllable (g) showing a decrease in fundamental frequency, and the second syllable (h) showing an increase in fundamental frequency. Green lines indicate where fundamental frequencies were quantified for (e) and (f). Note that each syllable was from a different bird.

### 4.4.5 Transformation from vocal muscle activation to vocal behavior is fixed for some acoustic parameters and context-dependent for others.

Despite the presence of context-dependency in some cases, we asked whether there were any transformations that did not vary across syllables. While a vocal muscle might exert a context-dependent effect on one acoustic parameter, that muscle might have an effect on another parameter that is constant across vocal gestures. Across all stimulation experiments, VS perturbation always significantly increased fundamental frequency, but the stimulation could either increase, decrease, or have no effect on amplitude and spectral entropy (Figure 13a). The relationship with fundamental frequency was found to be significantly different than an even distribution between increases and decreases ($p = 0.031$, binomial test). DTB perturbation always significantly decreased amplitude, but the stimulation could either increase, decrease, or have no effect on fundamental frequency and spectral entropy (Figure 13b). This relationship was found to be significantly different than an even distribution ($p = 0.016$, binomial test). These results suggest that a given muscle's activity can have a fixed relationship with one acoustic parameter (e.g. VS and fundamental frequency), while having a context-dependent relationship with other parameters.
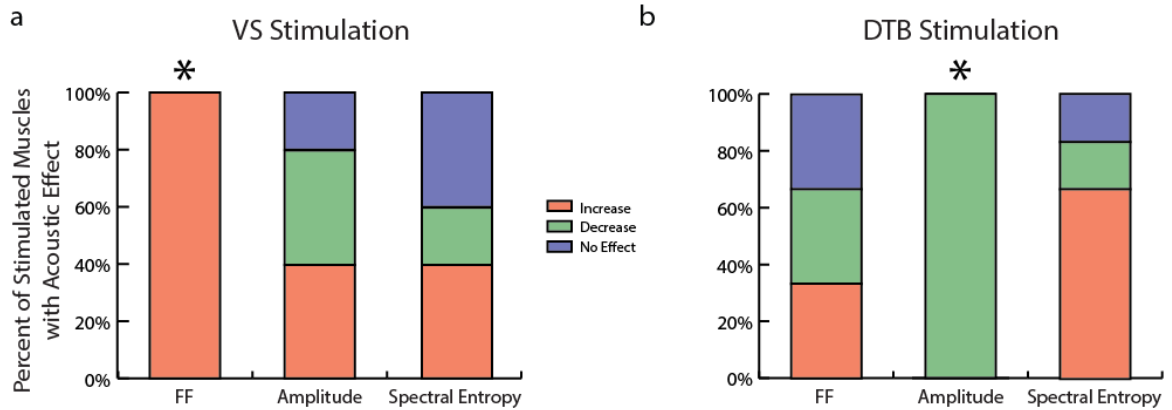
Figure 13: Vocal muscle perturbation effects are fixed for some acoustic parameters and context-dependent for others. (a) Across all VS perturbations, fundamental frequency (FF) always increased with stimulation (p = 0.031, binomial test, N = 5), but amplitude and spectral entropy effects varied by syllable. (b) Across all DTB perturbations, amplitude always decreased with stimulation (p = 0.016, binomial test, N = 6), while fundamental frequency and spectral entropy effects varied by syllable.

## 4.5    Discussion

We investigated whether individual vocal muscles can control multiple acoustic parameters during song. We found that 41% of muscle-syllable pairs had significant regressions between EMG activity and more than one acoustic parameter (Figure 7). Furthermore, *in vivo* stimulation showed that 90% of vocal muscle perturbations drove effects in multiple acoustic parameters (Figure 9d). *Ex vivo* perturbation of single muscles drove significant acoustic effects in both amplitude and fundamental frequency (Figure 10b). These results suggest that although songbirds can modulate single acoustic parameters independently [115], individual vocal muscles drive changes in multiple parameters.

We also asked whether the relationship between muscle activity and an acoustic parameter depended on the vocal gesture being produced. Our regression analysis showed that 50% of recorded muscles displayed context-dependency with at least one acoustic parameter (Figure 11). Furthermore, *in vivo* stimulation experiments suggested that the

43

acoustic effects of muscle perturbation varied by syllable (Figure 12). Interestingly, despite the prevalence of context-dependency, individual muscles drove constant-signed effects in some acoustic parameters. VS stimulation always increased fundamental frequency, and DTB stimulation decreased amplitude in every case (Figure 13). Although such constant-signed effects are consistent with prior models of syringeal function [41, 53], our results suggest the transformation from muscle activity to vocal behavior can be context-dependent for some parameters and fixed for others.

### 4.5.1   Isolating the functional role of single vocal muscles

Our finding that individual muscles affect a range of acoustic parameters constrains the functional architecture of neural control. A selective modification of fundamental frequency would require the modulation of muscles that also control other acoustic parameters, demanding extensive coordination across muscles (and the neurons that control them) to avoid unwanted acoustic changes. The activity of multiple muscles could be coordinated in fixed proportions using a single neural control signal through a muscle synergy [119], in which fewer control signals are needed than vocal muscles. While synergies have been studied in other behaviors [120-122], the computational technique has yet to be applied to EMG activity in vocal control and may further inform how the brain regulates vocal output.

To our knowledge, this study is the first to illustrate the effects of small variations in EMG activity during the production of individual song syllables. Previous studies have investigated the relationship between EMG activity and vocal output by combining data across many vocal gestures [41, 59]. While that transformation appears complex and highly nonlinear, investigating smaller variations across renditions of the same syllable

allows us to examine the marginal effects of single vocal muscles in shaping particular gestures.

This study implements online perturbation of vocal muscles via electrical stimulation to drive short-latency acoustic effects. The most obvious advantage to this approach is the elimination of the effects of correlations between muscles on our analysis. For instance, if a muscle's activity were highly correlated with the activity of another muscle that controlled fundamental frequency, a standard regression analysis would suggest that both muscles control fundamental frequency, when that may not be the case. Comparing stimulation to catch trials allows us to investigate the marginal effect of increasing a single vocal muscle's activity while, on average, holding other motor parameters constant. Online stimulation could be used to design more complex experiments investigating how muscles work together by altering the relative timing and amplitude of stimulation across multiple muscles.

As described in Results, although correlation analyses suggested that EXP modulates multiple acoustic parameters, we were unable to confirm this using electrical stimulation. Because the relationship between EXP activity and air sac pressure is poorly understood (see Methods), we must exercise caution when interpreting such correlative data. Significantly, *in vivo* and modeling studies have shown that perturbing pressure can affect both the fundamental frequency and amplitude of vocal output [82, 83], corroborating the results of our regression analysis on EXP activity (Figure 7) and suggesting that EXP activity might modulate multiple parameters. Therefore, although future work will be necessary to establish the effects of EXP perturbation *in vivo*, EXP might, via its effect on air sac pressure, affect multiple acoustic parameters.

Additionally, we used an *ex vivo* paradigm to visualize the consequences of electrical muscle stimulation and determine a range of current amplitudes that would restrict stimulation to a single muscle. Although we aimed to match the conditions of *ex vivo* and *in vivo* stimulation (electrode type and placement, current amplitude/duration, etc.) as closely as possible, potential differences between these conditions limit our ability to exactly duplicate *ex vivo* the stimulation parameters used *in vivo*. First, as the muscle reacts to the implanted electrode over time *in vivo*, electrode impedance will likely increase, whereas changes in electrode impedance are presumably less prevalent over the short time course of acute *ex vivo* experiments. The potentially greater impedance *in vivo* suggests that a smaller volume of tissue would be activated (i.e. greater muscle specificity) than that observed *ex vivo*. Second, our *ex vivo* tests were performed at room temperature rather than at body temperature, potentially altering the spread of current and reducing the efficacy of axonal activation, and electrical stimulation itself may have altered muscle temperature. Although it is therefore impossible to be certain whether the same number of motor units were activated in the *in vivo* and *ex vivo* conditions, given that the currents used *in vivo* were far smaller than those which evoked significant recruitment of nearby muscles *ex vivo* we consider it unlikely that accidental recruitment of adjacent muscles significantly influenced our results.

We found significant effects on fundamental frequency and amplitude from *in vivo* and *ex vivo* perturbations of VS. Interestingly, only *in vivo* stimulation produced changes in spectral entropy. One cause for this discrepancy could be the presence of a rigid tube instead of the upper vocal tract in the *ex vivo* assay (Figure 6a). In both songbirds and humans, the upper vocal tract, which includes the trachea, tongue, and beak/jaw, filters the acoustic source and can alter its resonance to accentuate certain

harmonics in the acoustic signal [84, 123]. The amount of filtering to certain harmonics could affect spectral entropy, which measures the noisiness of the spectral content. By substituting a rigid tube for the upper vocal tract, we may have prevented changes in spectral entropy due to stimulation. Additionally, the stimulation-induced changes in spectral entropy observed *in vivo* may reflect a mismatch between the source (the syrinx) and the filter (the upper vocal tract). If perturbing a vocal muscle results in a higher fundamental frequency, the resonance of the upper vocal tract may no longer match what is intended by the bird, possibly resulting in changes in spectral entropy in addition to fundamental frequency. At the very least, the *ex vivo* assay suggests that the technique used for *in vivo* stimulation can specifically perturb individual muscles and confirms that changes in fundamental frequency and sound amplitude are direct results of muscle perturbation rather than results of reflex mechanisms.

### 4.5.2 Vocal muscle function is context-dependent

In many cases, the relationship between vocal muscle activity and individual acoustic parameters depended on the vocal gesture being produced (Figure 11, Figure 12, and Figure 13). Similarly, our prior work has shown that the relationship between spiking activity in single neurons in vocal motor cortex and acoustic output can vary across vocal gestures (as when increases in spiking appear to increase fundamental frequency in one syllable but decrease fundamental frequency in a different syllable [15]). Together, these results suggest that inter-syllable differences in neural tuning in motor cortex reflect the context-dependency of vocal muscle function.

The context-dependency of vocal muscle function could result from nonlinearities in the force-producing properties of the muscles themselves or in the mechanics of the vocal motor system. Force generation is strongly affected by parameters such as muscle length and shortening velocity [124], which will vary across vocal gestures, and by a

muscle's recent history of contraction [125]. For the EXP muscle group, context-dependency might arise because the relationship between EXP activity and air sac pressure depends on the volume in the air sac and syringeal gating of airflow as noted above [114]. A recent study that modeled air sac pressure and labial tension concluded that the relationship between air pressure and frequency can take on different signs depending on where a given syllable is produced in the pressure-tension parameter space [86]. Similarly, in zebra finches, EMG activity in the VS muscle is correlated with frequency at low frequencies but no relationship is observed at higher frequencies [126]. In human vocal studies, stimulation of the thyroarytenoid muscle caused both increases and decreases in fundamental frequency depending on whether the fundamental frequency and intensity of the vocalization were high or low [109], suggesting that context-dependency is a common feature of vocal control in humans and songbirds. Examples of context-dependency can also be found in non-vocal motor systems such as in cockroach locomotion [110] and in mammalian joints [127]. Context-dependency therefore appears to be a general feature of complex motor control across species and systems.

# CHAPTER 5

# CHARACTERIZING FUNCTIONAL PROJECTIONS OF NUCLEUS RA TO THE VOCAL MUSCLES.

The objective of this Aim was to determine whether single premotor neurons control individual or multiple vocal muscles. This aim was not completed because of feasibility issues explained below. However, this aim did yield many important results for the field, particularly for those deciding to undertake a similar study.

## 5.1    Introduction

A gap in knowledge lies in the functional connectivity between RA neurons and vocal muscles (one-to-one vs. one-to-many). The neuroanatomy underlying birdsong production is relatively well-mapped [4, 5]. Premotor nucleus RA controls the activity of vocal muscles via motor neurons in the tracheosyringeal portion of the 12th motor nucleus, or nXIIts (Figure 2). A one-to-one mapping would give single RA neurons better control over individual muscles, but would also require more synaptic connections from upstream nuclei to induce changes in single acoustic parameters. Moreover, given the results of Aim 1, this would force single RA neurons to control multiple acoustic parameters. Alternatively, divergent mapping would reduce an individual RA neuron's ability to tune a single muscle's activity but might allow for simpler implementation of widespread changes to muscular activity for vocalization. In this scenario, a single RA neuron could use a muscle synergy, in which multiple muscles are activated in a fixed proportion by a single control signal [119], such that the effects on all parameters besides one would sum to zero. Therefore, in addition to quantifying how RA neurons control vocal muscles, Aim 2 investigated a physiological basis for muscle synergies, in which neurons control multiple muscles.

Spike-triggered electromyography (stEMG) studies in limb movements indicate single premotor neurons can control multiple muscles [22, 23], but the results from anatomical tracer studies in songbirds are less definitive. One of those songbird studies demonstrated a rough myotopy in nXIIts, but the boundaries between muscle representations overlap [20]. The other study showed a separation in the representation of rostral and caudal nXIIts in RA but does not show enough specificity to make inferences regarding the representation of vocal muscles in RA [21]. While these studies in songbirds suggest some anatomical specificity, it is not clear that the mapping in RA is truly myotopic. Thus, it is important to determine whether the discrepancy is due to a difference in methods or a fundamental difference between limb and vocal motor control.

Simultaneous neural and EMG recording is absolutely necessary in order to make inferences regarding the functional connectivity between RA neurons and vocal muscles. Furthermore, I chose to record from RA as opposed to the downstream nucleus nXIIts because the motor nucleus is known to have simple one-to-one mappings for the motor units associated with the vocal muscles [21]. Therefore, the ability of RA neurons to control single or multiple muscles is dependent on the synaptic connections between RA and nXIIts and not between nXIIts and the vocal muscles. In the song pathway, all information with respect to song production must be fed through nucleus RA to affect the vocalization. Moreover, individual neurons in the upstream nucleus HVC have been shown to burst sparsely (once per song) during song [13], which strongly points to the lower nucleus RA controlling the dynamics of song production and syllable structure.

I hypothesized that individual RA neurons control multiple vocal muscles. To demonstrate this, I simultaneously recorded from RA and multiple vocal muscles, and then employed stEMG to quantify the number of muscles functionally activated by each recorded neuron.

## 5.2    Methods

### 5.2.1    Surgical procedures

Because simultaneous recordings of RA and vocal muscles had never been performed in songbirds in a chronic setting, the experiment was performed in acute head-fixed birds. Preliminary data (Figure 14) demonstrate that vocal muscles are active in a stereotyped and syllable-locked manner when the bird is listening to a recording of its own song. Similarly, previous work has shown that RA neurons in anesthetized birds are active during playback of the bird's own song [128]. Therefore, while playing the bird's own song, multiple RA neurons could be sampled while recording from the vocal muscles. Moreover, the acute setup would allow the use of a bulkier 16 (as opposed to 4) channel electrode array (Neuronexus).
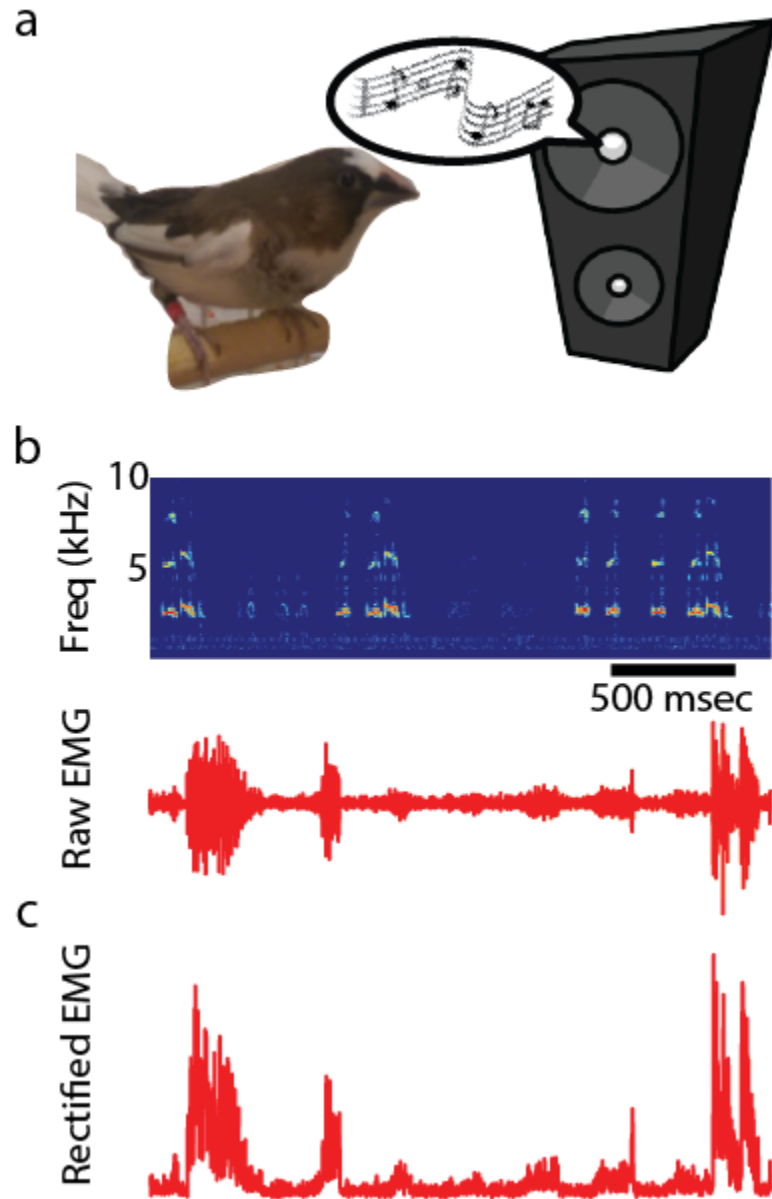
Figure 14: Vocal muscles were active when the bird's own song was played back to the bird. (a) The bird listened to a speaker playing the bird's own song. (b) Spectrogram of the audio played back to the bird with the accompanying raw EMG signal from the left DTB muscle. (c) The smooth rectified EMG showed activity during this playback, and some syllable locked activity seen in the beginning and end of this waveform.

Five Bengalese finches were to initially be used for this study. In previous studies studying anesthetized songbirds neural responses to their own song, the subjects were anesthetized with urethane [128-130]. For that reason, the subjects were anesthetized

with urethane (5 µL/g of 20% urethane in saline) instead of the typical combination of ketamine and midazolam used in the other aims. In additional experiments without urethane, subjects were placed on a reverse light-cycle (light from 7 PM to 9 AM) to help induce sleep during the procedure, with inhaled isoflurane (0-4% in $O_2$) used as supplemental anesthesia during electrode placement, but not during recordings. In a single surgery neural and muscular electrodes were implanted. When the experiment was conducted with zebra finches, the urethane anesthesia was used as above. A 16-channel electrode array (Neuronexus) was stereotactically implanted in RA at approximately 1.0 mm posterior and 2.25 lateral from y-zero (defined as the intersection of 3 arteries in a y-shape along the central sulcus). EMG electrodes were implanted in the left expiratory muscle group, left VS, left DTB, and right VS as in the other Aims.

### 5.2.2 Data collection

While recording from left RA and four vocal muscles (left EXP, left DTB, left VS, and right VS), the bird's own song (BOS) was played back to the bird over computer speakers. This stimulus was interleaved with reversed BOS (REV) and a conspecific song (CON) to control the responses. The actual playback was captured using a microphone (Knowles EM-23046-P16). Signals from RA, the vocal muscles, and the microphone were digitized and amplified at 30 kHz using the Intan RHD 2000 (Intan Technologies, Inc.).

### 5.2.3 Data analysis

To sort spikes in the neural recordings, a custom MATLAB script developed by Sober et al. (2008) was used. Once spike times were isolated, stEMG [18, 19, 131] was performed to determine the functional connectivity between individual RA neurons and motor neurons controlling the vocal muscles. In this technique, the smoothed-rectified EMG signal was aligned to each spike in a recorded RA neuron (Figure 15). This aligned signal was then averaged across every spiking instance from that RA neuron. The significance

threshold was calculated as the mean plus 2 standard deviations (across trials) of the 50 ms of the EMG signal prior to the RA neuron's spike. If the averaged, post-spike EMG signal crossed this threshold for at least 1 ms, the connection between the RA neuron and the specific muscle was determined to be significant as in previous studies [132]. Establishing functional connections showed whether mapping tended to be one-to-one or divergent. Observing functional connections to multiples could serve as the physiological basis of muscle synergies.
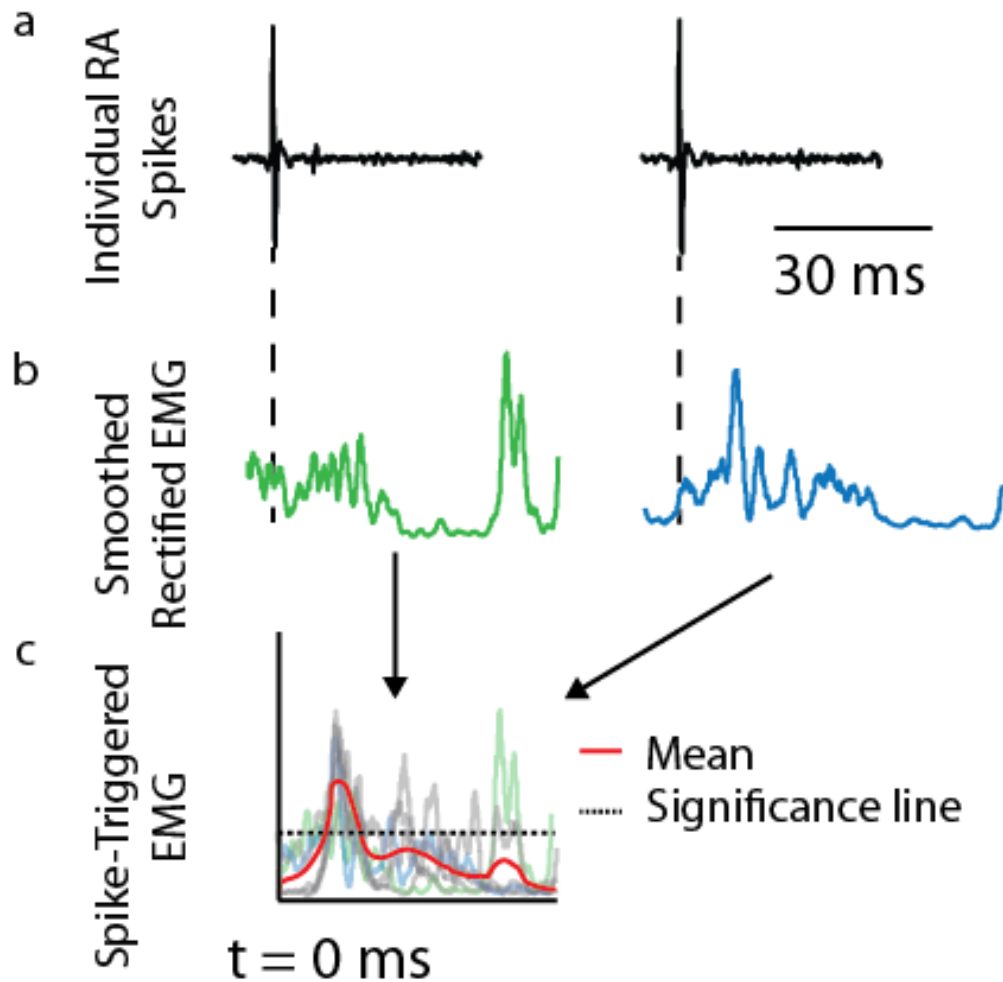


Figure 15: Hypothetical stEMG. (a) RA spikes are found in an extracellular recording during song. (b) The aligned EMG traces are (c) averaged across trials. Additional EMG traces are shown in grey. The red line denotes the average stEMG. The dashed line indicates the threshold for a significant post-spike effect. Note: this figure is hypothetical and not from a simultaneous recording.

## 5.3    Results
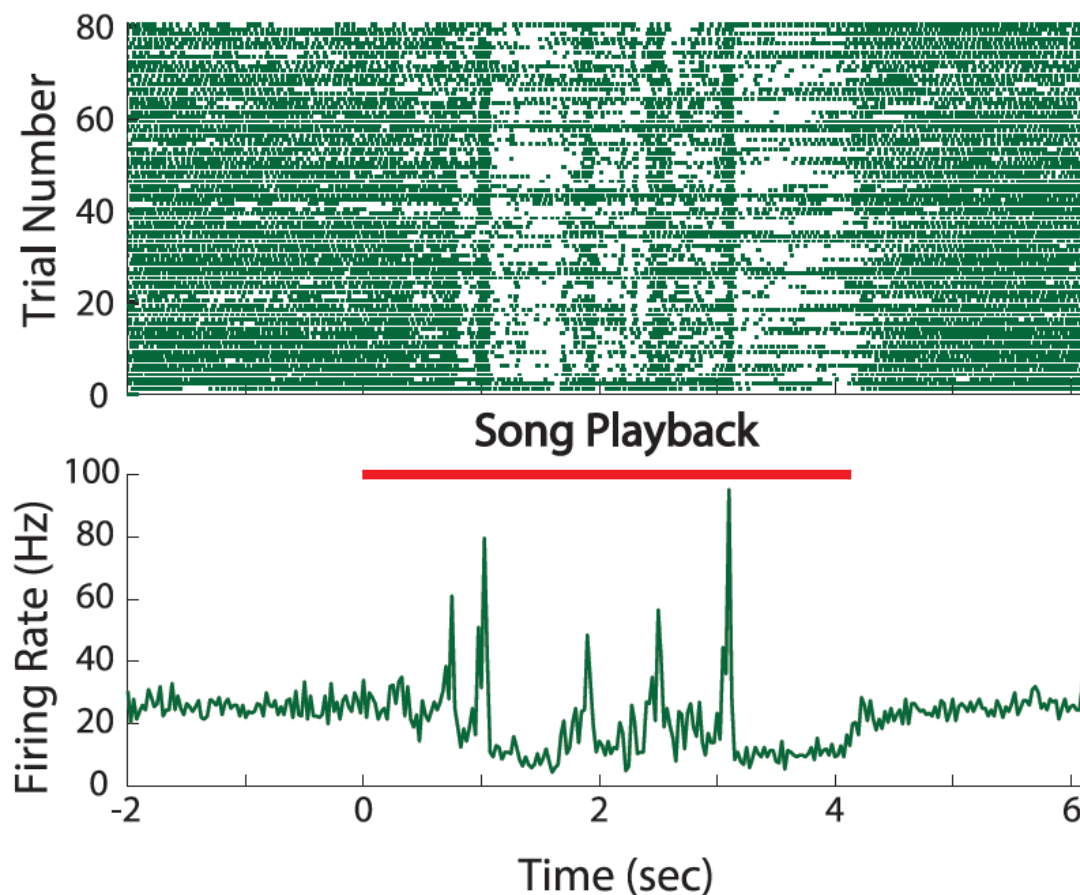


Figure 16: Neural modulation of an RA neuron in response to BOS playback in a sleeping Bengalese finch. The raster plot shows how tonic RA firing became phasic and aligned across trials once BOS playback began. The average firing rate over trials more than doubled at times during BOS playback, but also dropped below the tonic firing rate at times.

Upon recording and analyzing the results from three Bengalese finches, it was found that RA activity was not modulated under urethane, which was critical for this experiment and its analysis. This was in contrast to zebra finches, which were used in many of the previously published songbird studies that successfully modulated neural activity under urethane anesthesia [128-130]. As a result, the experiment was tried again with sleeping Bengalese finches, as another study demonstrated modulation of RA in sleeping zebra finches [133]. This experimental setup yielded RA modulation in response

to BOS playback (Figure 16), but the surgical procedure was difficult to reliably carry out under only inhaled anesthesia, which was transient. Even when the animals were placed on a reverse light-cycle, they did not consistently stay asleep during the experiment. While the aforementioned study looked at neural activity during sleep using chronic recordings in an unrestrained animal [133], I attempted to perform my experiment using an acute recording setup with a restrained animal.

Therefore, the experiment was switched to be performed on five zebra finches under urethane anesthesia, as they allowed me to perform the same experiment with reliable anesthesia that did not eliminate neural modulation during song playbacks. To summarize, Bengalese finches anesthetized with urethane did not produce neural modulation, asleep Bengalese finches did not consistently produce reliable recordings over a long enough time period, and zebra finches anesthetized with urethane allowed for neural modulation and enough recording trials.

In the urethane-anesthetized zebra finch setup, BOS playback drove modulation in both EMG and RA activity (Figure 17), but EMG modulation did not occur throughout the song. Moreover, EMG modulation often preceded neural modulation (red arrows in Figure 17b and d), bringing into question the causality of the transformation of modulation. EMG activity was not modulated on every trial, as was apparent in the fluctuations of individual trials as well as noting the difference in the magnitude of the EMG peaks in the mean versus individual trials (Figure 17b and c). Furthermore, a trial featuring EMG modulation at the same time as observed in the overall mean did not guarantee modulation at all of the time points where modulation was observed in the mean (blue trace in Figure 17c). When stEMG was performed on this dataset, no significant modulation relative to spiking of this specific RA neuron could be found (Figure 18). At this point, it was determined that the potential yield of this experiment was too small to continue (see Discussion).
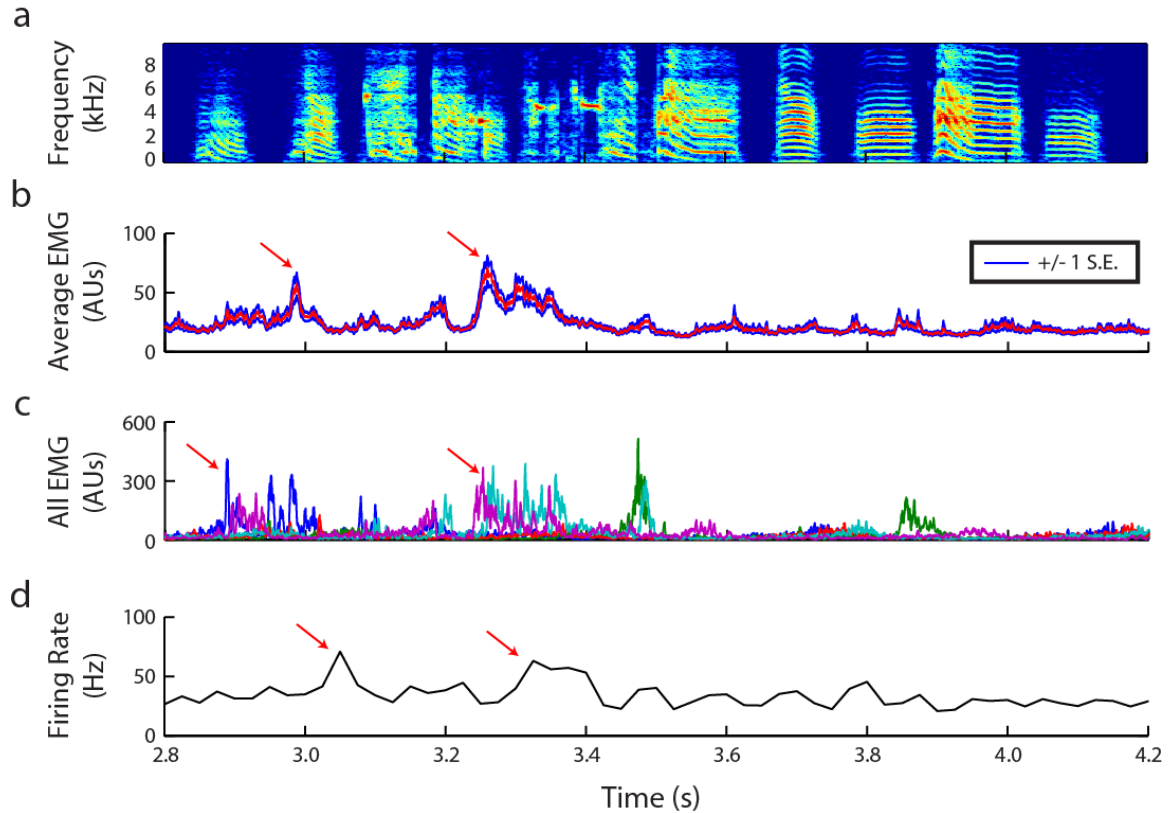
Figure 17: Neural and muscular modulation during BOS playback in a zebra finch anesthetized with urethane. (a) A spectrogram of the BOS recording played back to bird during the experiment. (b) BOS playback induced modulation in the mean EMG of left VS as particularly noted by the red arrows. (c) EMG from 5 of the 102 trials are shown to demonstrate that modulation did not occur in all trials (red trace), and even trials with modulation at one time point observed in the mean did not necessarily have modulation at all time points that are observed in the mean (blue trace). (d) Modulation of the recorded RA neuron was also apparent (red arrows), though they were surprisingly preceded by the EMG modulations.
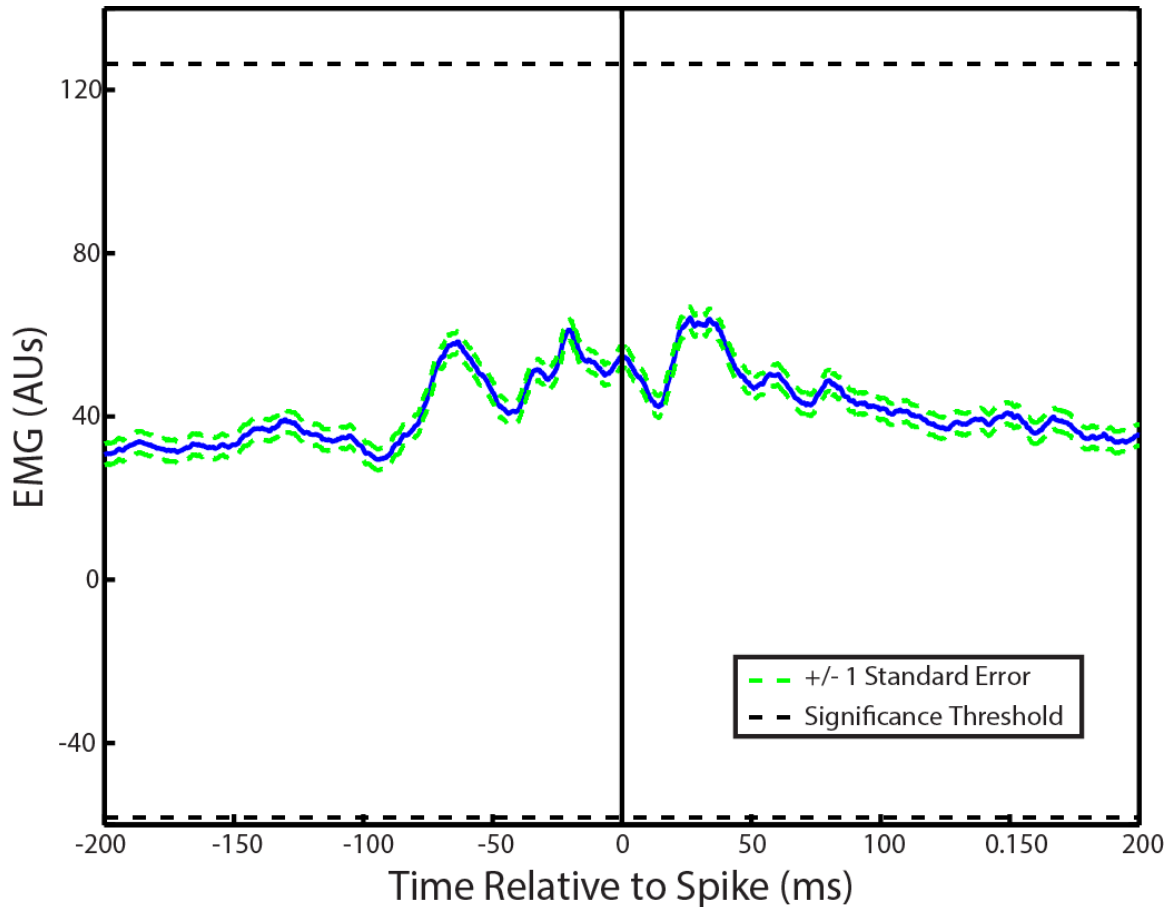
Figure 18: Sample spike-triggered EMG analysis from zebra finch in response to BOS playback. The mean EMG never crossed the significance threshold (two standard deviations above the mean baseline) in the vicinity of neural spiking.

## 5.4   Discussion

Future studies should exercise caution when attempting to drive modulation of neural activity in both Bengalese and zebra finches anesthetized with urethane. While no significant results could be found regarding the functional connectivity between RA and vocal muscles, this Aim did provide many learning points for future studies. First, it was found that RA neurons in Bengalese finches anesthetized with urethane do not modulate their activity in response to BOS playback. Neural modulation is found throughout the song system in zebra finches [128-130], a species closely related to the Bengalese finch. While this study only showed a lack of neural modulation in RA in urethane-anesthetized

Bengalese finches, it is quite likely to be the case in any song system nucleus. A recent study found that both HVC and RA did not increase their activity during song playback in awake zebra finches, but the nuclei did respond to the stimulus when gabazine, a $GABA_A$ antagonist was applied to HVC [134]. Their findings in awake subjects, which contrasted the findings in urethane-anesthetized subjects [128-130], suggest that urethane, also an antagonist for GABAergic transmission, was blocking inhibition in HVC. As we were investigating functional connections between RA and vocal muscles, urethane may have obscured our results by disinhibiting some connections.

The acute approach to determining functional connectivity between RA and vocal muscles shed light on some experimental drawbacks. EMG was only modulated at certain times during BOS playback, as opposed to modulation throughout song in a singing Bengalese finch. The number of opportunities to measure functional connectivity using stEMG was therefore limited in the acute setting. Moreover, EMG modulation did not occur on every single trial, thus weakening whatever effect we might quantify using stEMG. Initially, one might think a way to overcome this would be to only use trials where modulation occurred, but the observation that individual trials could have EMG modulation at some but not necessarily all time points where modulation was observed in the mean signal made it more difficult to implement such a technique. While all of these concerns might be improved by performing the experiment chronically, one might encounter another issue that was faced in this experiment. Though neural and EMG modulation was found in one experiment, the neural modulation preceded modulation of EMG activity. This exemplifies that over the course of several experiments, we might not even be sampling enough neurons that have connections with one or many vocal muscles. Even if this experiment was performed in a chronic setting, we might only be sampling up to 5 neurons with single-unit isolation. While we cannot say at this point how successful a chronic approach to this experiment would be, it is clear that the potential yield may be too low to provide significant results. However, it is still believed that

development of simultaneous chronic neural and EMG recordings will be useful in advancing this question as well as others. While this aim could not reveal the functional mapping from premotor neurons to vocal muscles, it did provide useful information for future studies.

# CHAPTER 6

# THE ROLE OF MOTOR NEURON SPIKE TIMING IN DRIVING

# VOCAL MUSCLE BEHAVIOR

This aim investigated the role of temporal precision in the code of motor neurons for driving activity in vocal muscles. While timing codes have traditionally been studied in sensory systems [135-137], recent studies have demonstrated the importance of spike timing in motor systems [138]. This system represents a perfect model for studying motor spike timing because of the quick dynamics of songbird vocal muscles [53]. In undertaking this study, we developed micro-scale, flexible, high-density electrode arrays for recording EMG signals. They are briefly described in this chapter discussed in more detail in the Appendix.

This chapter is broken up into two parts. The first portion (6.1-6.5) is adapted from a manuscript in preparation. The second portion (6.6) includes additional studies that were not included in the manuscript.

## 6.1    Introduction

The nervous system controls the body using patterns of action potentials (spikes) to activate the muscles. It is unclear how spike patterns encode motor output. Neurons could drive subsequent activity using spike rate, the precise timing of spikes, or a combination of both. However, nearly all prior studies of motor function in vertebrates have assumed that muscles are controlled with a rate code [24, 25, 139]. Recently, we demonstrated that in individual neurons in the songbird vocal motor cortex (the robust nucleus of arcopallium,or RA) the precise timing of action potentials at the timescale of milliseconds predicts behavioral output far better than does the spike rate [138]. This finding suggests an intriguing hypothesis – that small differences in spike timing in the

61

nervous system drive similarly precise timing patterns in muscle tissue, that these temporally precise motor commands cause significant differences in muscle force production, and that these differences in force output in turn cause measurable variations in behavior. Here, we evaluated this hypothesis by combining physiological, computational, and biomechanical analyses to examine the nervous system's control of a crucial motor parameter – air pressure in the respiratory system.

While motor timing precision has been investigated before, no study, to the best of our knowledge, has demonstrated together precise spike timing in muscles and its effect on force output and behavior. These three components are necessary to challenge long-held notions that cortical motor control is based solely on spike rates, as most motor studies have assumed [140, 141]. Previous studies have shown that small changes in the timing of muscle stimulation has a significant effect on force output but did not determine if those patterns of activation were physiologically relevant [26, 27, 142]. An invertebrate study revealed timing variability in motor neuron spike patterns and its effect on muscle force output, but it is not known if those effects cause differences in behavior [28]. While these studies support our hypothesis, combining approaches focusing on neural activity, muscle force, and behavior are necessary to determine that the neural code actually present in vertebrate motor systems relies on spike timing in addition to spike rate.

Songbirds represent an ideal system for studying motor timing because both cortical circuits controlling brainstem networks [130, 143] and the contributions of individual muscles to behavior [100] have been well-studied. Here, we focused on control of air sac pressure during breathing because we have a strong understanding of how muscle activity contributes to respiration [144, 145] and we could generate very large

62

datasets necessary for sophisticated analysis techniques. While previous studies have demonstrated how songbird muscles affect behavior using multi-unit EMG [100], analyzing the activity of single motor units will provide a window into the temporal dynamics of neural control. Our recent developments in single motor unit recording techniques have enabled us to examine whether temporal precision is significant at the level of muscles.

We hypothesized that the central nervous system precisely controls motor unit activation on a millisecond timescale, and that these fine temporal details significantly influence motor output. We used three different approaches to test our hypothesis. First, to demonstrate that precise spike timing is present at the level of motor neurons, we recorded single motor unit activity from a songbird respiratory muscle and analyzed whether variations in spike timing corresponded to differences in behavior. Second, to show that these differences in timing could drive changes in muscle force output, we stimulated the isolated respiratory muscle *in vitro* with spike patterns to isolate the effect of timing from rate. Finally, we applied the same stimulation patterns to the muscle *in vivo* while recording air sac pressure to reveal the effects of precise motor timing on behavior. These approaches together show, for the first time, the importance of spike timing in the neural code, muscle biomechanics, and behavior.

## 6.2    Methods

### 6.2.1    Surgical Procedure

We used electromyography (EMG) and electrical stimulation to determine the importance of motor timing in the expiratory muscle group (EXP) for avian respiration. All procedures were approved by the Emory University Institutional Animal Care and Use

Committee. Prior to surgery, adult male Bengalese finches (>90 days old) were anesthetized using 40 mg/kg of ketamine and 3 mg/kg of midazolam injected intramuscularly. Proper levels of anesthesia were maintained using 0-3% isoflurane in oxygen gas. Thoracic air sac pressure was monitored using a silastic tube inserted in the same manner as previous studies [14, 146, 147] with the pressure sensor 20INCH-D-4V (All Sensors, Morgan Hill, CA).

### 6.2.2 EMG recordings

To optimize our ability to isolate individual motor units, we developed micro-scale, flexible, high-density electrode arrays that sit on the surface of individual muscles to record EMG signals. The gold electrodes were fabricated on 20 micron thick photo-definable polyimide with a range of contact sizes and spacings (Premitec, Raleigh, NC). The electrode exposures ranged from 25 to 300 microns in diameter and were separated by as little as 25 microns. Several alignments of electrodes (16 per array) were fabricated including a four-by-four grid and four tetrodes. To record from the EXP, an incision was made dorsal to the leg attachment and rostral to the pubic bone. After spreading fascia on the muscle group, an electrode array was placed on its surface. The other end of the array connects to a custom-designed Omnetics adapter to interface with a digital amplifier (RHD2132, Intan Technologies, Los Angeles, CA). The Intan evaluation board delivered the EMG signals and the pressure signal to the computer at 30 kHz while providing the voltage supply for the pressure sensor.

With these arrays, we were able to acquire high-quality EMG recordings from 16 locations simultaneously during quiet respiration in eight male Bengalese finches. The increased number of channels allows the experimenter to decide which channels should

be subtracted from each other to create bipolar signals. Because of the high specificity and impedance of individual electrodes, we were able to extract single motor unit data in some cases. Because we can record sixteen unipolar signals in a very small area, we have increased the probability of recording a single motor unit while allowing us to test how different intramuscular segments are differentially recruited. Though EXP is made up of three sheet-like overlapping muscles (*m. obliquus externus abdominis*, *m. obliquus internus*, and *m. transversus abdominis*), we presumed that we were recording motor units from the most superficial muscle, *m. obliquus externus abdominis*. However, since all three muscles have similar functional roles involving contraction during respiration [148], recording a motor unit from any of these muscles would not affect our interpretation.

### 6.2.3 *In Vitro* Muscle Stimulation

The *in vitro* muscle preparation was conducted using five Bengalese finches (2 male, 3 female) and was set up as in Elemans, Mead [53]. That technique is described briefly here. The animal was euthanized using a 70%/30% $CO_2/O_2$ mixture and EXP was exposed as in the *in vivo* experiments. Fiber bundles were then isolated from the surface of *m. obliquus externus abdominis* (the most superficial muscle in the EXP group). The fiber bundles were then mounted in an aluminum test chamber while continuously being flushed with oxygenated Ringers solution at 21ºC. One end of the muscle was fixed to a servomotor (though it was not used) using silk suture while the other end was mounted on a force transducer (Model 400, Cambridge Technology, Bedford, MA). The muscle fibers were then stimulated through the solution using parallel platinum electrodes. To test the importance of motor timing, three stimulation pulses were delivered across 20ms,

with the middle pulse being placed either 2, 4, 10, or 12 ms after the first pulse. Additional trials were conducted with only a single pulse as a control. We could not fully survey the entire interval because the muscle fibers would die before a large enough sample size was achieved. Each stimulation pulse was a 250 µA biphasic pulse with a 500 µs duration. To account for muscle fibers dying over the course of the experiment, force measurements were normalized to the fiber bundles maximum tetanic force at 150Hz, which was measured after every 5 stimuli and linearly interpolated for each stimulus. Force transducer and stimulation signals were digitized at 20 kHz with a NIDAq board (PCI-MIO-16E4, National Instruments, Austin, TX).

### 6.2.4 *In Vivo* Muscle Stimulation

Stimulation of EXP was performed in six male Bengalese finches using two fine wire electrodes made of insulated multi-stranded alloy (50 µm diameter, Phoenix Wire Inc., Lawrenceville, GA). Pressure recordings were acquired using a NIDAq board (BNC-2090A, National Instruments), and used to trigger stimulation with custom-written LabVIEW code when the pressure crossed a user-defined threshold. The LabVIEW code then sent a stimulation pattern to an external stimulator (Model 2100, A-M Systems, Carlsborg, WA), which was connected to the fine wire electrodes in EXP.

To test the importance of motor timing on behavior, three stimulation pulses (also biphasic and 500 µs in duration) were delivered across 20ms, with the middle pulse being placed in 2 ms increments across the duration (9 different patterns) in addition to single pulse and no pulse control stimuli. All 11 patterns were interleaved during the experiment. Pressure and trigger times were recorded at 32 kHz for both of these experiments using the LabVIEW code.

The selection of an appropriate current was important for interpreting the results of these experiments. To properly compare them to EMG recordings, we wanted to stimulate using a current that activates the axons of motor neurons but not muscle fibers directly. One previous study that stimulated songbird muscle used currents as great as 2 mA [53], while a more recent one posited that currents below 500 µA were likely activating nerve fibers [100]. We therefore selected a current of 250 µA for EXP stimulation to ensure robust effects on air sac pressure. To test the theory that we were only stimulating the axons of motor neurons, we applied curare, which locally blocks the neuromuscular junction, to EXP and compared both EMG and stimulation effects versus when saline was applied to the muscle. Curare eliminated the recorded EMG signal observed when only saline was applied to the muscle (Figure 19a-b). Stimulation at 100 µA produced clear effects on air sac pressure when saline was applied to the muscle (Figure 19c), but those effects were abolished when curare was applied to the muscle (Figure 19d). The same strong stimulation effects observed at 250 uA when saline was applied (Figure 19e) were greatly reduced when curare was introduced to the muscle (Figure 19f). While we were unable to completely eliminate stimulation effects at 250 µA using curare, we believe that result was due to the current spreading further than the span of the drug. Applying too much curare and fully paralyzing EXP would endanger the well-being of the animal. However, conducting our full 3-pulse stimulation experiment at 100 µA produced quite similar air sac pressure effects (Figure 19g) as those observed using 250 µA (see 6.3). We therefore believe our muscle stimulation experiments were only activating the axons of motor neurons and not muscle fibers directly. This allowed

us to make insightful comparisons between the results of our spike pattern and stimulation analyses.
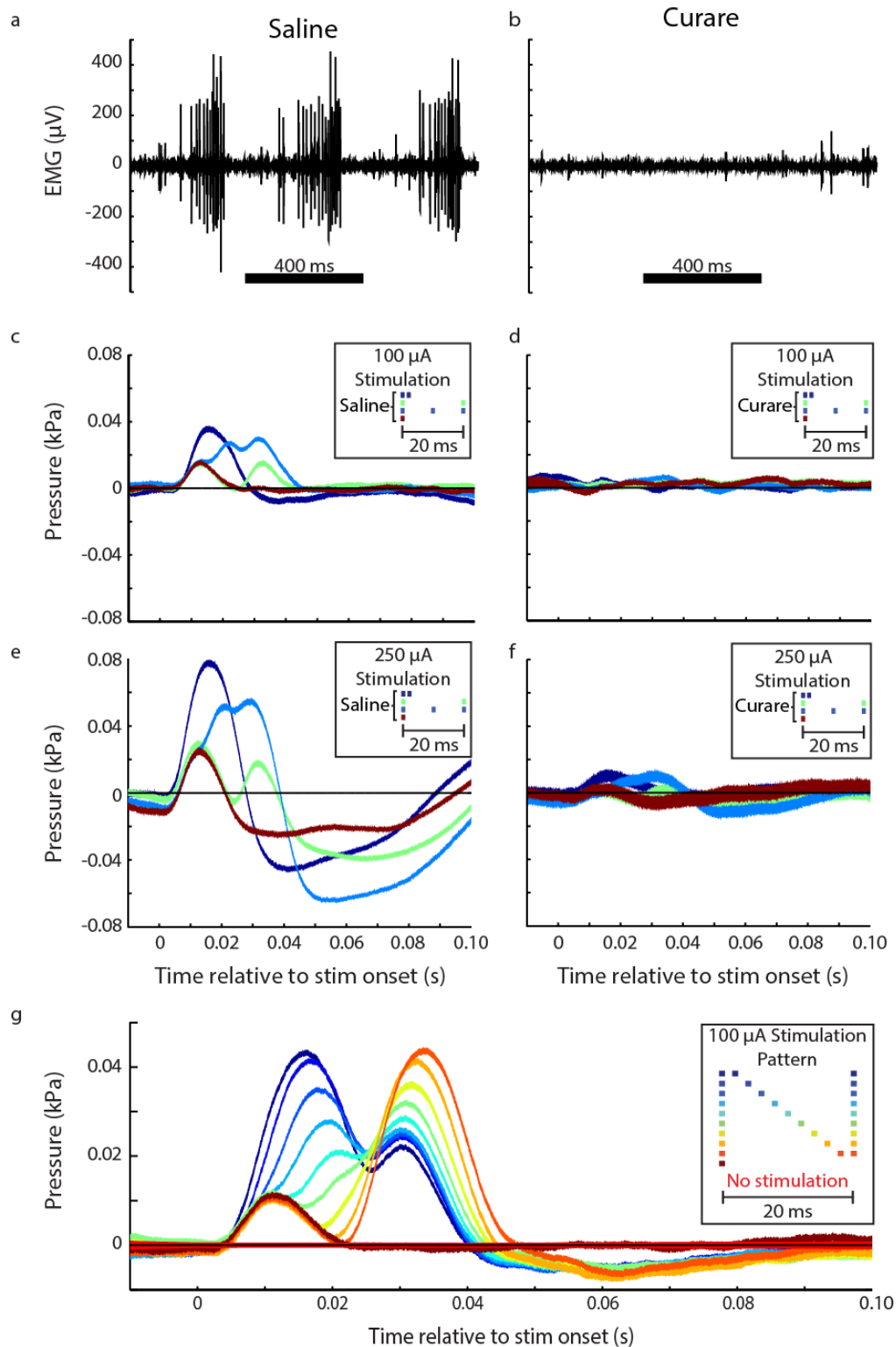
Figure 19: Curare experiments suggested that EXP stimulation activated the axons of motor neurons and not muscle fibers directly.(a) EMG recordings showed strong activity when saline was applied to the muscle, (b) but that activity quickly disappeared when curare, which locally blocked the neuromuscular junction, was applied to the muscle. (c)

Various stimulation patterns at 100 μA had clear effects on air sac pressure, (d) but curare abolished those effects at the same stimulation current. (e) The same stimulation effects at 250 μA were (f) greatly reduced by curare. (g) Though our experiments described effects of EXP stimulation at a current of 250 μA, we saw similar effects at currents where stimulation effects were abolished by curare as in (c), such as 100 μA shown here.

### 6.2.5   Data Analysis

All pressure recordings were converted from voltages to kPa via calibration measurements taken with a manometer, and then filtered between 1 and 50Hz. EMG recordings were filtered between 300 and 10,000 Hz. Pairs of EMG channels were subtracted to optimized motor unit isolation. Once a good pair was selected, motor unit spikes were sorted using custom-written MATLAB (Mathworks, Natick, MA) code.

To analyze the EMG and pressure recordings together, we searched through the pressure for occurrences of particular spiking patterns (words) and compared the pressures following those patterns. We assumed that the individual spikes of our single motor unit did not drive the overall pressure cycle, and so instead of comparing raw pressure measurements, we subtracted out average cycles (defined as the mean pressure waveform of 20 neighboring respiratory periods). We then compared these residuals following the chosen spiking patterns. This was done by finding the difference in residuals following these two patterns at every point and dividing by the square root of the sum of their variances at that point. So, for time t, if we define residuals following pattern 1 as x and residuals following pattern 2 as y,

$$d'(t) = \frac{\bar{x}(t) - \bar{y}(t)}{\sqrt{\sigma^2_{x(t)} + \sigma^2_{y(t)}}}$$

Error bars were then calculated by bootstrapping with 1000 trials.

*In vitro* force measurements were compared from different stimulation patterns using the same d' analysis referred to in the recording analysis above. Due to limited resources, we used two male and three female subjects for analysis. Despite other experiments only being conducted on male Bengalese finches, no qualitative differences were observed between sexes, aside from normal inter-subject variability (Figure 20). Because the sample size was small for each sex, we could not perform a statistical comparison between the two groups.
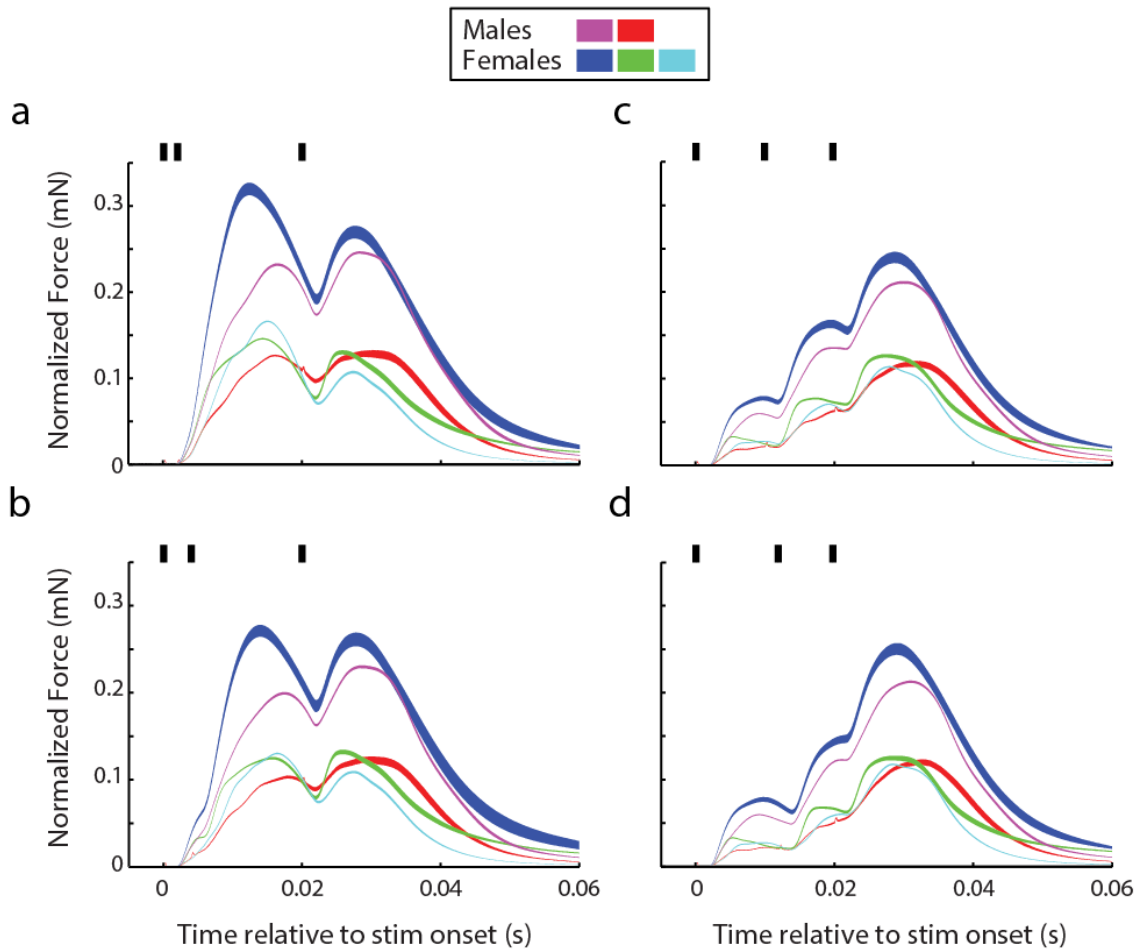


Figure 20: *In vitro* stimulation of EXP did not show any qualitative differences across sexes.Across all four stimulation patterns (a-d), all subjects showed approximately the same force trajectory, with no subjects showing differences, outside of normal inter-subject variability. Sample size for each group was too small to perform a statistical

comparison, but observations did not produce any notable concerns that would affect subsequent analysis.

To isolate the effects of EXP stimulation on air sac pressure, the mean pressure waveform of 10 neighboring unstimulated (catch) respiratory period was similarly subtracted from the stimulated pressure waveform. Waveforms were aligned to the phase of the respiratory pattern at which the stimulation, instead of the spike pattern, occurred. All catch-subtracted pressure waveforms were averaged within a given stimulation pattern with the standard error calculated at every time point. To compare responses from two different stimuli, d' was calculated as above.

### 6.2.5.1 Mutual Information: consecutive ISIs

In order to address the question of mutual information between consecutive ISIs, we approximated local rates as the spiking data passed through a Gaussian filter, where we varied the width (in ms) of the filter. We then used these rates to generate Poisson spike trains (assuming a refractory period of 2.5 ms). In order to estimate the mutual information, we relied on the estimator algorithm and code from Kraskov, Stögbauer [149], which relies on counts of $k$ − nearest neighbors in order to estimate densities of the relevant variables in each dimension. This allowed us to deal with continuous variables, such as, in this case, interspike intervals. In our implementation of the algorithm, we used $k = 10$, although values were similar for small changes in k. Error bars were calculated by dividing the data into non-overlapping subsamples, and then finding the standard deviation of the mutual information in these smaller data sets.

We performed this analysis on both the generated spike trains and the spike train from the actual data, and compared the two. The analysis was performed for all birds.

6.2.5.2 <u>Mutual Information: Spikes and Pressure</u>

We also calculated the mutual information between spiking in a particular window and the following pressure. Again we used the mutual information estimator algorithm and code in Kraskov, Stögbauer [149], although here due to an increase in dimensions and decrease in data set size we used $k = 3$.

In order to limit the size of the data sets and reproduce the effect of the residuals we had used in earlier analyses without having to process the data, we fixed the phase of occurrence of spikes (all spiking patterns compared began at $\phi \approx 0.8\pi$, and all pressure patterns compared to the spikes began at $0.8\pi + 10ms$). We chose this phase because the most spiking occurs at that phase – nearby choices reveal similar results, and distant phases rarely have any spikes in the window. Mutual information values used a subsampling of the pressure data to 10 points – this corresponded to a plateau in mutual information as a function of number of points representing the pressure. We used $k = 3$ for similar reasons to our earlier choice of k.

We were able to split the mutual information between spikes and pressure into components related to count and those related to precise timing. We did this by using the following property of mutual information, where $\bar{x}$ represents the spike count for a particular spiking window:

$$I(x, y) = I(\bar{x}, y) + \sum_{\bar{x}} P(\bar{x})I(x, y|\bar{x})$$

This follows from the definition of conditional mutual information,

$$I(x; y|\bar{x}) = H(x|\bar{x}) - H(x|y, \bar{x}),$$

and the fact that

$$H(x, \bar{x}) = H(x); H(\bar{x}|x) = 0.$$

73

6.2.5.3 Wavelet-based Functional ANOVA (wfANOVA)

To compare pressure and force waveforms while removing inter-bird variation, we implemented an analysis technique called wavelet-based functional ANOVA (wfANOVA), which does not treat each time point in a waveform independently as comparisons are performed in the wavelet domain [150]. While the above d-prime analysis provides fine temporal resolution for comparing pressure and force waveforms from different spike and stimulation patterns, it treats each time point as independent from other time points, when in fact that may not be the case. These two types of analyses, therefore, complement each other in terms of what we can learn from the data. The wfANOVA technique was first introduced and described in detail in McKay, Welch [150], but we will describe it briefly here. Our analysis used an adapted version of the MATLAB code used in McKay, Welch [150].

In our approach, each trial was zero-padded to make the total number of time points equal to an exponent of two, as was required for a wavelet transform. All trials were then transformed into the wavelet domain using the discrete wavelet transform, which is similar to the Fourier transform, as it produces coefficients for a family of wavelets that can be linearly transformed back into the time domain. We chose to use the third-order coiflet family, as McKay, Welch [150] used, because their symmetry does not introduce phase shifts into the data and their shapes approximated those of the pressure waveforms. The wavelets in this family are orthogonal to each other, which is important for implementing multivariate ANOVA, which performs more poorly when there are high correlations between data points, as is the case in the time domain. Because wavelets are localized in time and finite in time, unlike Fourier sinusoids, reconstruction does not depend on cancelation and instead features many small or zero magnitude wavelets.

74

Wavelet decomposition uses a combination of large time-scale wavelets that approximate the signal like a low-pass filter and small time-scale wavelets that provide the detail of the original signal. The coefficients determined for each of the wavelets in the family are used for subsequent ANOVA.

All trials were grouped by two factors: spike pattern and bird. Fixed-effect, two-factor ANOVA was performed on the wavelet-decomposed pressure waveforms from the EMG experiments. Significant wavelet coefficients ($\alpha = 0.05$, using F test) were then used to determine significant contrasts between pairs of spike patterns with separate post hoc Scheffé tests, with the null hypothesis being that the pressure waveforms from the pairs of spike patterns were equal. These post hoc tests were conducted using a significance level that was Bonferroni-corrected for the number of significant F-tests corresponding to the initial ANOVA with respect to spike pattern factor. Wavelet coefficients that were significantly different between spike patterns were subtracted to find the coefficient corresponding the difference between the two patterns. All nonsignificant coefficients were set to zero, and the entire decomposition was transformed back into the time domain. This produced a contrast curve between two spike patterns across birds that removed the effects of inter-subject variability on the result. This analysis technique was also used for the *in vitro* muscle stimulation experiments, with the input being the force waveforms instead of the pressure waveforms, and *in vivo* muscle stimulation experiments.

## 6.3     Results

EMG recordings were conducted using a custom-designed flexible microelectrode array (Figure 21, see 6.2.2) placed on the expiratory muscle group (EXP) during anesthetized

respiration. The high signal-to-noise ratio and isolation of the motor units allowed us to test the importance of precise spike timing in muscles when driving motor output.
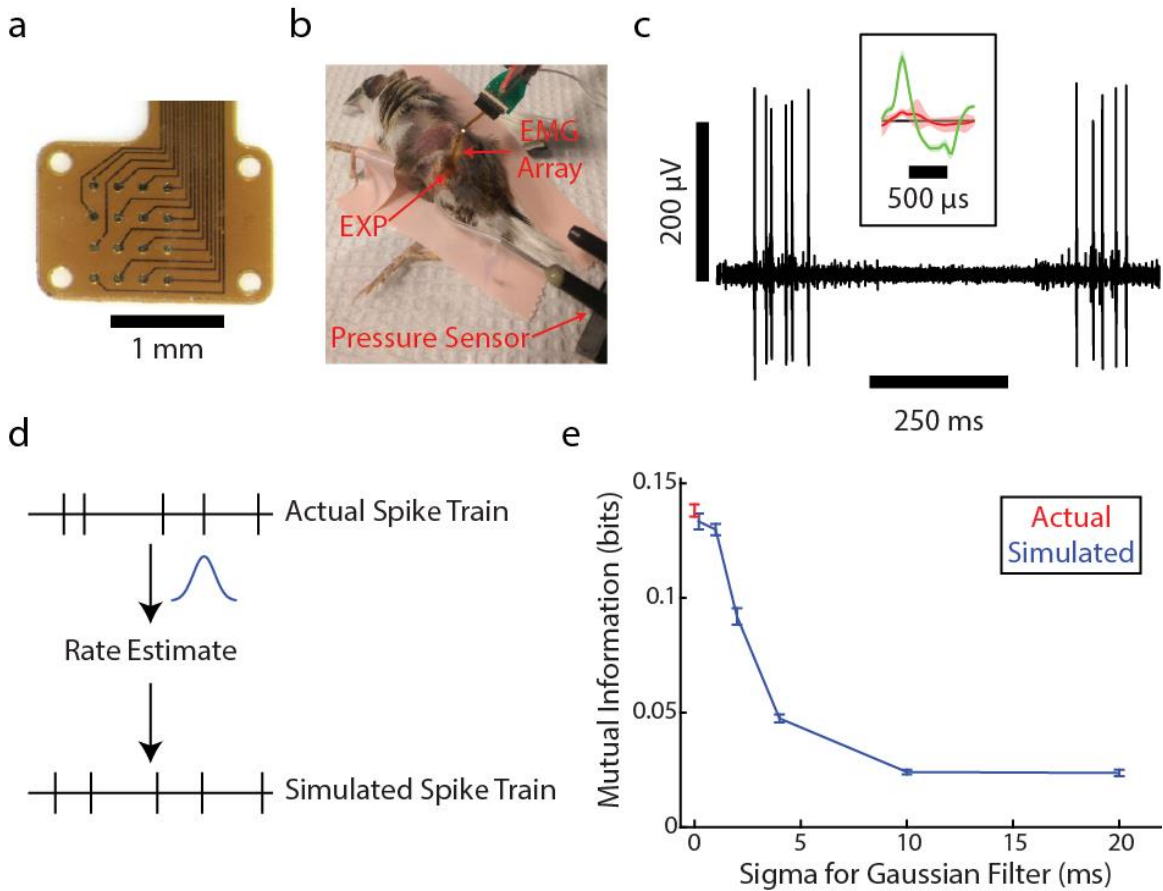


Figure 21: Flexible, microelectrode arrays were used to record single motor units in the expiratory muscle group (EXP).(a) There were 16 channels on the array with contacts 100 μm in diameter. (b) In these experiments, we recorded from EXP while simultaneously recording the thoracic air sac pressure. (c) A sample recording demonstrates the signal-to-noise ratio of the recording was enough to isolate single motor units. (d) To determine how well the spike pattern was approximated by a rate code, the rate estimates were taken from the actual spike train using different timescales, and then those rate estimates were used to generate simulated non-homogeneuous Poisson spike trains for comparison. (e) The mutual information between consecutive interspike intervals for the actual data was best approximated by a Poisson spike train with rates updating on a millisecond time scale.

Our first-pass analysis looked only at spiking activity in the motor units and found that their rates can only be accurately represented at a millisecond time scale. To

determine how well the spike pattern could be approximated by a rate code, we estimated mutual information between consecutive interspike intervals (Figure 21e). In a homogeneous Poisson spike train, we would expect the mutual information to equal zero; here, with a rate-varying Poisson, consecutive interspike intervals do carry information about each other. We find that the information in the Poisson approximations only approached that of the actual data for values of $\sigma$ on the order of 1 ms, which suggests that the spike trains of these motor units can only accurately be represented by rates that vary on that time scale. This does not mean that motor control occurs on that time scale, but it does suggest much more complicated interactions between spike timings than we would expect were this system to be controlled by a more slowly changing rate.

Having determined that there are complex patterns present in the spiking patterns of the motor units recorded from, we then asked if these timing-precise patterns corresponded to differences in behavior, here represented by air pressure in the respiratory system. We analyzed the pressure differences between spike trains that differed only in the timing of a single motor unit spike. In 3 spike patterns over 20 ms, having the middle spike occur 12 versus 10 ms after the first spike significantly increased the pressure waveform and subsequently decreased it over the following 100 ms (Figure 22b and c). This effect was seen across all six birds that showed a significant number of occurrences of this particular pattern (Figure 22d). After accounting for inter-subject variability using wavelet-based functional ANOVA (wfANOVA, see 6.2.5.3), we observed a strong pressure difference between the two spike patterns (Figure 22e). Therefore, millisecond-scale changes in single motor unit timing correlated with small, but significant changes in air sac pressure.
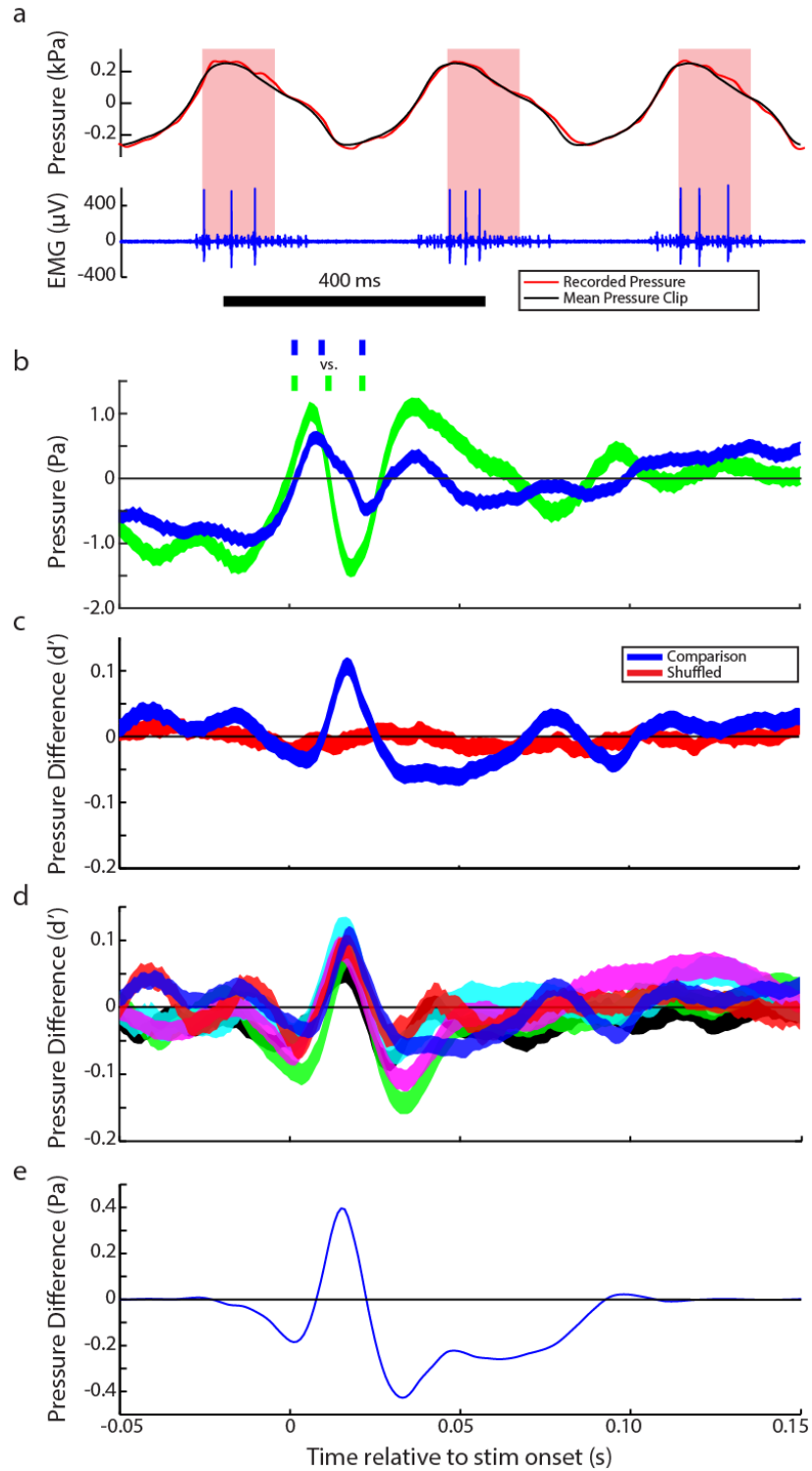
Figure 22: Comparison of pressure following similar spiking patterns.(a) The pressure waveform associated with every recorded spike pattern was extracted with the mean pressure waveform subtracted to reduce phase dependence. (b) The mean residual pressure waveform differed for two three-spike, 20 ms patterns where the middle spike occurred 10 ms after the first spike in the first pattern and 12 ms after the first spike in the

78

second pattern. (c) The blue represents the difference in residual pressure following two pressure words. The red trace was generated by shuffling the pressure data and demonstrates the expected result if there were no correlation between the timing of the middle spike and the subsequent pressure trace. (d) The various color traces represent d' for the six birds that demonstrated a significant number of occurrences of these two spiking patterns (blue trace is same as in (c)). Note the intervals in (b) represent the mean +/- 1 S.E. while the intervals in (c) and (d) represent the mean +/- 1 S.D. as determined by bootstrapping.

Although this result held qualitatively across a variety of similar patterns, the d' analysis method was necessarily limited to pairs of hand-selected patterns and relationships. In order to analyze relationships between spiking and the following pressure without this restriction, we turned to mutual information. We used a property of mutual information that allowed us to separate out the information between spikes and pressure into two components, as follows (see Methods for more detail):

$$I(spikes, pressure) = I(spike\ counts, pressure) + I(spike\ timing, pressure)$$

The ability to explicitly separate the mutual information between the spiking and the pressure into information from spike count (rate) and the mutual information between spike timing and pressure allowed us to precisely quantify how much of the information was encoded in each.

We did this by looking at a 20 ms window of spiking during anesthetized respiration, and comparing the spikes in that window to the air sac pressure over the subsequent 100 ms (Figure 23). We then calculated the two terms in the mutual information separately (I(spike counts, pressure) and I(spike timing, pressure), and added them in order to find the total mutual information. Mutual information between spike counts and pressure was 0.0309 +/- 0.0024 bits, while the mutual information between spike timing and pressure was 0.0283 +/- 0.0052 bits. Together, this yielded a total

mutual information between spike patterns and pressure of 0.0592 +/- 0.0057 bits. The difference between the two points in Figure 23 represents the information in the spike timing about the pressure waveform that is not contained in the in the firing rate. As can be seen, approximately half of the mutual information was not in the spike counts, and was instead found in spike timing.
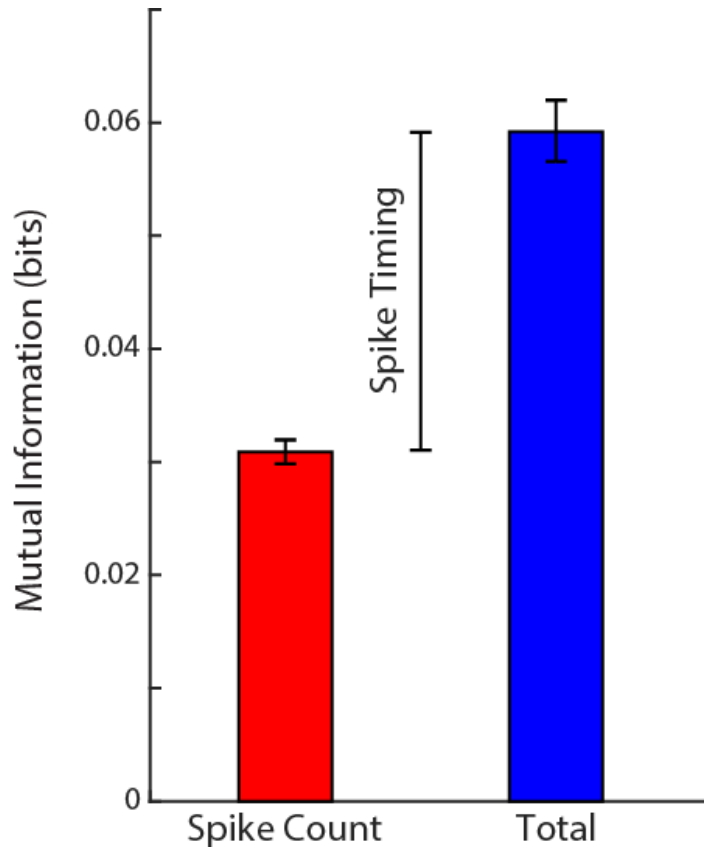


Figure 23: Mutual information between spiking (in a 20 ms spiking window) and the following pressure (100 ms).Mutual information between spike counts and pressure (red) made up approximately one half of the total mutual information between the spiking and pressure (blue). The difference between the two was the information contained in the timing of the spikes within those 20 ms.

Though the above results demonstrated that precise timing in motor neuron spiking patterns contains information about output not present in the rate of firing, we did not know if those variations in timing could affect muscle output. To test the effects of

these spike patterns on muscle force, we extracted *m. obliquus externus abdominis* from EXP and stimulated the muscle fibers using 3 pulses across 20 ms while varying the timing of the middle pulse, such that we could isolate the effects of pulse timing versus those of pulse rate. Moving the timing of the middle pulse in the 3 pulse sequence forward by 2 ms had a significant effect on force output regardless of when the middle pulse occurred (Figure 24). In fact, the d' measurements were several standard deviations greater than the average (Figure 24c and f). Again, we employed wfANOVA, which accounted for inter-subject variability, to reveal a consistent and significant difference between force outputs from respective pairs of stimulation patterns (Figure 24d and g). The results of these *in vitro* experiments revealed that the precise spike timing observed in motor neurons can have a significant effect on the force output generated by the muscle.
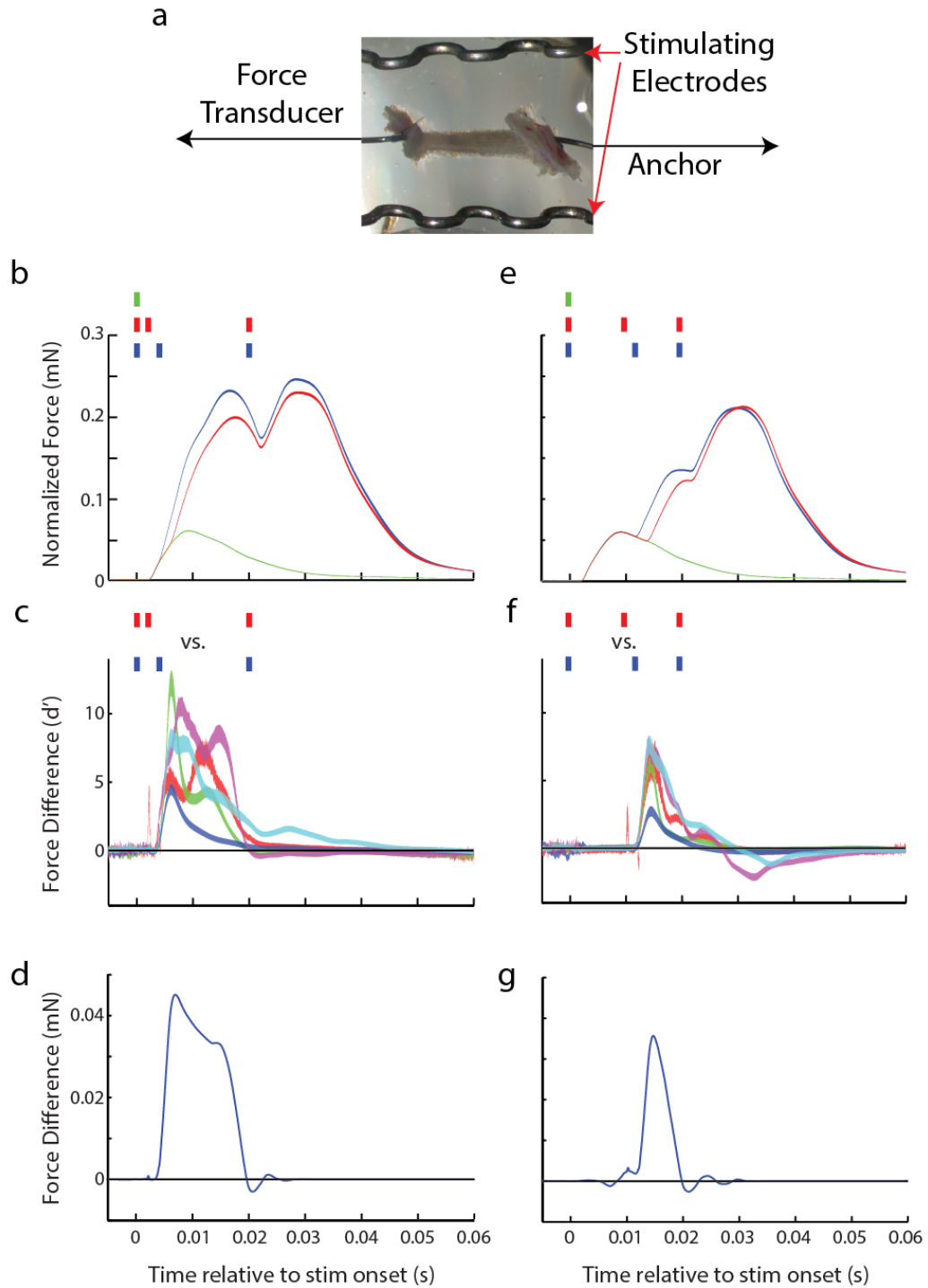
Figure 24: *In vitro* force measurements demonstrate importance of timing on a millisecond scale.(a) Isolated muscle fibers were anchored on one end and attached to a force transducer on the other end while different stimulation patterns were delivered via stimulating electrodes in an oxygenated Ringers solution. (b) The force profile showed a distinct difference when moving the middle pulse from 2 ms after the initial pulse to 4 ms after the initial pulse. (c) Quantifying this difference using the d' metric showed typical

results across five birds. (d) wfANOVA revealed the effect of moving the stimulation pulse, independent of inter-subject variability for the same stimulation pattern in (b) and (c). Similar results were found in the (e) force profiles, (f) d' waveforms, and (g) wfANOVA result when comparing stimulation patterns with the middle pulse at 10 ms and 12 ms, respectively. The examples shown in (b) and (e) are represented in (c) and (f), respectively, by the cyan traces. The intervals shown in (b) and (e) represent the mean +/- 1 standard error and the mean +/- 1 standard deviation in (c) and (f).

While we have shown that precise motor timing exists in motor neurons and can drive significant differences in muscle force output, we have not demonstrated that these effects are significant for behavior. To further probe the effects of timing on behavior, we recorded air sac pressure and stimulated EXP during respiration again using 3 pulses across 20 ms while varying the timing of the middle pulse. In this experiment, the middle pulse was located at each multiple of 2 ms after the first pulse, resulting in 9 different pulse trains of 3 pulses each. The differences in mean pressure response to these stimuli can be clearly observed in Figure 25a. When quantifying these differences using the d-prime (d') metric, the responses were significantly different when moving the middle pulse by just 2 ms regardless of when that middle pulse occurred in the 20 ms interval (Figure 25b-g). When the middle pulse was timed soon after the first pulse, moving the pulse by 2 ms had a significant effect on air sac pressure (Figure 25b-d). A similarly significant effect was observed when the middle pulse occurred near the center of the interval (Figure 25e-g). These effects were consistent across all six birds, as demonstrated by the similar d' waveforms in Figure 25c and f. Performing the same wfANOVA analysis on the pressure waveforms instead of the force waveforms demonstrated the effect of moving the stimulation pulse while accounting for inter-subject variability (Figure 25d and g). Significant differences were found using this method for all 36 pairs

of stimulation patterns (not shown). The results of these stimulation experiments demonstrate a causal link between millisecond-scale motor timing and air sac pressure.
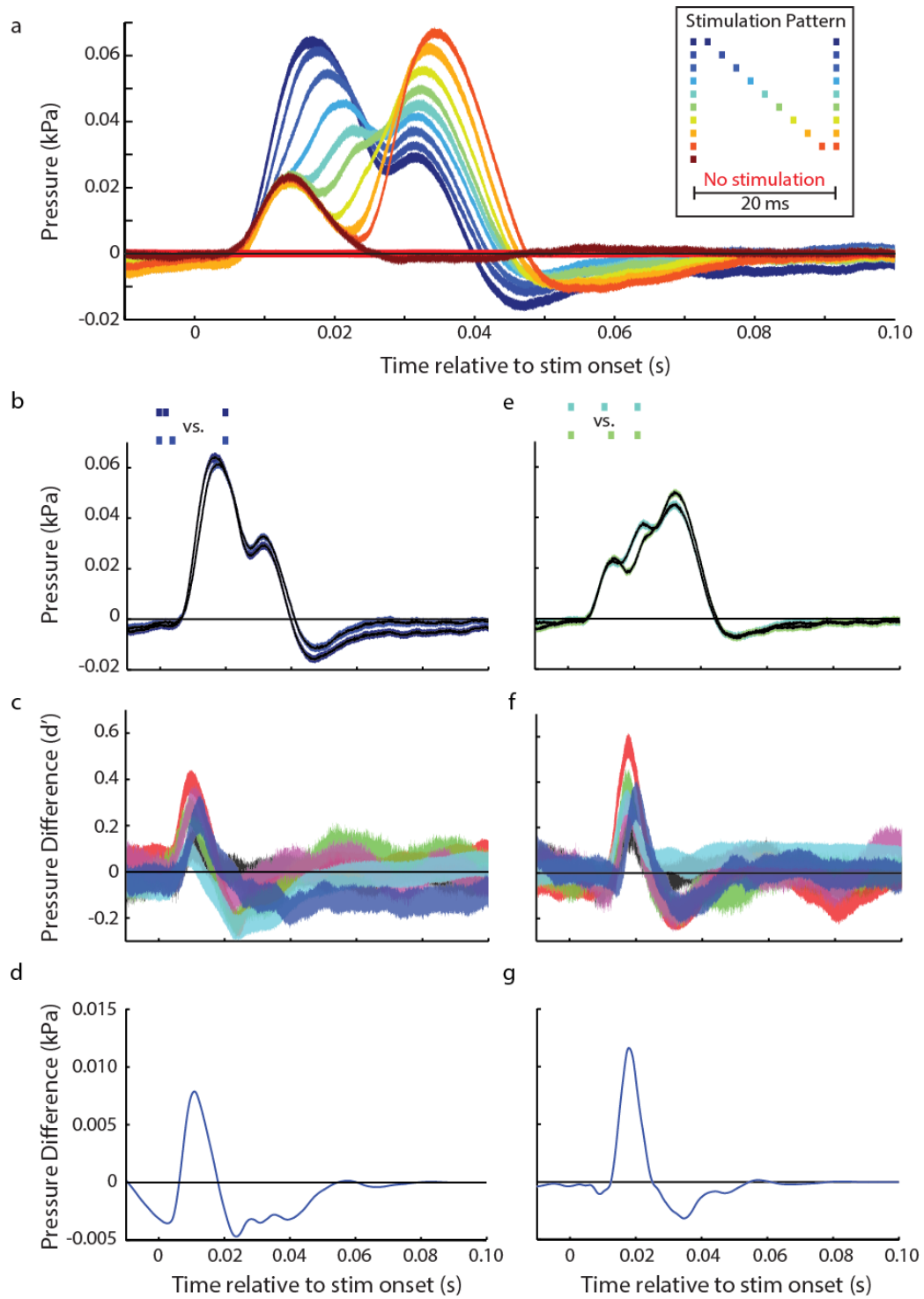


Figure 25: Changing stimulation pulse timing but not overall rate had a significant effect on air sac pressure.(a) The mean response varied significantly depending on the timing of

the middle pulse in the 3-pulse stimulation pattern. Calculating d' for the pressure effect between two stimuli with the middle pulse moved 2 ms showed a significant difference regardless of whether the middle pulse was towards an extremity of the pattern (b, c, d) or in the middle (e, f, g). (b) and (e) show examples from one bird, whereas (c) and (f) show the d' waveforms for all six birds, with the blue waveform corresponding to the examples in (b) and (e). (d) and (g) show the reconstruction of wavelets significantly different between pairs of stimulation patterns (in (b) and (e), respectively) after accounting for inter-subject variability, as determined by wfANOVA. Note that the intervals shown represent the mean +/- 1 standard error for the pressure waveforms in (a), (b), and (e) and the mean +/- 1 standard deviation for the d' waveforms in (c) and (f).

## 6.4    Discussion

In this study, we have compiled the first-ever demonstration of downstream decoding of a

timing code, from motor neuron activity to muscle force output to behavior. The mutual

information between consecutive interspike intervals in EXP motor units was shown to

surpass what would be expected with Poisson spiking, suggesting that even without

addressing motor output we were looking at complex temporal patterns in spike

positioning that could not be represented by rates that vary on scales significantly greater

than 1 ms. Regarding the relationship between the spiking and the behavioral output that

it induces, we also found that the mutual information between spike timing and pressure

was not only nonzero, but, for a 20 ms spiking window and the subsequent 100 ms of

pressure, was about equal to half of the total information in the spike trains. Moreover,

analysis of motor unit recordings demonstrated that 3-spike patterns with the middle

spike moved by just 2 ms resulted in significant changes in air sac pressure. By

stimulating EXP *in vitro*, we found that moving the middle pulse of a 3-pulse stimulus by

2 ms also resulted in significantly different effects on force output. A similar effect on air

sac pressure was observed during our *in vivo* muscle stimulation experiments, suggesting

that the force effects calculated from the *in vitro* data were enough to drive significant

effects on behavior. Because we were able to verify all of our effects using wfANOVA, we can conclude that both the EMG and stimulation results were due to motor timing and not just variability between subjects. Together, these findings suggest not only that the brain generates a precise neural code, but also that this code evokes meaningful differences in both muscle force output and behavior.

The relationship between the nature of signals originating from the brain and the capacity of the muscles to interpret incoming commands is key to understanding the capabilities of the entire system. The results of our analysis solely on motor unit activity demonstrated that the nervous system uses the timing of spikes to direct the downstream muscles. This result agrees with previous findings showing that cortical areas rely on spike timing in addition to spike rate when encoding motor behavior [138]. The motor unit spikes seemed to be precisely positioned relative to each other at scales of less than 1 ms, which suggests that rate approximations of firing at larger time scales will miss internal patterns. A study of proprioceptive encoding in macaques determined that the sensory portion of sensorimotor pathways used both temporal and rate codes [151]. Using similar sensory and motor codes would likely make it easier for the sensory pathway to "teach" the motor pathway in order to incorporate learned changes.

Deficiencies in current implementations of brain machine interfaces (BMIs), which often rely on neural firing rates to drive action [152-154], might be improved by taking spike timing into account. The use of local field potentials (LFP) and electroencephalography (EEG) over neural spike rate to control BMIs might suggest that precise timing across neurons in synchronized networks may be critical for properly translating neural activity to behavior [155, 156]. Extracting additional information from

86

neural spike trains in the form of spike timing may help BMIs overcome current obstacles towards greater efficacy.

To our knowledge, this study is the first to show the effect of physiologically relevant stimulation patterns on behavior in vertebrates. A previous study demonstrated variability in motor unit spikes played back to a muscle of *Aplysia* resulted in significant effects on force output, despite the muscle having slow dynamics [28]. A pair of studies showed that stimulating a flight muscle of the hawkmoth *in vitro* at different times relative to a physiologically relevant length cycle resulted in significantly different power outputs that were highly sensitive to the phase of activation on a millisecond-scale [157, 158]. Using the same model, another study showed that the nervous system could control synchrony between two opposing muscles at a sub-millisecond scale to modulate torque for flight [98]. We found similar results, even though our study looks at vertebrate skeletal muscle that can modulate behavior with relatively fast dynamics [53]. A key difference between invertebrate and vertebrate muscle is that an invertebrate motor unit can be innervated by more than one motor neuron, each of which can be excitatory or inhibitory [99]. On the other hand, because a single excitatory motor neuron, which can itself be inhibited, activates a vertebrate motor unit, it is difficult to compare the function of a motor timing code in invertebrates versus vertebrates. All of these studies focus on smaller muscles, which can theoretically contract with faster dynamics, though results may differ for larger muscles, which generally require more time to shorten [159]. For decades, the motor control field has investigated the importance of motor timing and its relevance to behavior, but those studies have generally focused on stimulation patterns that may or may not be physiologically relevant [26, 27] or correlations between recorded

87

doublet patterns and behavior [160, 161]. While doublets occur during firing onset and are hypothesized to ramp up force quickly, our timing analysis was always relative to an initial spike or stimulation pulse. Timing in multi-spike patterns may serve a different purpose than that of doublets. In this study, we are able to not only record motor unit timing and correlate it with behavior, but also use those recordings to inform our stimulation patterns to causally demonstrate the effect of motor timing on force output and behavior.

While we expected to discover behavioral changes due to stimulation timing, it was somewhat surprising to find correlational effects, based on mutual information calculations, as a result of motor timing in a single motor unit. Because there are likely on the order of hundreds of motor units across the respiratory muscles [17], one would expect variations in the timing of a single motor neuron to have a negligible effect on air sac pressure. This finding might suggest that there is a great deal of synchrony between motor units in the respiratory muscles, such that when a spike is relatively "late" in one motor unit, it may also be in others. On the other hand, this result may suggest that variation in motor timing in a single motor unit is enough to overcome any redundancy in motor units within the same muscle group. Future studies should look at motor timing while recording populations of motor units simultaneously.

Another important consideration was what electrical stimulation was actually doing to the muscle tissue. Based on the current used in previous studies [83, 100] as well as our curare experiments (see 6.2.4, Figure 19), we are inclined to believe that the 250uA stimulation current was activating motor neurons and not muscle fibers. Though that implies that we were activating whole motor units, it is quite likely that we were

activating multiple motor units. While the analysis of EMG recordings focus on single motor units, the stimulation experiments may only tell us about the importance of timing in groups of motor units. On one hand, this enabled us to potentially amplify the effects of precise timing observed in the EMG recordings. On the other hand, this prevents us from making strong conclusions about the causal effects of motor unit spike timing. If we were, in fact, activating multiple motor units, it is important to consider that recruitment was likely not the same as that experienced during normal contraction. A human study showed that the typical recruitment order of smallest to largest motor units, according to Henneman's size principle, was not observed during electrical stimulation [162]. Future studies should attempt to stimulate only single motor units. An important feature of this study is that the stimulation patterns attempted to mimic those observed in our EMG recordings. If we had found spike timing to be important for stimulation patterns that did not occur naturally in the EXP, it would not tell us anything physiologically relevant.

In this study, we demonstrated the importance of spike timing during respiration, which is generally believed to be controlled by central pattern generators (CPG) [71, 163]. Given control by a CPG, the variation in timing could arise either from intrinsically from the respiratory circuits or from upstream nuclei. The origin of this variation could be instrumental to understanding whether the central nervous system uses millisecond-scale timing to optimize behavior. Respiration is also critical to vocalization in songbirds. The brain nuclei responsible for controlling song in songbirds are able to assume control of the respiratory circuits to modulate breathing during song [164, 165]. One of those brain nuclei, RA, has demonstrated precise spike timing in controlling vocal output [138].

An interesting next step in this line of research would be to see if precisely-timed motor unit spikes and stimulation can drive significant effects in vocalizations.

## 6.5      Supplementary Information

We wanted to determine the salient duration to test 3-pulse stimulation experiments because finding the timing effect of two pulses separated by a large time interval may seem trivial. We therefore wanted to determine the time interval between two stimulation pulses required to completely separate their effects on pressure. In this experiment, two stimulation pulses (each pulse was biphasic with a 250 µs pulse width at 250 µA) were delivered with the interpulse interval (IPI) varied to include 1, 2, 3, 4, 5, 6, 7, 8, 9, 10, 12, 14, 16, 18, 20, 25, 30, 40, and 60ms. As controls, a single pulse and a no pulse stimulus were also delivered. All 21 patterns were interleaved during the experiment. This experiment would find the largest interpulse interval (IPI) that would have a nontrivial effect on the timing of the motor output. More specifically, if the IPI were greater than the duration of the impulse response to a single stimulation pulse, then it would seem trivial that moving a stimulation pulse outside of that interval would not stress the motor system's ability to reproduce millisecond-scale timing in its output.

To find this IPI threshold for meaningful motor timing analysis, we measured nonlinear summation by comparing the actual pressure response to a given stimulation pattern with the response constructed by adding the pressure response to a single stimulation pulse at the same times. The difference in area between the actual 2-pulse response and the constructed "linear" response was calculated for each IPI used in the 2-pulse stimulation experiments. To test whether this difference was significant, a baseline area difference interval was determined by calculating the mean +/- 1 S.E. of the area

difference between single pulse responses and the mean single pulse response. At a small IPI of 2 ms, the nonlinear summation was large (Figure 26b), while the difference was negligible at an IPI of 20 ms (Figure 26c). Quantifying the difference between these two responses at IPIs between 1 ms and 60 ms showed that the superlinear effect disappeared at IPIs above 20ms (Figure 26d). This experiment informed the salient time periods to test pulse timing in our subsequent 3 pulse stimulation experiments.
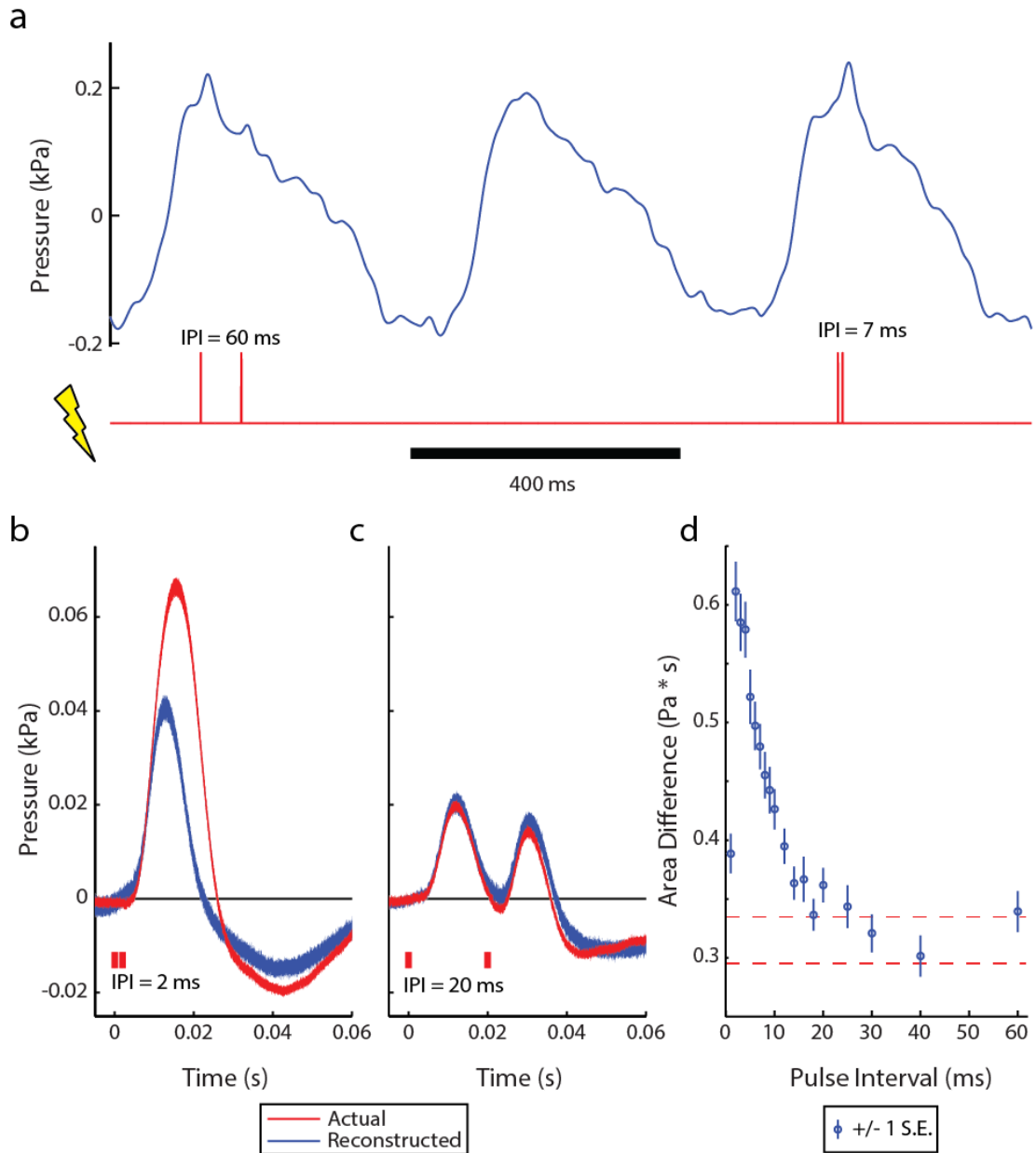
Figure 26: Nonlinear summation in thoracic air sac pressure in response to stimulation.(a) During respiration, stimulation of a varying interpulse interval (IPI) was delivered after air sac pressure crossed a user-defined threshold. (b) At small IPIs like 2ms, the actual pressure response was much greater than that produced from summing two single pulse responses separated by 2ms. (c) On the other hand, the responses were quite similar with an IPI of 20ms. Note that the intervals shown represent the mean +/- 1 S.E. (d) The difference between the actual and summed response dropped as IPI increased, leveling off after 20ms. The red dashed lines denote the mean +/- 1 S.E. when calculating the area difference between single pulse responses and the mean single pulse response. Note that the superlinear summation was relatively small for a 1 ms IPI, as the second pulse likely occurred within the motor neuron's refractory period.

In this study, we analyzed motor unit recording from anesthetized, breathing birds in order to generate very large data sets to conduct the analysis of mutual information between spike patterns and pressure waveforms. While we could have learned even more about motor control in this system performing the experiments during awake respiration, there were some limiting factors that prevented that. First, the pressure sensor we used (see 6.2.1) was too large (10 g) to attach to the bird. While previous studies have recorded pressure chronically by attaching a smaller sensor to a backpack on the bird [14, 146, 147], we needed a sensor with better resolution, in order to focus on small changes in pressure due to spike patterns. Those previous studies often used pressure to simply identify expiration onset or qualitatively look at changes in patterns. Secondly, we could not guarantee that we were holding the same motor unit over long durations of time as the bird moved around. We were, however, able to record single motor units in four awake birds for five minute samples, which we used to perform the analysis done in Figure 21e. Despite the bird being awake, we still observed spiking statistics that were best approximated by Poisson spike trains that updated their rates on a millisecond scale (Figure 27).
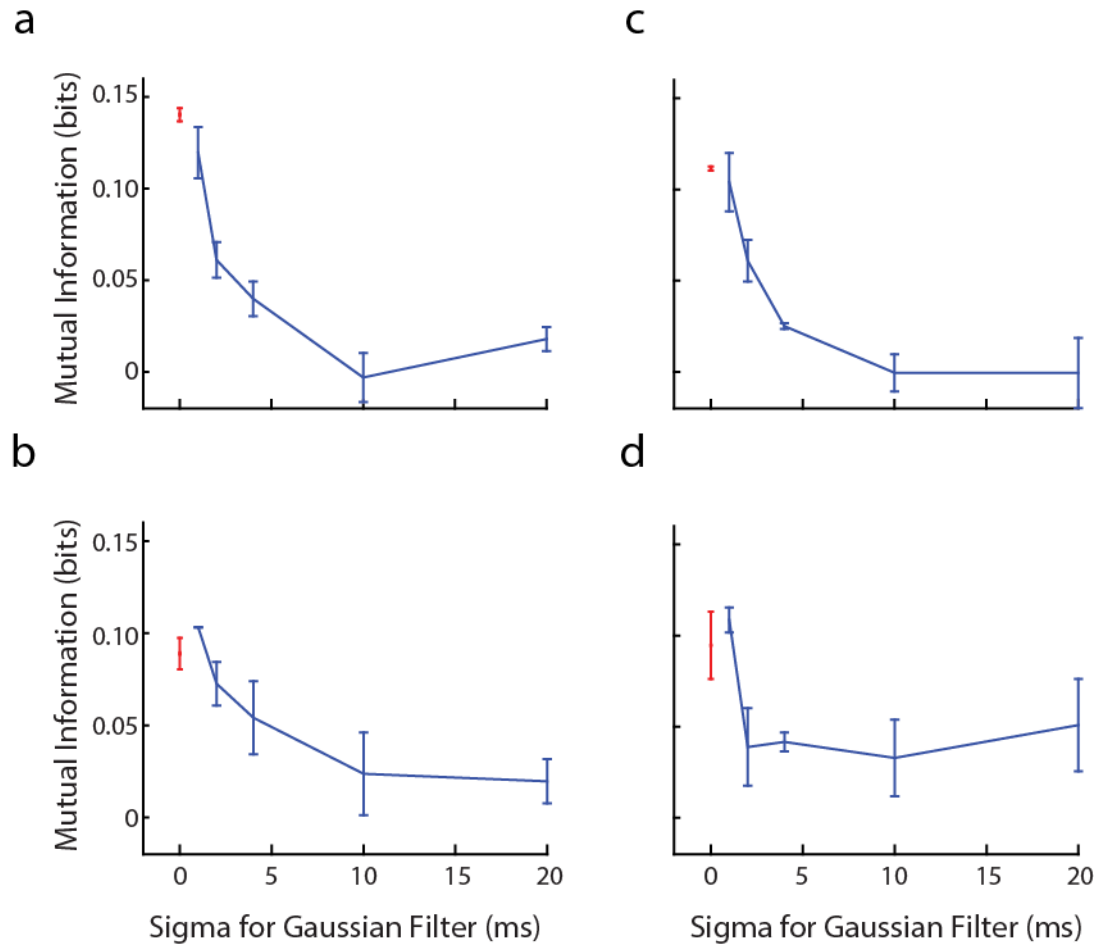
Figure 27: Mutual information between consecutive interspike intervals in awake birds was maximized by a Poisson spike train approximation that updated on a millisecond scale. Each of the four plots is from a 5-minute sample from a different awake bird. The shapes of these plots resembled those observed in anesthetized birds, suggesting that the observed importance of millisecond-scale spike timing was not due to anesthesia.

## 6.6    Effects of syringeal muscle stimulation pulse timing on vocalizations

While the previous sections shed much light on the importance of motor timing in respiration, it would be interesting to see if these effects carry over to an awake, behaving animal, where the behavior is not necessarily thought to be driven by a central pattern generator (CPG) [71, 163]. Because of technological limitations, we were not able to record single motor units from vocal muscles during song. In general, levels of activity are much higher during song than during breathing, and thus it is more difficult to isolate

individual motor units from the EMG recording. However, we were able to stimulate a syringeal muscle during song using different stimulation patterns in an attempt to demonstrate the importance of motor timing for vocal behavior

## 6.6.1  Methods

6.6.1.1 Experimental setup

Seven Bengalese finches were used for these experiments. Animal surgeries were conducted as in Aim 1 by implanting fine wire electrodes into the VS muscle (in six birds) and the DTB muscle (in one bird). Targeted stimulation for specific syllables was conducted in the same manner as in Aim 1. Briefly, a spectral template was created using a custom MATLAB script. This template was compared to online acoustic recordings in LabVIEW and triggered stimulation upon a successful match [115]. While in Aim 1, stimulation parameters were held constant, in this experiment, the number of pulses (3) and pulse parameters (pulse width = 500 μs, biphasic) were held constant, but the timing of the pulses was altered throughout. The different patterns were interleaved by changing the stimulation pattern every half-hour. Half of all triggered syllables were stimulated, and the other half ("catch" trials) were not, so there was a control for comparison. Because sample size was limited relative to the respiration experiments, only two pulse patterns were compared at a time. In some experiments, the three pulses occurred over a duration of 9 ms, with the middle pulse either occurring 3 or 6 ms after the first pulse. In other experiments, the three pulses occurred over a duration of 12 ms, with the middle pulse either occurring 3 or 9 ms after the first pulse. The 6 VS birds in this experiment yielded 11 syllables to be analyzed, while the single DTB bird yielded 3 syllables.

*In vitro* muscle stimulation experiments were also conducted on the VS muscle from the syrinx, as was done with the *m. obliquus externus abdominis* in the previous section of this Aim. All of the methods are identical, except for muscle fibers being excised from a different muscle.

6.6.1.2 <u>Data analysis</u>

Pitch contours were calculated for song syllables during which stimulation occurred using a MATLAB script adapted from [166]. Once pitch contours were calculated for every triggered syllable, trials were separated by which stimulation pattern occurred or did not occur in the case of catch trials. The mean pitch contour for catch trial was subtracted from the pitch contours for stimulated syllable. The pitch contour was then aligned relative to onset of stimulation and averaged across trials of the same stimulation pattern. As was done in previous sections of this Aim, the d' statistic was calculated when comparing pairs of patterns with the same pulse rate but different timing of the middle pulse. wfANOVA was also used to calculate the significant difference between stimulation patterns that could not be attributed to variability between birds. *In vitro* force measurements were also compared using the d' statistic and wfANOVA as was done earlier in this Aim.

## 6.6.2 Results

Stimulation of the VS muscle during song using patterns that were identical in rate but varied in timing produced markedly different pitch effects during vocalization. Though the pitch contours associated with different syllables are quite diverse, they were made comparable by subtracting away the mean pitch contour when the muscle was not stimulated. When the two compared patterns were three pulses across 9 ms with the middle pulse either 3 ms or 6 ms after the first pulse, the pitch contour demonstrated a significant difference, with the former pattern producing a greater pitch change (Figure 28a). Across all 11 syllables, there were significant differences between stimulation patterns as evidenced by the bumps in the d' statistic approximately 10 ms after stimulation onset (Figure 28b). Though all syllables had significant differences, the shapes of those d' waveforms varied considerably compared to what was observed in the air sac pressure experiments above. Despite the large amount of inter-syllable variability,

wfANOVA revealed a significant difference between the pitch changes, which can be attributed to the variation in stimulation pattern (Figure 28c). When the middle pulse during a 12 ms stimulation pattern occurs at either 3 ms or 9 ms after the initial pulse, the difference in pitch contours was even greater than with the 9 ms stimulation patterns (Figure 28d). Again, the d' waveforms were significant for all 11 syllables while still showing variability across syllables (Figure 28e). The larger magnitude of effect relative to the 9 ms stimulation patterns helped to reveal slightly more uniformity across syllables. This was verified by wfANOVA, which demonstrated a significant difference between patterns that was greater in magnitude than that found for the 9 ms stimulation patterns (Figure 28f). We were able to perform this experiment in a single bird with its left DTB muscle implanted with stimulating electrodes. Across three stimulated syllables, we found similar results to those demonstrated in VS (Figure 29). However, there was no significant difference between the two 9 ms stimulation patterns according to wfANOVA. The magnitude of pitch changes were smaller across all syllables relative to VS stimulation. A greater sampling across multiple birds is required to further investigate both of these result. Together, these results showed that small changes in stimulation timing could have significant effects on vocalizations.
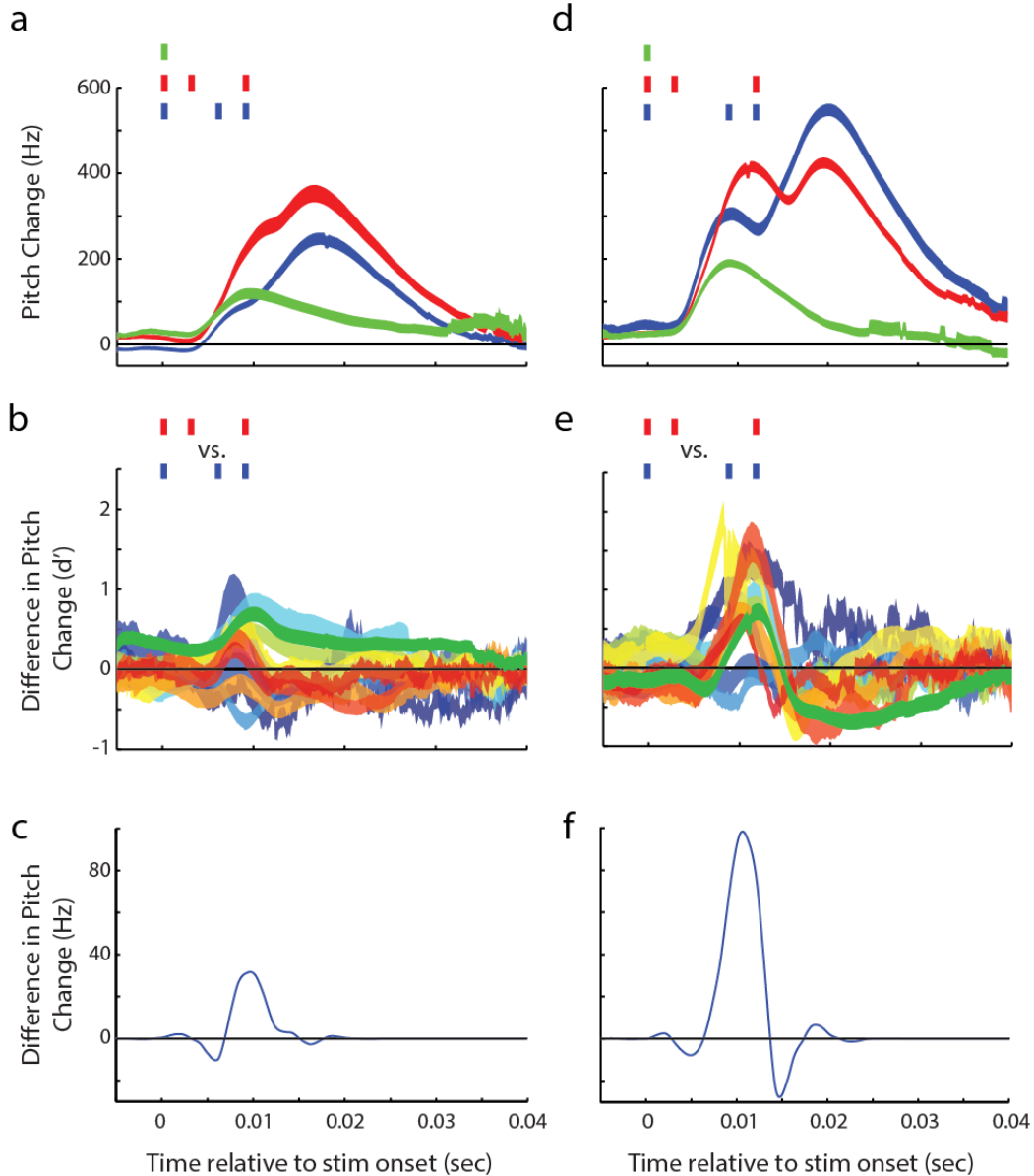
Figure 28: *In vivo* stimulation of the VS muscle during vocalizations produced significantly different pitch effects depending on the timing of the middle pulse in a 3-pulse train. (a) In one syllable, when the middle pulse occurs 3 ms after the initial pulse, a greater pitch change was achieved than when the middle pulse occurred at 6 ms, though the magnitudes aligned more closely after both patterns had featured a second pulse. (b) Across 11 syllables from 6 birds, the differences between pitch contours were all significant, but the shape of the d' waveform varied considerably across syllables. (c) Despite the large amount of variance across syllables, wfANOVA extracted a significant difference due to stimulation pattern, after accounting for inter-syllable variability. (d) When comparing the stimulation patterns with a middle pulse at 3 ms as opposed to 9 ms, the pitch contour difference was even more pronounced, with the two peaks easier to separate. (e) The differences, as measured by d', were even greater than in (b), though the variance across syllables remained. (f) wfANOVA extracted a significant difference that

was even greater in magnitude than that found between the pulse trains delivered in (a-c). The green traces in the foreground of (b) and (e) represent the d' statistic for examples shown in (a) and (d). Note that intervals represent the mean +/- 1 S.E. in plots (a) and (d) and the mean +/- 1 S.D. in plots (b) and (e).
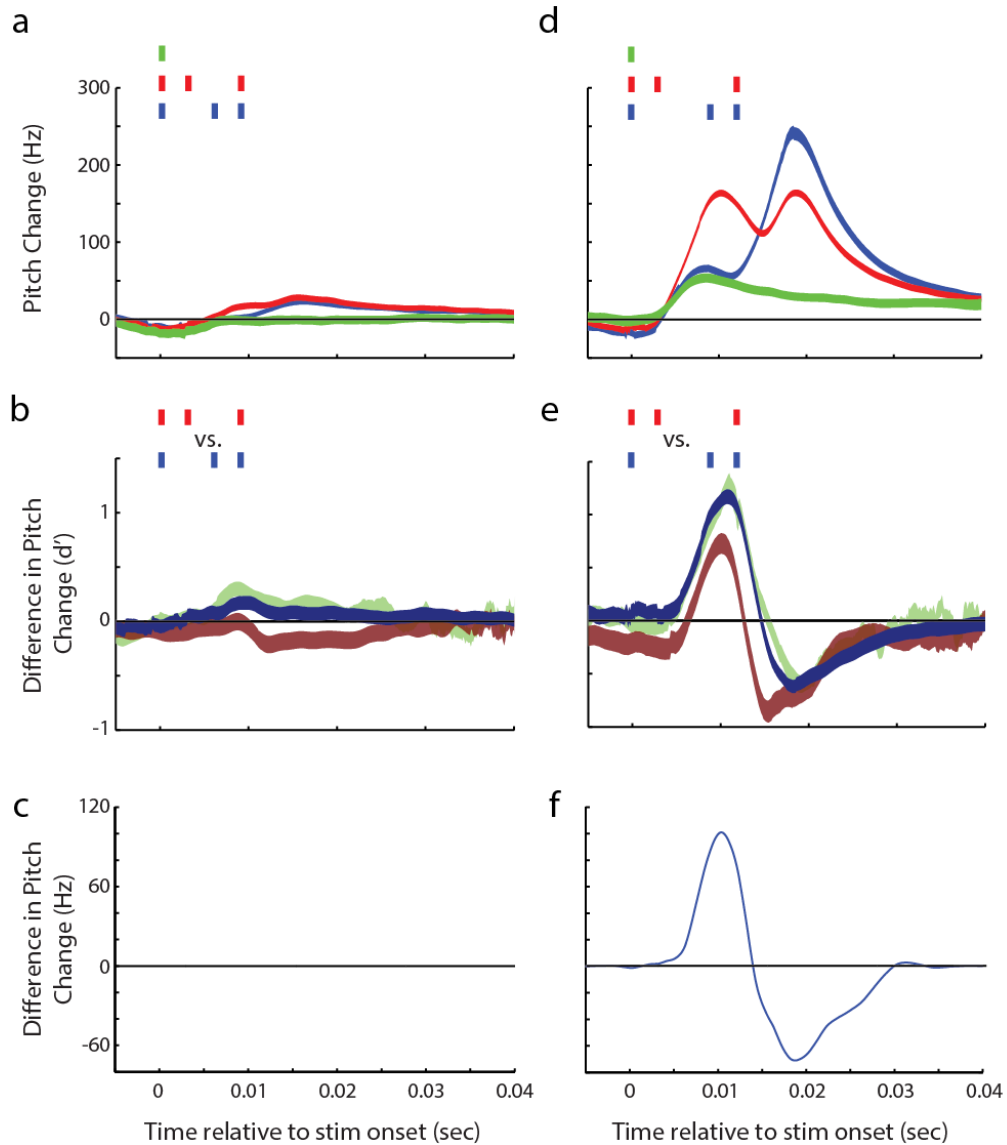


Figure 29: *In vivo* stimulation of the DTB muscle during vocalizations produced significantly different pitch effects depending on the timing of the middle pulse in a 3-pulse train. (a) In one syllable, when the middle pulse occurred 3 ms after the initial pulse, a greater pitch change was achieved than when the middle pulse occurs at 6 ms, though the magnitudes align more closely after both patterns have featured a second pulse. (b) Across 3 syllables in a single bird, the differences between pitch contours were clearly significant for two of the syllables, while the maroon waveform did not leave zero at the critical time point. (c) wfANOVA was not able to extract a significant difference between stimulation patterns, even after accounting for inter-syllable variability. (d)

When comparing the stimulation patterns with a middle pulse at 3 ms as opposed to 9 ms, the pitch contour difference was quite pronounced, with two separable peaks. (e) The differences, as measured by d', were much greater than in (b). (f) wfANOVA extracted a significant difference between 12 ms stimulation patterns after removing inter-syllable variability. The blue traces in the foreground of (b) and (e) represent the d' statistic for examples shown in (a) and (d). Note that intervals represent the mean +/- 1 S.E. in plots (a) and (d) and the mean +/- 1 S.D. in plots (b) and (e).

Similar to the previous section, we wanted to see if the importance of timing was mediated by the dynamics of the muscle. To test this, we excised fiber bundles from VS and stimulated them *in vitro*. The normalized force waveforms over 9 ms showed distinct differences, which could be attributed to the timing of the middle pulse and the fast dynamics of the muscle (Figure 30a). The d' statistic further demonstrated the differences between the two force responses with the metric depicting significant differences for all three birds (Figure 30b). Performing wfANOVA analysis revealed a significant difference between the stimulation patterns after accounting for inter-subject variability (Figure 30c). As expected, the resulting force waveforms were also significantly different when comparing two patterns over 12 ms (Figure 30d-f).
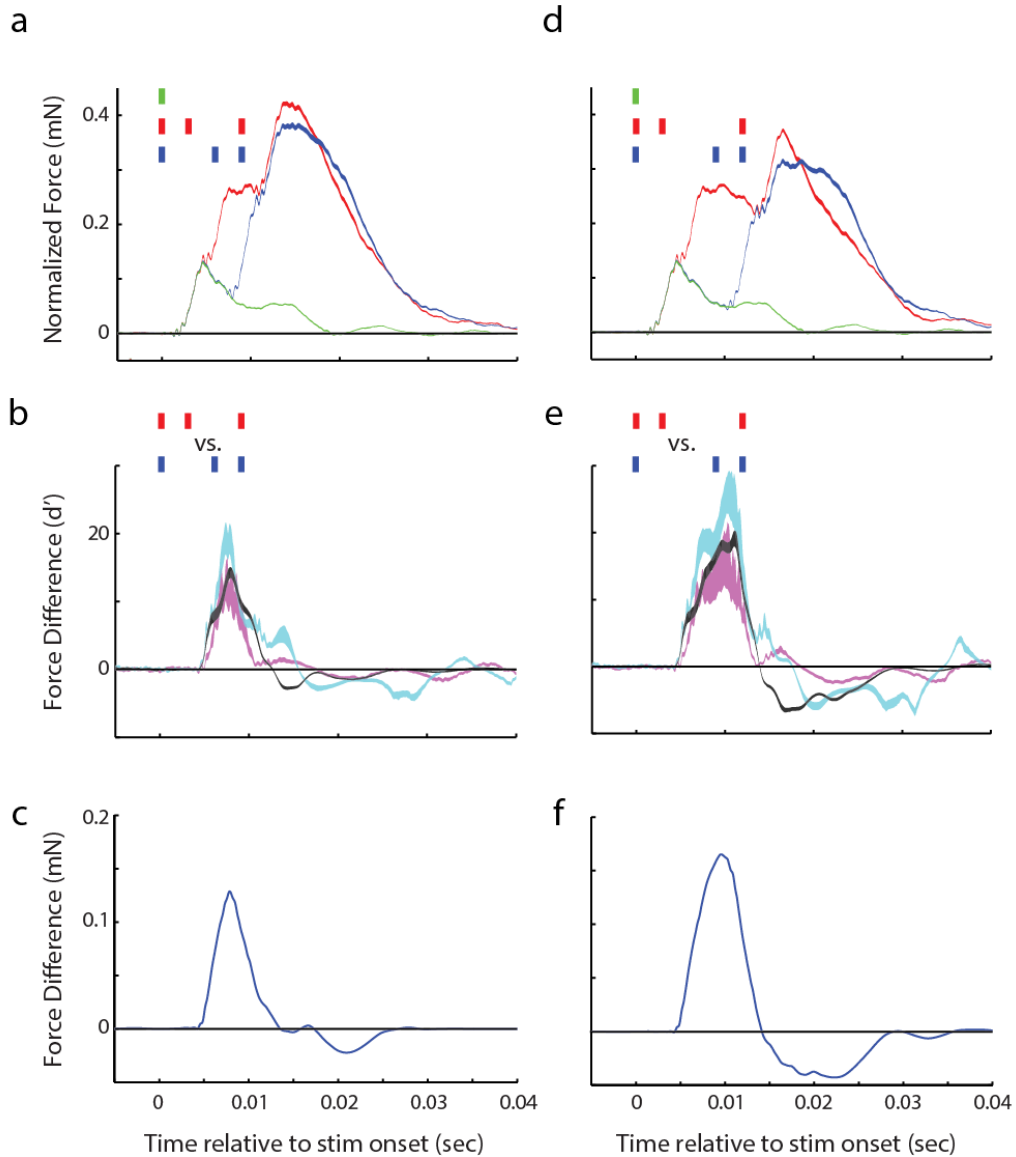
Figure 30: *In vitro* stimulation of the VS muscle demonstrated the importance of stimulation pulse timing on force. (a) The force waveforms showed clear differences between the two 9 ms patterns, with 3 levels corresponding to the onset of each pulse. (b) The difference between the two patterns was significant according to the d' statistic across all three birds. (c) Using wfANOVA, there was a significant difference between stimulation patterns even after accounting for inter-subject variability. (d-f) Same plots as (a-c) but with two different 12 ms stimulation patterns. The magenta traces in (b) and (e) represent the d' statistic for examples shown in (a) and (d). Note that intervals represent the mean +/- 1 S.E. in plots (a) and (d) and the mean +/- 1 S.D. in plots (b) and (e).

### 6.6.3 Discussion

The results of this section demonstrated that vocal behavior is sensitive to the timing of stimulation of a syringeal muscle. By adjusting the timing but not the rate of a 3 pulse stimulus, significant effects were observed on both the pitch of the vocalization as well as the force output of the muscle. The magnitude of the difference between stimulation patterns with the same rate was greater for the 12 ms patterns than for the 9 ms patterns. This was observed to a lesser degree in the *in vitro* force measurements. This difference could arise beyond the force output of the muscle itself but rather due to the biomechanics of the vocal organ. Interestingly, there was a considerable amount of variance in the effects of stimulation on pitch across different syllables relative to what was observed in previous experiments in which we measured air sac pressure while stimulating EXP. This result was not that surprising when considering the complexity of the acoustic transformation from muscle contraction to vocal behavior [85, 167]. This implication was further supported by the results of *in vitro* stimulation of VS, which were dramatically less variable. Moreover, the context-dependency of vocal muscles, as demonstrated in CHAPTER 4 [100], indicates that the effect of vocal muscle stimulation can vary depending on the syllable being produced as well as the activity of other vocal muscles. Despite all of the variability arising from stimulating across different syllables, we were still able to demonstrate a significant difference attributable to solely the stimulation pattern using wfANOVA. Therefore, it is important to consider the effect of syllable variability on the observed results in both this study and others that attempt to aggregate results across multiple birds' vocalizations.

In a limited sample size, we were able to analyze the effects of stimulation timing on the DTB muscle. The magnitude of pitch effects across all stimulation patterns appeared to be smaller than those observed during VS stimulation. This relates closely to the results of Aim 1, where VS stimulation was strongly associated with an increase in pitch, while DTB stimulation could have context-dependent effects on pitch. Another

interesting result was that wfANOVA did not find a significant difference between the two 9 ms stimulation patterns. Because we were able to see significant d' waveforms for two of the syllables, this result and the previous one likely need to be investigated further with a larger sample size. Future analysis may look to see if other acoustic parameters respond to stimulation timing as well as pitch did, particularly given that DTB appeared to be more closely associated with sound amplitude in Aim 1.

Whereas the previous section focusing on respiratory patterns was able to employ physiologically relevant stimulation patterns determined by motor unit recordings on respiration, we were limited to user-defined stimulation patterns. The timescale of stimulation patterns was informed by previous work indicating that vocal muscles could modulate behavior over 250 Hz, which computes to a period of 4 ms [53]. On the other hand, the syrinx may use its biomechanical properties to achieve modulation at this high of a rate [72], without the motor unit spiking that frequently. A previous study showed that songbirds in a reinforcement paradigm could learn changes within syllables on timescales of several milliseconds [166]. Songbirds may therefore implement this fine temporal control using the precise timing mechanisms observed in our stimulation experiments. It is important for future studies to bridge this gap by capturing single motor unit recordings from vocal muscles during song.

# CHAPTER 7

# CONCLUSIONS AND FUTURE DIRECTIONS

This thesis thoroughly investigated the role of vocal muscles in actuating signals from the brain into acoustic behavior. The results of all three Aims have significant impact on the field of motor control.

In Aim 1, vocal muscles were shown to be both multi-functional and context-dependent in their effects on acoustic behavior. This was demonstrated using *in vivo* EMG recordings, syllable-targeted *in vivo* muscle stimulation, and *ex vivo* muscle stimulation. These findings will shed light on the general principles of vocal behavior, especially for human speech. The results of Aim 1 suggest potential drawbacks to speech therapies focusing only on the activity of individual muscles. While this approach may be effective for muscles with fixed relationships with specific acoustic parameters, the context-dependency of some of these relationships may lead to undesired consequences. More effective therapy will likely need to focus on multiple vocal muscles as their coordination allows changes in single parameters despite each muscle being multi-functional. Future research focusing on the complex coordination of vocal muscles will help to unlock appropriate therapies for speech pathologies.

In Aim 2, I attempted to determine the functional connections between the premotor nucleus RA and vocal muscles in the songbird as a means of determining whether individual neurons controlled single or multiple muscles. While the Aim was unsuccessful due to low yield, multiple lessons were learned, which could be applied to future attempts beyond this project. The results of this Aim provide guidance for the vocal motor control field when studying neuromuscular activation patterns in anesthetized subjects. Broadly speaking, this Aim set the stage for future studies in any motor control system to identify the physiological existence of muscle synergies. Finding these synergies will help to distinguish between a mathematical outcome and the brain

actually using a simplified control scheme to control muscles, and subsequently, behavior.

In Aim 3, I demonstrated the importance of precise timing for vocal muscles in controlling both respiration and vocalizations. This was accomplished using both EMG and muscle stimulation with simultaneous air sac pressure recordings for respiration and *in vivo* muscle stimulation for song. These results will impact how the motor control field interprets the neural code, by adding another dimension (timing) to a code that is generally modeled by the neural firing rate. From a research perspective, the field can attempt to find more information about behavior in the timing of neural firing. Our results may also suggest a way for sensory and motor pathways to interact during motor learning. From a clinical perspective, these results will lead to potentially better implementations of BMIs, which could take spike timing into account when translating neural activity in machine outputs. Improving the efficiency of BMIs is critical for properly rehabilitating and replacing motor function in patients with paralysis or other peripheral motor loss.

## 7.1    Future directions for Aim 1

In Aim 1, we were able to correlate the activity of multiple muscles with acoustic output. However, in most cases, only one muscle was recorded at a time. By extending this project to record from multiple muscles at once, future work could investigate the presence of muscle synergies in songbirds. A muscle synergy exists when the control system exploits a reduction in dimensionality, in which there are fewer control signals than vocal muscles, which are activated in fixed proportions to each other [119]. A reduction in dimensionality of vocal muscles' activities would suggest a simpler model for neural control. Previous work has demonstrated muscle synergies in other motor systems like locomotion and fine hand movement [121, 168]. Because multiple muscles in songbirds are activated simultaneously during song production [41, 59], there is likely

to be a reduction in dimensionality in the activity of vocal muscles. To determine whether vocal muscle activity undergoes dimensionality reduction, future studies could use nonnegative matrix factorization (NMF) [122], which decomposes the muscles' EMG signals into the components that contribute the greatest variability to the overall signal. NMF has been used to identify muscle synergies in other systems [120]. To perform this analysis, multiple muscles must be recorded from, with successful analysis using at least six muscles [121]. Therefore, implementation of this approach would likely require the recording of EXP, VS, DTB, VTB, DS, and some combination of those muscles on the other side of the syrinx.

Another further extension of this work would be to look at the activity of vocal muscles during learning. Previous work has shown the ability to induce learning in both pitch and amplitude [48, 52]. In fact, by shifting auditory feedback, significant syllable pitch changes can be learned within one day [169], while syllable amplitude changes can be learned within minutes [52]. Both setups would allow the measurement of how vocal muscle activity changes during learning. While previous work has demonstrated adaptive changes in vocalizations [48, 52, 115], it is unknown how single muscles are used to drive vocal learning. Aim 1 examined the functionality of vocal muscles only in the steady state. A single muscle may control more than one acoustic parameter during unperturbed song, but it is important to establish whether the song system will use that muscle to implement learning changes in any of those individual acoustic parameters. Additionally, if future work detected the presence of muscle synergies during learning, it would suggest that the brain can tune individual control signals to implement vocal changes.

### 7.2    Future directions for Aim 2

While Aim 2 failed to characterize the projections from premotor neurons in RA to vocal muscles, it did shed light on how this experiment could be conducted in future iterations.

One of the limitations of Aim 2 was the inability to drive modulation during song playback in Bengalese finches. This was overcome by using zebra finches, whose neural substrates of song experience modulation in response to BOS playback [128-130]. A stronger form of the approach attempted in this Aim would be to perform the experiment in behaving Bengalese finches. By performing the experiment in a chronically behaving animal, future studies would not be concerned with the sparseness of EMG activity that is observed during BOS playback (Figure 14). The experimenter would thus be more likely to encounter a relationship between a neuron and a muscle that is short-latency and prospective, i.e. the neuron fires before the muscle. Though it will likely be more difficult to record from RA and vocal muscles in a chronically behaving animal, we have recorded from both in succession, so would not expect an issue as far as the bird carrying the necessary weight while singing. This approach would better investigate the hypothesis that Aim 2 originally set out to do.

A more ambitious version of the above future direction would look to record from both RA and the vocal muscles during the vocal learning described in "Future directions for Aim 1." Though the behavioral effects of pitch-adjusted auditory feedback on birdsong have been shown, the neuromuscular mechanism for this phenomenon remains unknown. During simultaneous RA and vocal muscle recording, vocal learning would be induced by delivering either pitch-shifted auditory feedback through headphones [48, 103, 170, 171] or a punishing white noise stimulus conditioned on pitch [115, 166, 172]. This study would be key to determining how the premotor activity of RA is reshaped during error correction. Localizing plasticity to RA would allow subsequent studies to look upstream for inputs onto RA that guide learning.

### 7.3    Future directions for Aim 3

A feasible extension of the studies in Aim 3 would be to look at how motor timing is regulated across populations of motor units. We had found that millisecond-scale changes

in motor unit firing correlated with significant differences in respiratory pressure. However, it is not clear if the result was due to one specific motor unit or synchrony among motor units. One way to analyze this further would be to record multiple motor units at the same time during respiration. Not only could one investigate the synchrony within these populations but also look at the effects of motor timing across populations. These studies may help to understand how the timing of the neural signal is being implemented in motor output.

In Aim 3, we were limited to investigating the activity of motor units during respiration because muscle activity tends to be much greater during song, and thus swamps the EMG signal [173]. While we were able to show the importance of timing through stimulation during song, a further extension of that work would be to apply the analysis used on motor units during breathing to motor units during song. This would go a lot further in explaining how the brain controls muscles, as respiration is often thought to behave like a CPG [71, 163] while song is believed to be controlled more actively by the brain. As is suggested in the Appendix, it is not currently easy to record single motor units during song. One way to overcome this issue is to redesign the electrode arrays by optimizing electrode size and layout. Another option for recording motor unit activity would be to record from neurons in the nXIIts, though one would not be able to differentiate muscles and the nucleus contains both sensory and motor neurons. A third option is to return to using high impedance fine wire electrodes. We were previously able to record what we believe to be a single motor unit once in the DTB muscle using fine wire electrodes. Though the sample size was limited, we were able to apply an analysis similar to that used in [138]. By applying metric space analysis [138, 174, 175] on the motor unit spike patterns in the 40 ms preceding a given syllable, we found that the mutual information was maximized when $q > 0$, indicating that each case was a temporal case rather than a rate case, where only spike count mattered (Figure 31). For a full description of the analysis techniques, consult [138]. All of this analysis is very

preliminary but suggests that future work should look to record single motor units during song.
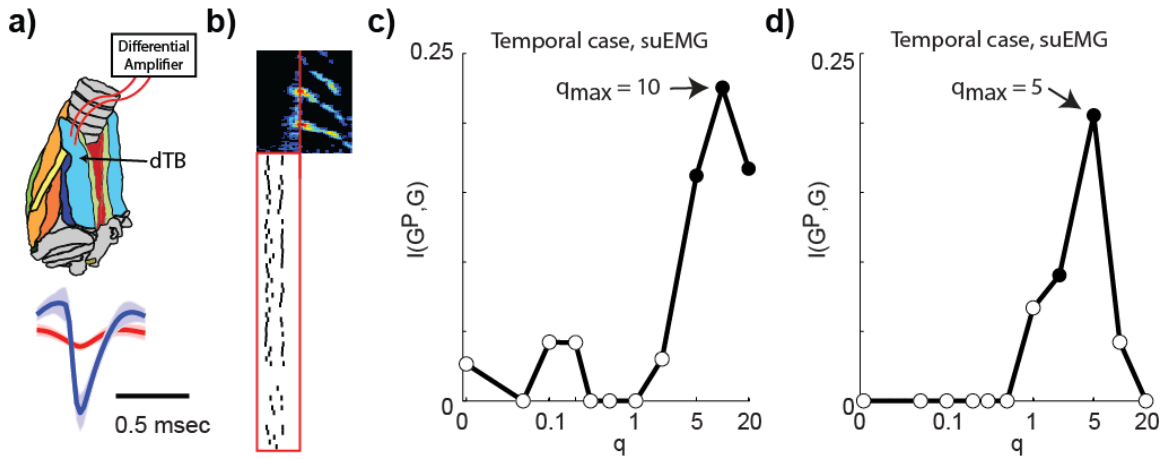


Figure 31: Single-unit EMG recordings suggest temporal encoding in vocal muscles. (a) Fine wires implanted in a single vocal muscle (DTB) yielded a recording of a single motor unit. Anatomical schematic shows a dorsal and posterior view of the left side of the syrinx, with vocal muscles shown in color and non-muscular structure shaded gray. Blue and red waveforms at bottom show the single motor unit and background noise waveforms (dark lines show mean waveform, shaded region shows 1 S.D.). (b) Raster of single-unit EMG (suEMG) activity during a song syllable. Red box shows the 40 ms premotor window. (c) Temporal case, acoustic groupings by amplitude for the syllable shown in panel (b). (d) Another temporal case, here with acoustic groupings by spectral entropy, for another syllable produced during the same suEMG recording.

# APPENDIX

## A.1.  A micro-scale, flexible, high-density electrode array for performing multi- and single-unit electromyographic recordings[2]

### A.1.1.  Introduction

EMG provides researchers and clinicians with a window into the activity of individual muscles. This technique is often employed using skin-level surface arrays or intramuscular fine wire electrodes. Skin-level surface arrays are noninvasive but can prove problematic when recording very small or deep muscles. Intramuscular fine wire electrodes, in contrast, can often cause damage to the muscle it is recording, preventing its use for long-term recordings. Moreover, it can be difficult to record from multiple muscles in a very small area using either method. Furthermore, isolating the signals arising from a single motor units, which is made up of a motor neuron and the muscle fibers it innervates, using fine wire or surface EMG remains challenging. To help remedy the shortcomings of traditional EMG techniques, we developed micro-scale, flexible, high-density electrode arrays that sit on the surface of individual muscles to record EMG signals.

### A.1.2.  Device development

To fabricate these electrodes, we collaborated with Premitec, Inc. (Raleigh, NC). The gold electrodes were fabricated on 20 micron thick photo-definable polyimide with a

---

[2] **Srivastava, K.H.** & Sober, S.J. "A Micro-scale, flexible, high-density electrode array for performing multi- and single-unit electromyographic recordings [abstract]." Program No. ThBT1.42. Montpellier, France: *Neural Engineering*, 2015. Online.

range of contact sizes and spacings. The electrode exposures ranged from 25 to 300 microns in diameter and were separated by as little as 25 microns. Several arrangements of electrodes (16 per array) were fabricated including a four-by-four grid, four tetrodes, and configurations designed specifically for the vocal organ in Bengalese finches (Figure 32).
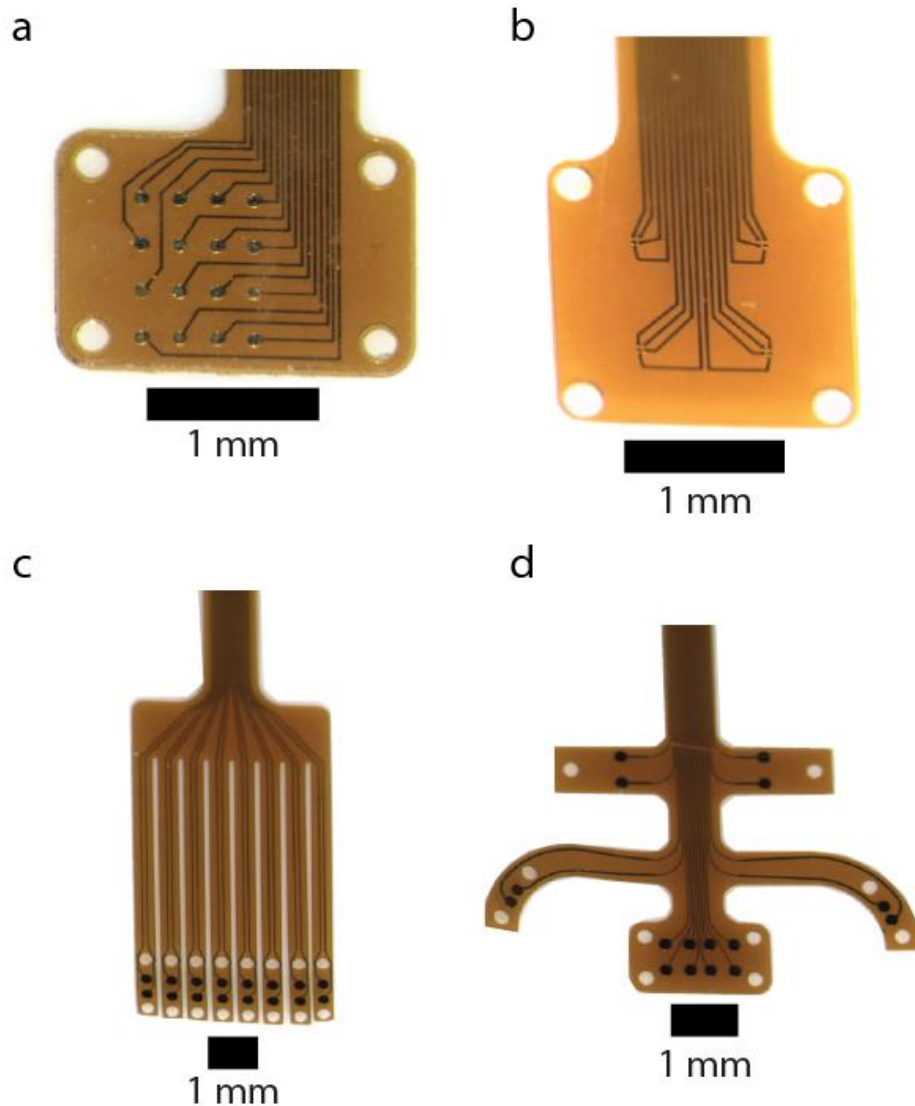


Figure 32: Zoomed in photographs of different arrangements of 16 electrodes on micro-scale, flexible, high-density electrode arrays. (a) In the first design, the 16 electrodes (200 μm diameter) were spaced evenly in a 4 x 4 grid. This array could be used on the EXP muscle group as well as the ventral surface of the syrinx to record left and right VS and VTB. (b) The 16 electrodes (25 μm diameter) could also be arranged as 4 tetrodes to be placed on EXP or the ventral syrinx. (c) The 8-finger array allowed pairs of electrodes (300 μm diameter) to be sutured in place on the syrinx. (d) The tree branch design

featured electrodes (300 μm diameter) designed to target, from top to bottom, TL, DTB, and the ventral syrinx (VS and VTB).

### A.1.3. Device testing

The different arrays were sutured to their respective muscle groups (either EXP or around the syrinx, Figure 33). When suturing the array (either Figure 32a or b) to the EXP group, usually 3 sutures sufficed. The neck of the array was then fed under the skin to the bird's back, where it plugged into an adapter that interfaced with the RHD 2132 digital amplifier (Intan Technologies). The adapter rested on a bird "backpack" as was used in previous studies [41, 59, 60]. A lead was plugged into the amplifier and a commutator for recording. For syringeal recordings, the neck of the array was fed under the skin to the base of the neck to plug into an adapter for the amplifier before the array was sutured in place. For the designs that wrap around the syrinx or trachea (Figure 32d), it was better to suture the flaps together behind the syrinx, rather than suture directly to the muscle. Suturing to the muscle caused too much strain on the tissue. When performing this difficult technique, one must poke the suture needle through one flap, then through a clear membrane attaching the back of the syrinx to the esophagus, then through the other flap, then back through the clear membrane before tying a knot. Once in place, this held the array against the muscle remarkably well. In both EXP and syringeal recordings, birds were trained with the amplifier plugged in (before array was implanted), to ensure the bird would sing in the given setup.
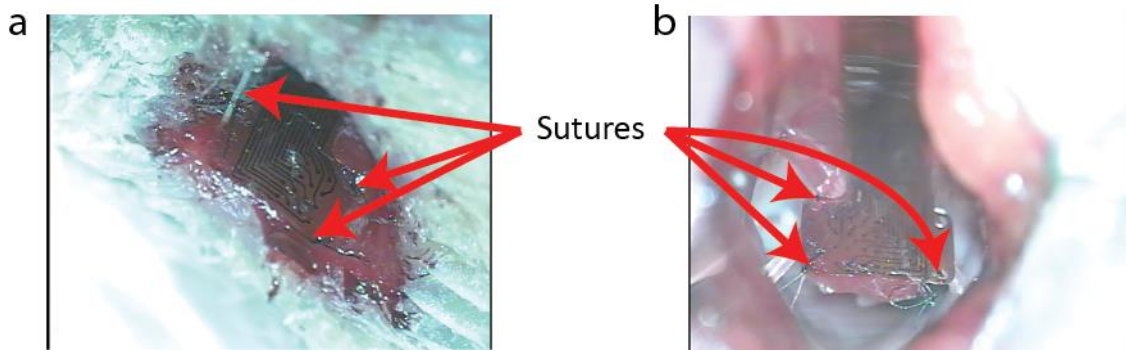
Figure 33: Flexible, microelectrode arrays were attached to the surface of muscles. Sutures were used to fix the array on the expiratory muscle group (a) as well as the ventral surface of the syrinx (b) which covered the left and right VS and VTB muscles.
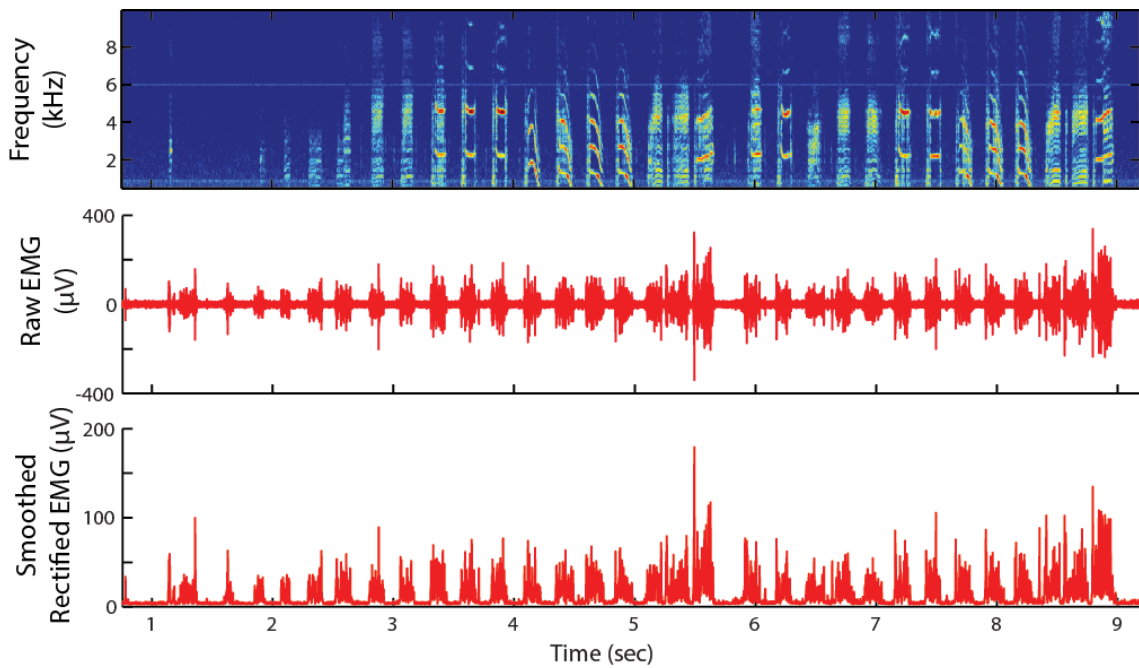


Figure 34: Flexible, microelectrode array recorded EMG activity in vocal muscle during song. Recording demonstrated periodic, syllable-locked EMG activity that was featured a relatively high SNR.
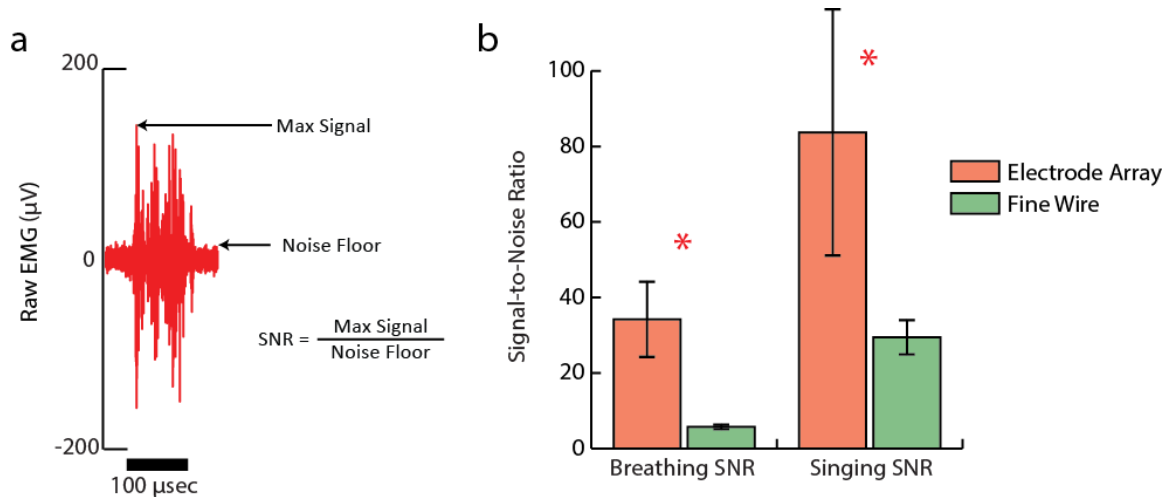
Figure 35: Flexible, microelectrode arrays significantly improved SNR of EMG recordings compared to fine wire electrodes. (a) The maximum signal divided by the noise floor was used to calculate SNR. (b) The SNR for recordings using the electrode array was significantly greater than that of fine wire recordings both during breathing and singing.

With these arrays, we were able to acquire high-quality EMG recordings from 16 locations simultaneously during both quiet respiration and vocalization (Figure 34). The increased number of channels allowed the experimenter to select which channels should be subtracted from each other to create bipolar signals. The signal-to-noise ratios (SNRs) achieved during these recordings were compared to previous recordings made using intramuscular electrodes. During both vocalization and breathing, the SNR was significantly greater using the flexible arrays than with intramuscular electrodes (Figure 35). Additionally, the quality of EMG recordings lasted over several days, indicating that these arrays could be used in both acute and chronic experiments. Because of the high specificity and impedance of individual electrodes, we were able to extract single motor unit data in some cases in addition to the multiunit signals more commonly used in EMG analysis (Figure 36). This result was more common when looking at low levels of muscle activity, such as during quiet respiration, as compared to high levels during vocalization.

Because we could record sixteen unipolar signals in a very small area, we had increased the probability of recording a single motor unit while allowing us to test how different intramuscular segments were differentially recruited. In the case of very small muscles, as are found in the Bengalese finch vocal organ (~2 mm x ~4 mm), we could record from multiple muscles simultaneously using the electrode array. The ability to isolate single motor units with these arrays also presents the opportunity to study spiking patterns in individual motor neurons during behavior. Further development of this micro-scale, flexible electrode array will let us compare the precision of single motor units across muscles and behavioral contexts.
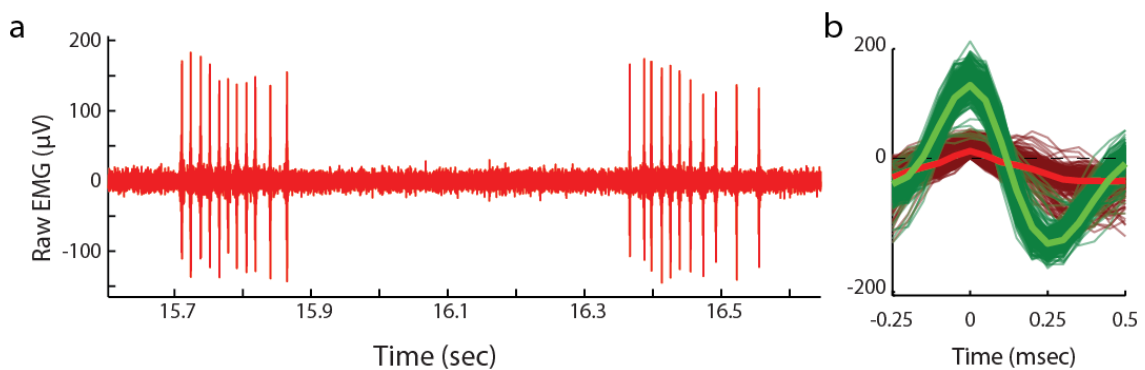


Figure 36: Array recordings enabled the isolation of single motor units. (a) A sample recording from the expiratory muscle group during breathing revealed a spiking motor unit. (b) Clustering the spikes against noise showed a well-isolated single motor unit.

### A.1.4. Issues to be solved in future generations and applications of arrays

It was much easier to record from muscles with these arrays in acute settings where one can move the array to optimize recording of single motor units and not worry about the array breaking. During chronic EXP recordings, the neck of the array exited the skin and plugged into the adapter, leaving the array exposed for several millimeters. The array often broke at this location after a few days. Reinforcement of this area with tape often led to the array breaking at the point where the tape ends. The latest generation of the arrays has silicone gel around this area, though this has not been fully tested.

115

During syringeal recordings, the array typically broke at the insertion point into the adapter. This area is coated with dental cement during implantation, but the array would break just below the dental cement. Again, these arrays now have silicone gel in this area, though it has not been fully tested. Strengthening the array could help, but it often just moved the breakpoint to the weaker areas while sacrificing flexibility. Another potential solution is to interface the array to wires under the intraclavicular skin above the air sac, and then run wires to the head. This might reduce the potential for breakage but also reduce the number of feasible channels to wire to the head. Often it was difficult to get the bird to sing during syringeal array recordings. In general, surgical outcomes were much better when the air sac was sutured closed, with bird sometimes singing the next day. This could be sometimes more difficult, when one needs more space in the air sac to implant the array, thus requiring more air sac to be cut back. One way to improve this was to ensure the air sac stayed moist with saline throughout the surgery.

As was demonstrated in the methods in Aim 3, it was much easier to record and isolate single motor units when the bird was breathing. This was likely due to the fact that vocal muscle activity levels are, in general, lower during respiration than they are during song [173]. Being able to extract single motor units during song would enable many interesting future research projects. While the manner in which to solve this problem is not clear at the moment, future work should focus on redesigning electrode size and layout to increase the probability of isolating single motor units during high levels of activity, such as those observed during song.

### A.1.5. Other applications

Because these devices are designed to be used on small muscles, they could be applied to EMG recordings of any size muscles. In fact, using them on large muscles might allow researchers to better focus on the activity of sections of muscles which might be made up of motor units that behave differently than the whole. Despite these electrode arrays

being designed for EMG applications, they could theoretically be used to record any electrophysiological signal because of its biocompatibility.

# REFERENCES

1.      Maguire, G., et al., *Exploratory randomized clinical study of Pagoclone in persistent developmental stuttering: The EXamining Pagaclone for peRsistent dEvelopmental Stuttering Study.* J Clin Pyschopharm, 2010. **30**(1): p. 48-56.

2.      Immelman, K., *Song development in the zebra finch and other estrilid finches. Bird vocalizations*, ed. R.A. Hinde. 1969, New York: Cambridge UP.

3.      Konishi, M., *The role of auditory feedback in the control of vocalizations in the white-crowned sparrow.* Z Tierpychol, 1965. **22**: p. 770-783.

4.      Nottebohm, F., T.M. Stokes, and C.M. Leonard, *Central control of song in the canary.* J Comp Neurol, 1976. **165**(4): p. 457-486.

5.      Reiner, A., et al., *Songbirds and the revised avian brain nomenclature.* Ann N Y Acad Sci, 2004. **1016**(77-108).

6.      *Statistics on Parkinson's*. 2015   [cited 2015 October 19]; Available from: http://www.pdf.org/en/parkinson_statistics.

7.      *Amyotrophic Lateral Sclerosis (ALS) Fact Sheet*. 2015  [cited 2015 October 19]; Available                                                                          from: http://www.ninds.nih.gov/disorders/amyotrophiclateralsclerosis/detail_ALS.htm.

8.      *What You Need to Know About Stroke*. 2015  [cited 2015 October 19]; Available from: http://stroke.nih.gov/materials/needtoknow.htm.

9.      Parnes, S.M., A.S. Lavorato, and E.N. Myers, *Study of plastic dysphonia using videofiberoptic laryngoscopy.* Ann Otol Rhinol Laryngol, 1978. **87**(3): p. 322-326.

10.     Sapir, S., L. Ramig, and C. Fox, *Speech and swallowing disorders in Parkinson disease.* Curr Opin Otolaryngol Head Neck Surg, 2008. **16**(3): p. 205-210.

11.     Lincoln, M., A. Packman, and M. Onslow, *Altered auditory feedback and the treatment of stuttering: a review.* J Fluency Disord, 2006. **31**(2): p. 71-89.

12.     Fee, M.S., A.A. Kozhevnikov, and R.H. Hahnloser, *Neural mechanisms of vocal sequence generation in the songbird.* Ann N Y Acad Sci, 2004. **1016**: p. 153-170.

13.     Hahnloser, R.H., A.A. Kozhevnikov, and M.S. Fee, *An ultra-sparse code underlies the generation of neural sequences in songbird.* Nature, 2002. **419**(6902): p. 65-70.

14. Ashmore, R.C., J.M. Wild, and M.F. Schmidt, *Brainstem and forebrain contributions to the generation of learned motor behaviors for song.* J Neurosci, 2005. **25**(37): p. 8543-8554.

15. Sober, S.J., M.J. Wohlgemuth, and M.S. Brainard, *Central contributions to acoustic variation in birdsong.* J Neurosci, 2008. **28**(41): p. 10370-10379.

16. Kao, M.H., A.J. Doupe, and M.S. Brainard, *Contributions of the avian basal ganglion-forebrain circuit to real-time modulation of song.* Nature, 2005. **433**(7026): p. 638-343.

17. Leonardo, A. and M.S. Fee, *Ensemble coding of vocal control in birdsong.* J Neurosci, 2005. **25**(3): p. 652-661.

18. Cheney, P.D. and E.E. Fetz, *Functional classes of primate corticomotoneuronal cells and their relation to active force.* J Neurophysiol, 1980. **44**(4): p. 773-791.

19. Davidson, A.G., M.H. Schieber, and J.A. Buford, *Bilateral spike-triggered average effects in arm and shoulder muscles from the monkey pontomedullary reticular formation.* J Neurosci, 2007. **27**(30): p. 8053-8058.

20. Vicario, D.S., *Organization of the zebra finch song control system: II. Functional organization of outputs from nucleus Robustus Archistriatalis.* J Comp Neurol, 1991. **309**(4): p. 486-494.

21. Vicario, D.S. and F. Nottebohm, *Organization of the zebra finch song control system: I. Representation of syringeal muscles in the hypoglossal nucleus.* J Comp Neurol, 1988. **271**(3): p. 346-354.

22. Fetz, E.E. and P.D. Cheney, *Postspike facilitation of forelimb muscle activity by primate corticomotoneuronal cells.* J Neurophysiol, 1980. **44**(4): p. 751-772.

23. McKiernan, B.J., et al., *Corticomotoneuronal postspike effects in shoulder, elbow, wrist, digit, and intrinsic hand muscles during a reach and prehension task.* J Neurophysiol, 1998. **80**(4): p. 1961-1980.

24. Fuglevand, A.J., D.A. Winter, and A.E. Patla, *Models of recruitment and rate coding organization in motor-unit pools.* J neurophysiol, 1993. **70**(6): p. 2470-2488.

25. Callahan, D.M., B.R. Umberger, and J.A. Kent-Braun, *A computational model of torque generation: neural, contractile, metabolic and musculoskeletal components.* PLoS One, 2013. **8**(2): p. e56013.

26. Burke, R., *Motor units: anatomy, physiology, and functional organization.* Comprehensive Physiology, 1981.

27.     Binder-Macleod, S.A. and C.B.r. Barker, *Use of a catchlike property of human skeletal muscle to reduce fatigue.* Muscle Nerve, 1991. **14**(9): p. 850-857.

28.     Zhurov, Y. and V. Brezina, *Variability of motor neuron spike timing maintains and shapes contractions of the accessory radula closer muscle of Aplysia.* J Neurosci, 2006. **26**(26): p. 7056-7070.

29.     Krakauer, J.W. and R. Shadmehr, *Consolidation of motor memory.* Trends Neurosci, 2006. **29**(1): p. 58-64.

30.     Wolpert, D.M., *Probabilistic models in human sensorimotor control.* Hum Movement Sci, 2007. **26**(4): p. 511-524.

31.     Doupe, A.J. and P.K. Kuhl, *Birdsong and human speech: common themes and mechanisms.* Annu Rev Neurosci, 1999. **22**: p. 567-631.

32.     Paton, J.A.M., K R and F. Nottebohm, *Bilateral organization of the vocal control pathway in the budgerigar, Melopsittacus undulatus.* J Neurosci, 1981. **1**(11): p. 1279-1288.

33.     Brenowitz, E.A., A.P. Arnold, and P. Loesche, *Steroid accumulation in song nuclei of a sexually dimorphic duetting bird, the rufous and white wren.* J Neurobiol, 1996. **31**(2): p. 235-244.

34.     Wild, J.M., *Neural pathways for the control of birdsong.* J Neurobiol, 1997. **33**(5): p. 653-670.

35.     Perkel, D., *Origin of the anterior forebrain pathway.* Ann N Y Acad Sci, 2004. **1016**: p. 736-748.

36.     Olveczky, B., A. Andalman, and M.S. Fee, *Vocal experimentation in the juvenile songbird requires a basal ganglia circuit.* PLoS Bio, 2005. **508**(5): p. e153.

37.     Garst-Orozco, J., B. Babadi, and B. Olveczky, *A neural circuit mechanism for regulating vocal variability during song learning in zebra finches.* Elife, 2014: p. e03697.

38.     Gale, S.D., A.L. Person, and D.J. Perkel, *A novel basal ganglia pathway forms a loop linking a vocal learning circuit with its dopaminergic input.* J Comp Neurol, 2008. **508**(5): p. 824-839.

39.     Ohman, S.E., *Numerical model of coarticulation.* J Acoust Soc Am, 1967. **41**(2): p. 310-320.

40.     Fowler, C.A. and E. Saltzman, *Coordination and coarticulation in speech production.* Lang Speech, 1993. **36**(2,3): p. 171-195.

41.     Goller, F. and R.A. Suthers, *Role of syringeal muscles in controlling the phonology of bird song.* J Neurophysiol, 1996a. **76**(1): p. 287-300.

42.     Roubeau, B., C. Chevrie-Muller, and J. Lacau Saint Guily, *Electromyographic activity of strap and cricothyroid muscles in pitch change.* Acta Otolaryngol, 1997. **117**(3): p. 459-464.

43.     Reinke, H. and J.M. Wild, *Identification and connections of inspiratory premotor neurons in songbirds and budgerigar.* J Comp Neurol, 1998. **391**(2): p. 147-163.

44.     Larsen, O.N. and F. Goller, *Direct Observation of syringeal muscle function in songbirds and a parrot.* J Exp Biol, 2002. **205**(1): p. 25-35.

45.     Waldstein, R.S., *Effects of postlingual deafness on speech production: implications for the role of auditory feedback.* J Acoust Soc Am, 1990. **88**(5): p. 2099-2114.

46.     Okanoya, K. and A. Yamaguchi, *Adult Bengalese finches (Lonchura striata var. domestica) require real-time auditory feedback to produce normal song syntax.* J Neurobiol, 1997. **33**(4): p. 343-356.

47.     Houde, J.F. and M.I. Jordan, *Sensorimotor adaptation in speech production.* Science, 1998. **279**(5354): p. 1213-1216.

48.     Sober, S.J. and M.S. Brainard, *Adult birdsong is actively maintained by error correction.* Nat Neurosci, 2009. **12**(7): p. 927-931.

49.     Nagel, K.I. and A.J. Doupe, *Organizing principles of spectro-temporal encoding in the avian primary auditory area field L.* Neuron, 2008. **58**(6): p. 938-955.

50.     Mello, C.V., F. Nottebohm, and D.F. Clayton, *Repeated exposure to one song leads to a rapid and persistent decline in an immediate early gene's response to that song in zebra finch telencephalon.* J Neurosci, 1995. **15**(10): p. 6919-6925.

51.     Mello, C.V., D.S. Vicario, and D.F. Clayton, *Song presentation induces gene expression in the songbird forebrain.* Proc Natl Acad Sci U S A, 1992. **89**(15): p. 6818-6822.

52.     Osmanski, M.S. and R.J. Dooling, *The effect of altered auditory feedback on control of vocal production in budgerigars (Melopsittacus undulatus).* J Acoust Soc Am, 2009. **126**(2): p. 911-919.

53.     Elemans, C.P., et al., *Superfast vocal muscles control song production in songbirds.* PLoS One, 2008. **3**(7): p. e2581.

54.     During, D.N., et al., *The songbird syrinx morphome: a three-dimensional, high-resolution, interactive morphological map of the zebra finch vocal organ.* BMC Biol, 2013. **11**(1).

55.    Goller, F. and R.A. Suthers, *Implications for lateralization of bird song from unilateral gating of bilateral motor patterns.* Nature, 1995. **373**: p. 63-66.

56.    Suthers, R.A., et al., *Bilateral song production in domestic canaries.* J Neurobiol, 2004. **60**(3): p. 381-393.

57.    Allan, S.E. and R.A. Suthers, *Lateralization and motor stereotypy of song production in the brown-headed cowbird.* J Neurobiol, 1994. **25**(9): p. 1154-1166.

58.    Goller, F. and B.G. Cooper, *Peripheral motor dynamics of song production in the zebra finch.* Ann N Y Acad Sci, 2004. **2004**(1016): p. 130-152.

59.    Goller, F. and R.A. Suthers, *Role of syringeal muscles in gating airflow and sound production in singing brown thrashers.* J Neurophysiol, 1996b. **75**(2): p. 867-876.

60.    Suthers, R.A., F. Goller, and R.S. Hartley, *Motor dynamics of song production by mimic thrushes.* J Neurobiol, 1994. **25**(8): p. 917-936.

61.    Suthers, R.A., *Peripheral control and lateralization of birdsong.* J Neurobiol, 1997. **33**(5): p. 632-652.

62.    Williams, H., et al., *Right-side dominance for song control in the zebra finch.* J Neurobiol, 1992. **23**(8): p. 1006-1020.

63.    Secora, K.R., et al., *Syringeal specialization of frequency control during song production in the Bengalese finch (Lonchura striata domestica).* PLoS One, 2012. **7**(3): p. e34135.

64.    Goller, F. and R.A. Suthers, *Bilaterally symmetrical respiratory activity during lateralized birdsong.* J Neurobiol, 1999. **41**(4): p. 513-523.

65.    Brackenbury, J.H., *Lung-air-sac anatomy and respiratory pressures in the bird.* J Exp Biol, 1972. **57**(2): p. 543-550.

66.    Brackenbury, J.H., *Airflow dynamics in the avian lung as determined by direct and indirect methods.* Respir Physiol, 1971. **13**(3): p. 319-329.

67.    Brackenbury, J.H., *Respiratory mechanics in the bird.* Comp Biochem Physiol A Comp Physiol, 1973. **44**(2): p. 599-611.

68.    Gaunt, A.S., R.C. Stein, and S.L.L. Gaunt, *Pressure and air flow during distress calls of the starling, Sturnus vulgaris (Aves; Passeriformes).* Journal of Experimental Zoology, 1973. **183**(2): p. 241-261.

69.    Schmidt, M.F., R.C. Ashmore, and E.T. Vu, *Bilateral control and interhemispheric coordination in the avian song motor system.* Ann N Y Acad Sci, 2004. **1016**: p. 171-186.

70.     Wang, C.Z., et al., *Rapid interhemispheric switching during vocal production in a songbird.* PLoS Biol, 2008. **6**(10): p. e250.

71.     Suthers, R.A., F. Goller, and J.M. Wild, *Somatosensory feedback modulates the respiratory motor program of crystallized birdsong.* Proc Natl Acad Sci U S A, 2002. **99**(8): p. 5680-5685.

72.     Elemans, C.P.H., et al., *Universal mechanisms of sound production and control in birds and mammals.* Nat Comm, in press.

73.     Van den Berg, J., *Myoelastic-aerodynamic theory of voice production.* Journal of Speech, Language, and Hearing Research, 1958. **1**(3): p. 227-244.

74.     Titze, I.R., *Comments on the myoelastic-aerodynamic theory of phonation.* Journal of Speech, Language, and Hearing Research, 1980. **23**(3): p. 495-510.

75.     Titze, I.R., *Principles of voice production.* 2000: National Center for Voice and Speech.

76.     Titze, I.R. and F. Alipour, *The myoelastic aerodynamic theory of phonation.* 2006: National Center for Voice and Speech.

77.     Herbst, C.T., et al., *How low can you go? Physical production mechanism of elephant infrasonic vocalizations.* Science, 2012. **337**(6094): p. 595-599.

78.     Titze, I.R., *On the relation between subglottal pressure and fundamental frequency in phonation.* The Journal of the Acoustical Society of America, 1989. **85**(2): p. 901-906.

79.     Titze, I.R. and W.J. Strong, *Normal modes in vocal cord tissues.* The Journal of the Acoustical Society of America, 1975. **57**(3): p. 736-744.

80.     Švec, J.G., et al., *Resonance properties of the vocal folds: In vivo laryngoscopic investigation of the externally excited laryngeal vibrations.* The Journal of the Acoustical Society of America, 2000. **108**(4): p. 1397-1407.

81.     Berry, D.A., *Mechanisms of modal and nonmodal phonation.* Journal of Phonetics, 2001. **29**(4): p. 431-450.

82.     Amador, A. and D. Margoliash, *A mechanism for frequency modulation in songbirds shared with humans.* J Neurosci, 2013. **33**(27): p. 11136-11144.

83.     Elemans, C.P., R. Zaccarelli, and H. Herzel, *Biomechanics and control of vocalization in a non-songbird.* J R Soc Interface, 2008. **5**(24): p. 691-703.

84.     Daley, M. and F. Goller, *Tracheal length changes during zebra finch song and their possible role in upper vocal tract filtering.* J Neurobiol, 2004. **59**(3): p. 319-330.

85.     Fee, M.S., et al., *The role of nonlinear dynamics of the syrinx in the vocalizations of a songbird.* Nature, 1998. **396**(6697): p. 67-71.

86.     Alonso, R., F. Goller, and G.B. Mindlin, *Motor control of sound frequency in birdsong involves the interaction between air sac pressure and labial tension.* Phys Rev E Stat Nonlin Soft Matter Phys, 2014. **89**(3): p. 032706.

87.     Amador, A., et al., *Elemental gesture dynamics are encoded by song premotor cortical neurons.* Nature, 2013. **495**(7439): p. 59-64.

88.     Sitt, J.D., et al., *Dynamical origin of spectrally rich vocalizations in birdsong.* Phys Rev E Stat Nonlin Soft Matter Phys, 2008. **78**(1 Pt 1): p. 011905.

89.     Purves, D., et al., *The Motor Unit.* 2001.

90.     Buchthal, F. and H. Schmalbruch, *Motor unit of mammalian muscle.* Physiological Reviews, 1980. **60**(1): p. 90-142.

91.     Partridge, L., *Muscle properties: a problem for the motor controller physiologist.* Posture and movement, 1979: p. 189-229.

92.     Day, B.L., et al., *Electric and magnetic stimulation of human motor cortex: surface EMG and single motor unit responses.* J Physiol, 1989. **412**(1): p. 449-73.

93.     Garland, S.J. and L. Griffin, *Motor unit double discharges: statistical anomaly or functional entity?* Can J Appli Physiol, 1999. **24**(2): p. 113-130.

94.     Adams, L., A.K. Datta, and A. Guz, *Synchronization of motor unit firing during different respiratory and postural tasks in human sternocleidomastoid muscle.* J Physiol, 1989. **413**(1): p. 213-231.

95.     Mrówczyński, W., et al., *Physiological consequences of doublet discharges on motoneuronal firing and motor unit force.* Front Cell Neurosci, 2015. **9**(81): p. doi: 10.3389/fncel.2015.00081.

96.     Hoffer, J.A., et al., *Discharge patterns of hindlimb motoneurons during normal cat locomotion.* Science, 1981. **213**(4506): p. 466-467.

97.     Sandercock, T.G. and C.J. Heckman, *Doublet potentiation during eccentric and concentric contractions of cat soleus muscle.* J Appl Physiol, 1985. **82**(4): p. 1219-1228.

98.     Sponberg, S. and T.L. Daniel, *Abdicating power for control: a precision timing strategy to modulate function of flight power muscles.* Proc Biol Sci, 2012. **279**(1744): p. 3958-3966.

99.     Barnes, J., *Feedback and motor control in invertebrates and vertebrates*. 2012: Springer Science & Business Media.

100.    Srivastava, K.H., C.P. Elemans, and S.J. Sober, *Multifunctional and context-dependent control of vocal acoustics by individual muscles.* J Neurosci, 2015. **35**(42): p. 14183-14194.

101.    Stevens, K.N., *Scientific substrates of speech production*, in *Introduction to Communication Sciences and Disorders*, F.D. Minifie, Editor. 1994, Singular: San Diego, CA. p. 399-437.

102.    Jones, J.A. and K.G. Munhall, *Perceptual calibration of F0 production: evidence from feedback perturbation.* J Acoust Soc Am, 2000. **108**(3 Pt 1): p. 1246-1251.

103.    Hoffmann, L.A. and S.J. Sober, *Vocal generalization depends on gesture identity and sequence.* J Neurosci, 2014. **34**(16): p. 5564-5574.

104.    David, G., et al., *EMG and strength correlates of selected shoulder muscles during rotations of the glenohumeral joint.* Clin Biomech (Bristol, Avon), 2000. **15**(2): p. 95-102.

105.    Carvell, G.E., et al., *Electromyographic activity of mystacial pad musculature during whisking behavior in the rat.* Somatosens Mot Res, 1991. **8**(2): p. 159-164.

106.    Ludlow, C.L., *Central nervous system control of the laryngeal muscles in humans.* Respir Physiol Neurobiol, 2005. **147**(2-3): p. 205-222.

107.    Sawashima, M., Y. Kakita, and S. Hiki, *Activity of the extrinsic laryngeal muscles in relation to Japanese word accent.* Ann Bull RILP, 1973. **7**: p. 19-25.

108.    Erickson, D., *Laryngeal muscle activity in connection with Thai tones.* Ann Bull RILP, 1993. **27**: p. 135-149.

109.    Titze, I.R., E.S. Luschei, and M. Hirano, *Role of the thyroarytenoid muscle in regulation of fundamental frequency.* J Voice, 1989. **3**(3): p. 213-224.

110.    Sponberg, S., et al., *A single muscle's multifunctional control potential of body dynamics for postural control and running.* Phil Trans R Soc B, 2011. **366**: p. 1592-1605.

111.    Li, C.R., C. Padoa-Schioppa, and E. Bizzi, *Neuronal correlates of motor performance and motor learning in the primary motor cortex of monkeys adapting to an external force field.* Neuron, 2001. **30**(2): p. 593-607.

112.    Hartley, R.S., *Expiratory muscle activity during song production in the canary.* Respir Physiol, 1990. **81**(2): p. 177-187.

113.    Wild, J.M., *The avian nucleus retroambigualis: a nucleus for breathing, singing, and calling.* Brain Res, 1993. **606**(2): p. 319-324.

114. Goller, F. and B.G. Cooper, *Peripheral motor dynamics of song production in zebra finch.* Ann N Y Acad Sci, 2004. **1016**: p. 130-152.

115. Tumer, E.C. and M.S. Brainard, *Performance variability enables adaptive plasticity of 'crystallized' adult birdsong.* Nature, 2007. **450**(7173): p. 1240-1244.

116. Sakata, J.T. and M.S. Brainard, *Online contributions of auditory feedback to neural activity in avian song control circuitry.* J Neurosci, 2008. **28**(44): p. 11378-11390.

117. Elemans, C.P.H., et al., *Superfast muscles set maximum call rate in echolocating bats.* Science, 2011. **333**(6051): p. 1885-1888.

118. Rall, J.A. and R.C. Woledge, *Influence of temperature on mechanics and energetics of muscle contraction.* Am J Physiol, 1990. **259**(2 Pt 2): p. R197-203.

119. Bernstein, N., *The Coordination and Regulation of Movements*. 1967, New York: Pergamon Press.

120. Ting, L.H. and J.M. Macpherson, *A limited set of muscle synergies for force control during a postural task.* J Neurophysiol, 2005. **93**(1): p. 609-613.

121. Weiss, E.J. and M. Flanders, *Muscular and postural synergies of the human hand.* J Neurophysiol, 2004. **92**(1): p. 523-535.

122. Tresch, M.C., V.C. Cheung, and A. d'Avella, *Matrix factorization algorithms for the identification of muscle synergies: evaluation on simulated and experimental data sets.* J Neurophysiol, 2006. **95**(4): p. 2199-2212.

123. Fant, G., *Acoustic Theory of Speech Production*. 1970, The Hague: Mouton.

124. Huxley, A.F., *Muscle structure and theories of contraction.* Prog Biophys and Biophys Chem, 1957. **7**: p. 255-318.

125. Herzog, W. and T.R. Leonard, *The history dependence of force production in mammalian skeletal muscle following stretch-shortening and shortening-stretch cycles.* J Biomech, 2000. **33**(5): p. 531-542.

126. Goller, F. and T. Riede, *Integrative physiology of fundamental frequency control in birds.* J Physiol Paris, 2013. **107**(3): p. 230-242.

127. De Luca, C.J. and B. Mambrito, *Voluntary control of motor units in human antagonist muscles: coactivation and reciprocal activation.* J Neurophysiol, 1987. **58**(3): p. 525-542.

128. Doupe, A.J. and M. Konishi, *Song-selective auditory circuits in the vocal control system of the zebra finch.* Proc Natl Acad Sci U S A, 1991. **88**(24): p. 11339-11343.

129. Mooney, R., *Different subthreshold mechanisms underlie song selectivity in identified HVc neurons of the zebra finch.* J Neurosci, 2000. **20**(14): p. 5420-5436.

130. Sturdy, C.B., J.M. Wild, and R. Mooney, *Respiratory and telencephalic modulation of vocal motor neurons in the zebra finch.* J Neurosci, 2003. **23**(3): p. 1072-1086.

131. Baker, S.N., E. Olivier, and R.N. Lemon, *Coherent oscillations in monkey motor cortex and hand muscle EMG show task-dependent modulation.* J Physiol, 1997. **501**(Pt 1): p. 225-241.

132. Griffin, D.M., et al., *Do corticomotoneuronal cells predict target muscle EMG activity?* J Neurophysiol, 2008. **99**(3): p. 1169-1186.

133. Dave, A.S. and D. Margoliash, *Song replay during sleep and computational rules of sensorimotor vocal learning.* Science, 2000. **290**(5492): p. 812-816.

134. Vallentin, D., et al., *Inhibition protects acquired song segments during vocal learning in zebra finches.* Science, 2016. **351**(6270): p. 267-271.

135. Lawhern, V., et al., *Spike rate and spike timing contributions to coding taste quality information in rat periphery.* Front Integr Neurosci, 2011. **5**: p. 18.

136. Fairhall, A., E. Shea-Brown, and A. Barreiro, *Information theoretic approaches to understanding circuit function.* Curr Opin Neurobiol, 2012. **22**(4): p. 653-659.

137. Berry, M.J., D.K. Warland, and M. Meister, *The structure and precision of retinal spike trains.* Proc Natl Acad Sci U S A, 1997. **94**(10): p. 5411-5416.

138. Tang, C., et al., *Millisecond-scale motor encoding in a cortical vocal area.* PLoS Biol, 2014. **12**(12): p. e1002018.

139. Todorov, E., *Direct cortical control of muscle activation in voluntary arm movements: a model.* Nat Neurosci, 2000. **3**(4): p. 391-398.

140. Churchland, M.M., et al., *Neural population dynamics during reaching.* Nature, 2012. **487**(7405): p. 51-56.

141. Georgopoulos, A.P., A.B. Schwartz, and R.E. Kettner, *Neuronal population coding of movement direction.* Science, 1986. **233**(4771): p. 1416-1419.

142. Hoffer, J., et al., *Discharge patterns of hindlimb motoneurons during normal cat locomotion.* Science, 1981. **213**(4506): p. 466-467.

143. Roberts, T.F., et al., *Telencephalic neurons monosynaptically link brainstem and forebrain premotor networks necessary for song.* J Neurosci, 2008. **28**(13): p. 3479-3489.

144. Kadono, H., T. Okada, and K. Ono, *Electromyographic studies on the respiratory muscles of the chicken.* Poultry Science, 1963. **42**(1): p. 121-128.

145. Fedde, M., P. DeWet, and R. Kitchell, *Motor unit recruitment pattern and tonic activity in respiratory muscles of Gallus domesticus.* Journal of Neurophysiology, 1969. **32**(6): p. 995-1004.

146. Wild, J.M., F. Goller, and R.A. Suthers, *Inspiratory muscle activity during bird song.* J Neurobiol, 1998. **36**(3): p. 441-453.

147. Goller, F. and O.N. Larsen, *A new mechanism of sound generation in songbirds.* Proc Natl Acad Sci U S A, 1997. **94**(26): p. 14787-14791.

148. Fedde, M., *Respiratory muscles.* Bird respiration, 1987. **1**: p. 3-37.

149. Kraskov, A., H. Stögbauer, and P. Grassberger, *Estimating mutual information.* Physical review E, 2004. **69**(6): p. 066138.

150. McKay, J.L., et al., *Statistically significant contrasts between EMG waveforms revealed using wavelet-based functional ANOVA.* J Neurophysiol, 2013. **109**(2): p. 591-602.

151. Witham, C.L. and S.N. Baker, *Information theoretic analysis of proprioceptive encoding during finger flexion in the monkey sensorimotor system.* Journal of neurophysiology, 2015. **113**(1): p. 295-306.

152. Donoghue, J.P., *Connecting cortex to machines: recent advances in brain interfaces.* Nature neuroscience, 2002. **5**: p. 1085-1088.

153. Andersen, R.A., S. Musallam, and B. Pesaran, *Selecting the signals for a brain–machine interface.* Current opinion in neurobiology, 2004. **14**(6): p. 720-726.

154. Marsh, B.T., et al., *Toward an autonomous brain machine interface: integrating sensorimotor reward modulation and reinforcement learning.* The Journal of Neuroscience, 2015. **35**(19): p. 7374-7387.

155. Waldert, S., et al., *Hand movement direction decoded from MEG and EEG.* The Journal of neuroscience, 2008. **28**(4): p. 1000-1008.

156. Ranade, G.V., K. Ganguly, and J. Carmena. *LFP beta power predicts cursor stationarity in BMI task*. in *Neural Engineering, 2009. NER'09. 4th International IEEE/EMBS Conference on*. 2009. IEEE.

157. Tu, M.S. and T.L. Daniel, *Submaximal power output from the dorsolongitudinal flight muscles of the hawkmoth Manduca sexta.* J Exp Biol, 2004. **207**(Pt 26): p. 4651-4662.

158.     Tu, M.S. and T.L. Daniel, *Cardiac-like behavior of an insect flight muscle.* J Exp Biol, 2004. **207**(Pt 14): p. 2455-2464.

159.     Hill, A.V., *The dimensions of animals and their muscular dynamics.* Science Progress (1933-), 1950. **38**(150): p. 209-230.

160.     Gorassini, M., et al., *Activity of hindlimb motor units during locomotion in the conscious rat.* J Neurophysiol, 2000. **83**(4): p. 2002-2011.

161.     Person, R.S. and L.P. Kudina, *Discharge frequency and discharge pattern of human motor units during voluntary contraction of muscle.* Electroencephalogr Clin Neurophysiol, 1972. **32**(5): p. 471-483.

162.     Jubeau, M., et al., *Random motor unit activation by electrostimulation.* Int J Sports Med, 2007. **28**(11): p. 901-904.

163.     Gracco, V.L. and J.H. Abbs, *Central patterning of speech movements.* Exp Brain Res, 1988. **71**(3): p. 515-526.

164.     Brenowitz, E.A., D. Margoliash, and K.W. Nordeen, *An introduction to birdsong and the avian song system.* J Neurobiol, 1997. **33**(5): p. 495-500.

165.     Wild, J.M., *Descending projections of the songbird nucleus robustis archistriatalis.* J Comp Neurol, 1993. **338**(2): p. 225-241.

166.     Charlesworth, J.D., et al., *Learning the microstructure of successful behavior.* Nat Neurosci, 2011. **14**(3): p. 373-380.

167.     Elemans, C.P.H., et al., *Universal mechanisms of sound production and control in birds and mammals.* Nat Comm, 2015. **6**(8978): p. 1-13.

168.     Ivanenko, Y.P., R.E. Poppele, and F. Lacquaniti, *Five basic muscle activation patterns account for muscle activity during human locomotion.* J Physiol, 2004. **556**(Pt 1): p. 267-282.

169.     Sober, S.J. and M.S. Brainard, *Vocal learning is constrained by the statistics of sensorimotor experience.* Proc Natl Acad Sci U S A, 2013. **In press**: p. 1-6.

170.     Hoffmann, L.A., et al., *A lightweight, headphones-based system for manipulating auditory feedback in songbirds.* J Vis Exp, 2012. **69**: p. e50027.

171.     Sober, S.J. and M.S. Brainard, *Vocal learning is constrained by the statistics of sensorimotor experience.* Proc Natl Acad Sci U S A, 2012. **109**(51): p. 21099-21103.

172.     Andalman, A. and M.S. Fee, *A basal ganglia-forebrain circuit in the songbird biases motor output to avoid vocal errors.* Proc Natl Acad Sci U S A, 2009. **106**(30): p. 12518-12523.

173. McGill, K.C., Z.C. Lateva, and H.R. Marateb, *EMGLAB: an interactive EMG decomposition program.* Journal of neuroscience methods, 2005. **149**(2): p. 121-133.

174. Victor, J.D., *Spike train metrics.* Current opinion in neurobiology, 2005. **15**(5): p. 585-592.

175. Victor, J.D. and K.P. Purpura, *Metric-space analysis of spike trains: theory, algorithms and application.* Network: computation in neural systems, 1997. **8**(2): p. 127-164.